LASER INTERFEROMETER GRAVITATIONAL WAVE OBSERVATORY
- LIGO -
================================
LIGO SCIENTIFIC COLLABORATION

Technical Note	LIGO-T15TBI–v1	2016/08/31
Instrument Science White Paper		
LIGO Scientific Collaboration		

California Institute of Technology
LIGO Project, MS 100-36
Pasadena, CA 91125
Phone (626) 395-2129
Fax (626) 304-9834
E-mail: info@ligo.caltech.edu

Massachusetts Institute of Technology
LIGO Project, Room NW22-295
Cambridge, MA 02139
Phone (617) 253-4824
Fax (617) 253-7014
E-mail: info@ligo.mit.edu

LIGO Hanford Observatory
Route 10, Mile Marker 2
Richland, WA 99352
Phone (509) 372-8106
Fax (509) 372-8137
E-mail: info@ligo.caltech.edu

LIGO Livingston Observatory
19100 LIGO Lane
Livingston, LA 70754
Phone (225) 686-3100
Fax (225) 686-7189
E-mail: info@ligo.caltech.edu

http://www.ligo.org/

Contents

List of Figures

1 Introduction

The LIGO Scientific Collaboration (LSC) conducts research and development directed toward the improvement of the current generation of LIGO and GEO interferometers as well as toward the development of concepts, prototypes, components, and modelling for future interferometer configurations.

The research is roughly separated into the following categories and working groups:

- The Advanced Interferometer Configurations Working Group (AIC)
- The Quantum Noise Working Group (QNWG)
- The Lasers and Auxiliary Optics Working Group (LAWG)
- The Optics Working Group (OWG)
- The Suspensions and Isolation Working Group (SWG)

The intent of this white paper is to provide a synopsis of the current and future R&D directions of these working groups.
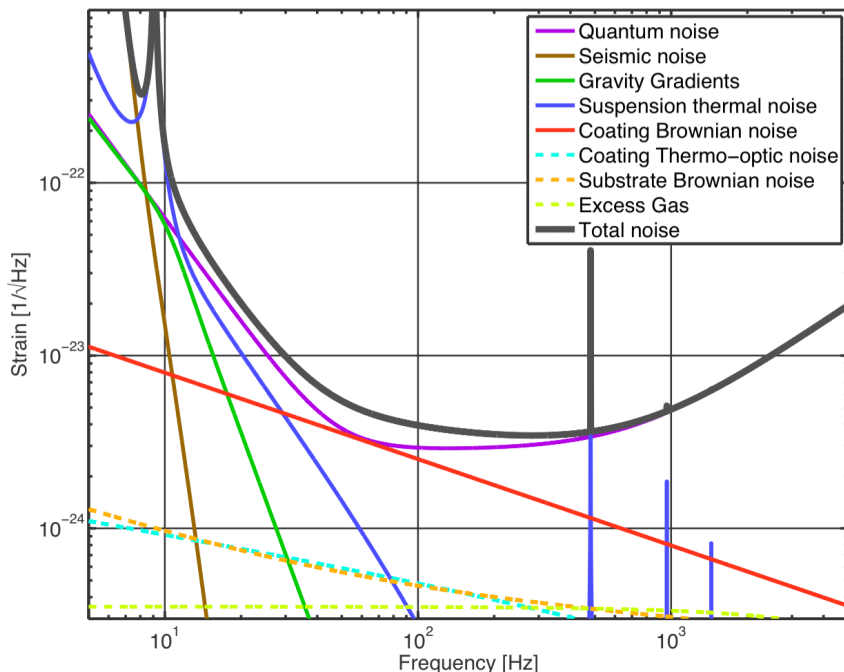
Figure 1: Baseline aLIGO Noise Budget (GWINC v2.0). 125 W input power; broadband RSE tuning. Experience to date with the aLIGO instruments has not uncovered any barrier to achieving performance consistent with these curves.

Interferometer development is a broad topic. One part of the effort is in the design, building, and characterization of test systems and prototypes for future detector upgrades and new detectors. Another element, of growing importance as we push the envelope of system performance, is the physics of materials and condensed matter systems. As this often requires scientists and skills beyond the existing groups, the Collaboration must expand these efforts in order to succeed in the larger goal of gravitational wave astrophysics. Finally, much

of the ongoing and planned research commands interest in and of itself; adaptive optics, precision measurement, and quantum interactions with matter are both integral elements of gravitational wave detectors and exciting areas of physics.

As with Initial and Enhanced LIGO, the success of the aLIGO and upgrade programs depends on the input from a robust next-generation research program, and vice-versa. This white paper represents the current thinking of the LSC technical working groups. From experience, we know that it will be updated routinely based on our ongoing R&D and both the experimental and observational results of Advanced LIGO.

Figure 1 presents our current best understanding of the noise sources that will limit Advanced LIGO in the high power, broadband tuning configuration. The sensitivity is determined by shot noise at high frequencies, by mirror thermal noise in the middle frequencies, and by a combination of thermal, seismic and quantum radiation pressure noises at low frequencies.

As is now well known, on September 14, 2015, the aLIGO interferometers recorded the first detection of gravitational waves, when at about 40 percent of their design sensitivity. We appear to be on track to have two interferometers in interleaved commissioning and observing from September 2016 for the O2 observing run. The optical, mechanical, and electronics systems appear to be compatible with the near-term improvements envisioned (e.g. the optical losses are low enough in the main cavities to make squeezing interesting). However there are a number of technical issues which are currently limiting the performance of the aLIGO detectors. In the the following chapters each working group, begins begin by identifying the R&D and effort needed to help resolve these problems.

This White Paper uses a Roadmap for the next 25 years, 2016-2040, in order to focus effort and aid prioritization. This Roadmap will be revised and refined each year.

2   Roadmap 2016-2040 and Executive Summary

Whilst it was major event in the history of science, the detection of gravitational waves using aLIGO heralded only the beginning of gravitational wave astronomy. The need to probe further into the universe and backward in time will drive instrument science to develop and deliver more and more sensitive detectors. Future detectors will study novel astrophysics, cosmology and gravitational phenomena employing technology beyond the current state of the art. These sources are well described in the ET Design Study [1] as well as in LSC technical notes e.g. [2].

The predicted gravitational-wave sources emit in a variety frequency bands with a variety of durations, which places a corresponding requirement on the detector sensitivity. Ideally, the design of future detectors will match the gravitational wave sources and the noise performance will be optimized accordingly. The required sensitivity then dictates the detector technology and design. However, at the current epoch audio-band upgrades must still pursue a general goal to push on the sensitivity across the broadest frequency range including pushing down the low frequency cutoff.

The long lead time from conception to operation (from experience about 15 years or more) dictates that we begin planning now for detectors that may begin operation 20 years from

now. A typical detector cycle includes: Simulation of ideas and concepts; Experimental tests; Conceptual design and prototyping phases; Proposal and engineering; construction and Installation; Commissioning and observing phases.
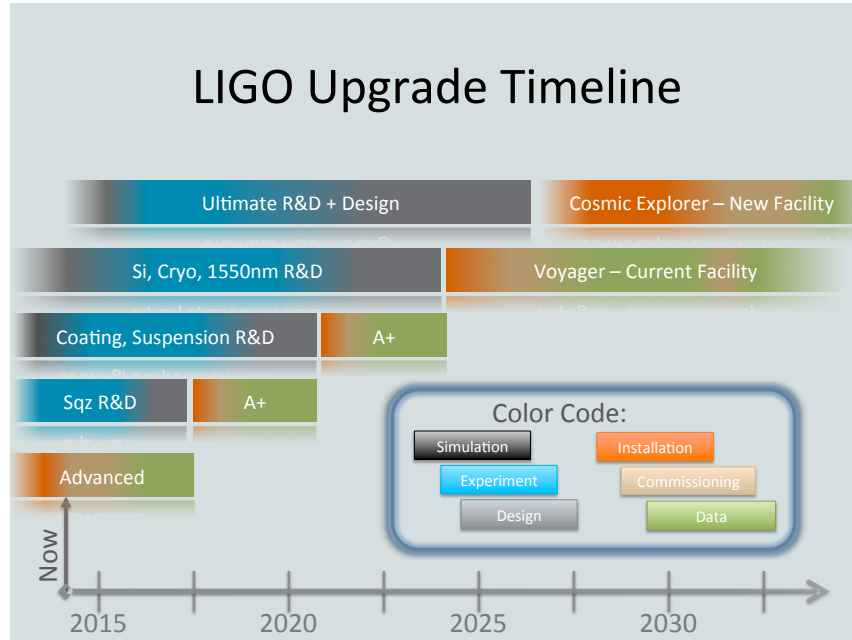
Figure 2: Estimated timeline for A+, LIGO Voyager and LIGO Cosmic Explorer.

We envisage potentially three detector epochs post Advanced LIGO baseline over the next 25 years with working titles A+, LIGO Voyager and LIGO Cosmic Explorer, see Figure 2. The funds required to implement the upgrades are classified as: modest, less than $10M to $20M; medium, $50M to $150M; major, greater than $200M. This strategy will be modified according to signals observed, technology readiness and funds available.

2.1 A+

A+ is a modest cost upgrade to aLIGO, implemented in a series of incursions. The goal binary neutron star inspiral range would be approximately 1.7 times aLIGO (around 340 Mpc), (see Figure 3). Each A+ stage could be implemented 1-2 years after the first 3 phases of the detector cycle (simulation, experimental testing and prototyping) have been completed. These phases of the detector cycle for frequency dependent squeezing were completed in the first half of 2016, allowing installation around 2017-18.

- frequency dependent squeezing, implemented in stage 1,
- bigger masses, bigger laser beam sizes in the optical cavities and better mirror coatings to reduce coating thermal noise, implemented in a second stage.

Miller et al [3] have shown that squeezing and coating thermal noise reduction must be combined to achieve maximum benefit. The goal is to minimise downtimes for these upgrades
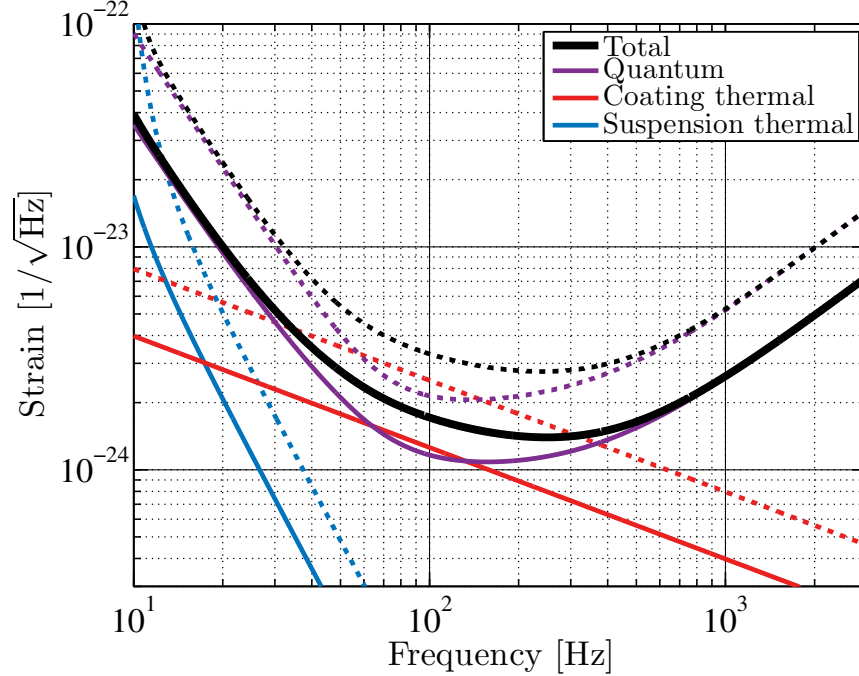
Figure 3: Strain sensitivity of A+. Improved thermal noise (factor of two), improved quantum noise (16 m filter cavity and 6 dB of measured squeezing at high frequency) and possibly heavier test masses (also a factor of two) are shown. The equivalent Advanced LIGO curves are shown as dashed lines.

to, preferably, three to six months. A realistic schedule would see stage 1 implemented after aLIGO's second observing run, O2.

R&D for A+ includes:

- Coating studies- sources of optical and mechanical loss in 1064 nm coatings
- Suspensions to allow heavier masses
- Seismic isolation performance tweaks
- Charge mitigation
- Stray light control
- Frequency dependent squeezing at 1064 nm.
- parametric instability control
- Newtonian noise reduction

2.2   LIGO Voyager

LIGO Voyager (LV) would be a more major upgrade still within the existing, or with perhaps minor modifications to the, LIGO vacuum envelope. A further factor of 3 increase in BNS range (to 1100 Mpc) is envisaged with a low frequency cutoff down to 10 Hz . To be operational by the latter half of next decade (2025 -), simulation and experimentation is underway now (2016) with the design to be completed with components ready for installation by 2025 (see Figure 7 for the noise budget).

LV will push a sensitivity across the audio-band. Subsystem improvements are tightly coupled with decisions made on one subsystem likely to place requirements on other subsystems. High frequency improvements achieved but using much higher laser power and suspension thermal noise reduction may drive the need for low temperature operation to both reduce thermal distortions (optimize thermal conductivity) and mechanical loss. This would necessitate a change of suspension material (perhaps) and mirror substrate material, and therefore laser wavelength. The need to reduce scatter loss to maximise the effectivenss of squeezing across the spectrum may also be a driver for longer wavelength operation. This in turn needs the development of high power lasers and quantum noise reduction at the new wavelength. The development of ultra low loss optical and mechanical loss coatings a factor of ten better than what is currently available on large substrates is required regardless of the operating wavelength. R&D is needed on (not prioritized):

- Bulk absorption measurements in new substrate materials
- Bulk Index/Birefringence Non-uniformity
- Procure / develop / qualify large test masses
- Initial Cooldown of Test Masses and suspensions
- Cryogenic Engineering of Test masses
- low opt/mech loss coatings at cryogenic temperatures
- Bond loss for new suspensions: ears, ribbons, etc.
- longer wavelength PSL operating at $200\,\mathrm{W}$
- longer wavelength squeezing
- High power IO components (modulators, isolators) at new wavelengths
- Ion milling level metrology for chosen wavelength
- Thermal Compensation
- Black Coatings for Mirror Barrels
- LWIR emissivity of HR/AR Coatings
- Low Phase Noise cryogenic interferometer prototype

LV will draw on technologies ready for large-scale prototyping in roughly 5 years (to be ready for implementation in ~ 2025). Given this timeline, a decision on operating wavelength must be made very soon to enable timely development of the required technologies. This decision could be informed by a cost estimate for each technology. For example, could a cryogenic interferometer be built under the proposed LV funding envelope? If the answer is no, this does not mean that such R&D should not be carried out. Its implementation may simply be delayed.

The question of what technologies could be ready for Voyager should the NSF find $100M around the middle of the next decade should be considered over the next year.

2.3 LIGO Cosmic Explorer

Once observations of gravitational waves with aLIGO, A+ and LIGO Voyager have established gravitational-wave astronomy, it will be timely to make a significant investment in a new Observatory with a binary neutron star reach well beyond a redshift of one, at a new

location. We refer to this new facility as LIGO Cosmic Explorer with operation to commence post 2035, probably in concert with LIGO Voyager. There is scope for bluesky R&D but the ideas and concepts that will form the basis of LIGO Cosmic Explorer (CE1) need to be maturing by by the end of this decade. A+ and LIGO Voyager may prototype some of the LIGO Cosmic Explorer technology.

The first instrument installed in LIGO Cosmic Explorer facility (CE1) will use extrapolations of techniques from previous instruments, as well as innovations unique to the new infrastructure. One relatively straight forward way to achieve the strawman design sensitivity is to adapt relevant A+ and Voyager technology for a much longer interferometer, for example, 40 km in length. Alternatively, shorter baseline designs with breakthroughs in Newtonian noise removal, other cancelation techniques and mirror, coating and mechanical system engineering, may exploit Quantum Non Demolition interferometry (e.g. speed-meters) to reach similar sensitivities. Another approach may be to use the Xylophone strategy with a series of interferometers targeting limited frequency spans. The European Einstein Telescope [1] (ET) forecasts technologies which overlap LIGO Voyager and LIGO Cosmic Explorer.

However, the facility infrastructure can be decoupled from the instrument which will be first installed. The facility should be designed to have a long lifetime a 50 year (say) so capable of housing instruments starting with sensitivities 10 times aLIGO allowing upgrades to at least 100 times aLIGO. Such a facility will by necessity be much longer that 4 km. It may be on the surface or it may be underground. The CE1 interferometer design will be determined following extensive R&D and informed by advanced interferometer observations. CE1 should be the best interferometer that can install when the time comes.

The question of 1-10Hz sensitivity, in terms of science/dollar, is likely to be a critical factor in the surface vs underground decision. This is a facility level decision and will impact on the direction of mid-term and long-term R&D. This critical "science case" question may be difficult to answer quantitatively without any detections, but a variety of scenarios should be considered as soon as possible.

2.4 Structure of this White Paper

This vision dictates that

- Prototyping for the second phase of the A+ upgrade, needs to be completed by mid 2017.
- LIGO Voyager R&D should be transitioning to the experimental phase in preparation for the design phase beginning around 2020; ideas need to be tested now in order to be mature enough for incorporation into Voyager.
- thinking about the new facility (simulation phase) that will become LIGO Cosmic Explorer needs to begin now.

.

In the remainder of this paper, the five working groups begin by identifying key issues which are currently limiting the performance of Advanced LIGO and investigations that need to

be carried out to overcome these problems. R&D needed for A+, LIGO Voyager and LIGO Cosmic Explorer is then reviewed in detail.

3 Advanced Interferometer Configurations

The AIC group has two chief purposes:

- Coordinate the integration of interferometers systems and make trade-offs between components to optimize the sensitivity.

- Design the sensing and feedback control for the interferometer length, alignment, and wavefront (thermal compensation) systems.

The following sections are organized in terms of the progress of detector technologies presented in the roadmap (section 2), followed by a section on interferometer sensing and control (ISC) which describes R&D that is relevant to all of the anticipated detectors.

3.1 A+

A few minor upgrades to aLIGO may be possible between major observing runs, given sufficient technical readiness and scientific payoff. These upgrades, when considered together, promise a significant increase in astrophysical event rate while incurring minimal downtime between observing runs [3].

Given our current understanding of the aLIGO observing schedule, a plausible progression of upgrades is:

- after O2 install a squeezed light source with a filter cavity (2017);

- after O3 swap end test-masses (and possibly ITMs) to improved coatings, possibly along with low-risk target of opportunity changes to the suspensions (2018-2019).

These upgrades target the 2 dominant noise sources in aLIGO: quantum noise and coating thermal noise.

Both of these upgrades also serve as risk reduction for aLIGO, squeezing in case of difficultly reaching high power operation, and improved coatings in case coating thermal noise has been underestimated. In the following sections we also consider improved suspensions with lower thermal noise and higher mass optics, but find that these have little impact on the astrophysical output of aLIGO. Possible low-risk changes to the suspensions include modifications to reduce gas damping, improve bounce and roll mode damping, mitigate parametric instabilities, etc.

3.1.1 Squeezed light for quantum noise reduction

Squeezed states of light [4] have already been used to improve the sensitivity of gravitational-wave interferometers [5, 6]. However, any reduction in quantum shot noise at high frequencies is accompanied by a commensurate increase in quantum radiation pressure noise (for frequency independent squeezing). If applied to Advanced LIGO, squeezing would reshape the
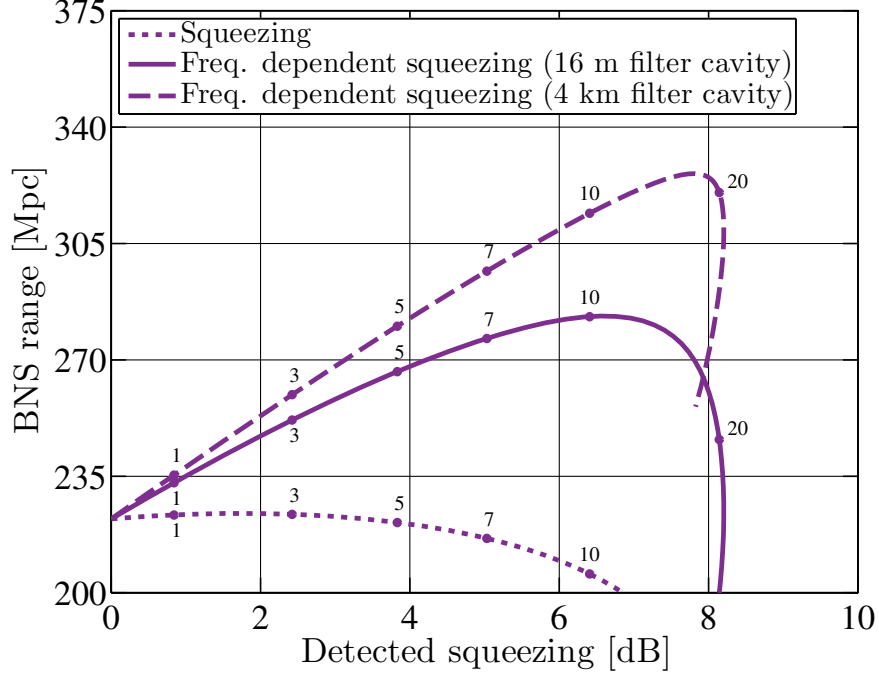
Figure 4: Impact of squeezing in Advanced LIGO on BNS range as a function of measured high-frequency quantum noise reduction. Numerical labels indicate the level of injected squeezing in dB (the best experimentally measured value currently stands at approximately 12 dB [7]). A number of loss mechanisms couple anti-squeezing into the measurement quadrature [8]. These effects are most noticeable with high levels of injected squeezing and are responsible for the curious double-valued nature of the frequency dependent curves.

sensitivity of the detector as a function of frequency to the detriment of binary black-hole (BBH) and binary neutron star (BNS) range (see Fig. 4).

By reflecting a squeezed beam from a detuned high-finesse optical resonator, known as a filter cavity, one can produce frequency dependent squeezing which can simultaneously reduce shot noise at high frequencies and radiation pressure noise at low frequencies [9, 10]. With a realistic implementation of frequency dependent squeezing (see parameters in Table 1, and methods described in [8]), broadband improvements are available, leading to increases of 30% and 15% in BNS and BBH ranges, respectively. With 10 dB of injected squeezing, realistic loss mechanisms, mainly the filter cavity intra-cavity loss, limit the BNS range achievable with a 16 m filter cavity to 280 Mpc.

A longer filter cavity can mitigate the impact of intra-cavity losses but, as shown in Fig. 4, would only yield a further 10% improvement assuming no change in other noises (e.g., coating thermal noise). For this reason, a 16-20 m filter cavity is an acceptable initial option for upgrading Advanced LIGO [11], while a longer filter cavity will be of considerable interest when combined with other improvements. Frequency dependent squeezing has recently been demonstrated at audio frequencies, and a prototype 16 m system is under construction at MIT [12, 8, 13].

Parameter	Value
Filter cavity length	16 m
Filter cavity input mirror transmissivity	67(47) ppm
Filter cavity detuning	49(35) Hz
Filter cavity half-bandwidth	56(41) Hz
Filter cavity losses	8 ppm
Injection losses	5%
Readout losses	5%
Mode-mismatch (squeezer-filter cavity)	2%
Mode-mismatch (squeezer-interferometer)	5%
Frequency independent phase noise (RMS)	5 mrad
Filter cavity length noise (RMS)	0.3 pm
Injected squeezing	9.1 dB

Table 1: Parameters used in evaluating the performance of an Advanced LIGO interferometer incorporating frequency-dependent squeezing. Interferometer parameters are as given in Table I of [8]. Values in parentheses correspond to an interferometer with 80 kg mirrors.

3.1.2 Coating thermal noise reduction

The optical coatings used in gravitational-wave detectors have extraordinary optical properties: absorption below 1 ppm, scatter losses around 10 ppm and very tightly controlled reflectivities. Conversely, these coatings are mechanically much more lossy than the mirror substrates on which they are deposited. Thus, they constitute the dominant source of thermal noise [14].

Coating research has received considerable attention in the past decade as the use of resonant optical cavities has become widespread in frequency standards, gravitational-wave detectors and other optical precision measurements [15]. Informed by this work, the coatings used in Advanced LIGO are composed of alternating layers of amorphous silica and titania-doped tantalum pentoxide [16, 17]. There is significant ongoing effort to develop amorphous coatings with reduced mechanical loss and acceptable optical properties (section 5.2). In addition, there has been a search for new coating materials and technologies for use in future GW detectors.

One potential solution is the use of crystalline coatings. A leading candidate is epitaxial layers of GaAs and AlGaAs, which can be grown on a GaAs wafer and then transferred to a fused-silica substrate. Multilayer AlGaAs Bragg reflectors have been shown to provide at least a factor of three reduction in the amplitude of coating thermal noise [18]. Alternative crystalline materials such as AlGaP/GaP are also under investigation, see [19, 20].

While crystalline coatings are promising, they have yet to be demonstrated on a 40 cm-scale mirror. Scaling this technology up presents several technical challenges, both in the manufacturing process and in meeting the extremely stringent surface-figure specification associated with multi-kilometer resonant cavities. As such, **crystalline coatings are not considered practical for use in A+**, though they may be very useful in Voyager or Cosmic Explorer given sufficient and successful technology development.

3.1.3 Increased mirror size and mass

While we recognize that **changing the mirror masses on the scale of A+ is not feasible**, we explore here the impact of higher mass for completeness and to inform the Voyager and Cosmic Explorer discussions which come later.

Radiation pressure noise scales inversely with the core optics' mass. Increasing the mirror mass is therefore a straightforward way of mitigating the impact of radiation pressure noise. The test masses in Advanced LIGO are made from ultra-low absorption fused silica, which is available in sizes allowing for up to about 10 times the present mass (400kg and 1m diameter available from Heraeus).

Polishing large masses with Ion Beam Figuring (as used for aLIGO) can handle up to 50 cm diameter, but would need work to handle greater weight and possible thickness (not technically challenging, but requires up front investment). Coating larger masses may also be challenging. CSIRO is currently limited to 40 cm diameter; their experts think they could do any size and weight with development, and our understanding of their technique is compatible with that assertion. LMA is also planning to scale-up their coating capabilities in the near future (see G1500687).

Larger masses should allow the use of larger beams and thus lower coating thermal noise. From this standpoint, the optimal mirror aspect ratio (radius/thickness) is approximately unity. With such a geometry, coating thermal noise amplitude scales as $m^{-1/3}$, where m is the mirror mass—if the diffraction loss is held constant. Increased mass also reduces suspension thermal noise. This effect scales as $m^{-1/4}$ in amplitude [21] and has been included in the values presented in this work.

Increasing the size of the laser beam reflected from the test masses reduces the impact of coating thermal noise in proportion to the beam diameter, simply due to averaging over a larger coating area [15]. While this solution is conceptually simple, feasible beam diameters are limited by optic size, optical stability considerations of the arm cavities and challenges in fabricating suitable mirror surfaces. In the context of Advanced LIGO, even with larger mirrors **only a small increase in beam size is likely to be achieved without compromising the stability of the interferometer** [22, 23, 24]. Given the expense and downtime associated with refitting the optical chain for a different beam size, this is not currently considered a feasible option for A+, though larger beams may play a role in Voyager, and will certainly be relevant in Cosmic Explorer (simply due to its length).

3.1.4 Suspension thermal noise reduction

As part of a multi-stage seismic isolation system, the test masses of the Advanced LIGO interferometers are suspended from four 60 cm-long low-loss fused silica fibers. The fibers have a circular cross section whose diameter varies to best cancel thermoelastic damping, to maintain low bounce mode and high violin mode frequencies and to ease handling and bonding to the test masses. Thermal noise from this suspension system dominates the total thermal noise below ~10 Hz (see Fig. 6). Several low risk methods are available for reducing suspension thermal noise [25].

The amplitude of suspension thermal noise scales as $1/l$, where l is the length of the sus-

pension fibers. This scaling includes equal contributions from "dissipation dilution" and the improved isolation resulting from a downward shift of the resonant frequency.[1] Further gains can be realized by refining the geometry of the fibre ends to improve dilution factors and by heat treatment of the fibers to reduce surface losses.

One recent study estimates that the above techniques can reduce the amplitude of suspension thermal noise by a factor of 2.5 . In this work we assume a factor of two gain, realizing this improvement solely through increased suspension length, but find that this change has little impact on the scientific output of A+.

Modifying the geometry could involve pulling fibres from thicker 5mm stock to ensure that bending energy remains in the thin section of the fibre, where thermoelastic cancellation takes place, and not the stock ends. In terms of surface loss, one recent study estimates that the above techniques can reduce the amplitude of suspension thermal noise by a factor of 2.5 [25]. In this work we assume a factor of two gain, realizing this improvement solely through increased suspension length, but find that this change has little impact on the scientific output of A+. In order to explore the surface loss one only has access to the product of surface loss multiplied by the surface layer which causes the loss, or $\phi_s \simeq 6 \times 10^{-12}$ for aLIGO. It will be interesting to be able to split the contributions to understand whether this is a very thin lossy layer, or a thicker layer with overall lower loss. For such a study we propose to pull thick fibres in the diameter range 1μm -10μm. Measuring properties such as breaking stress, Youngs modulus and the Shear modulus should enable a study to be made on whether there is an outer layer with different mechanical properties. Shear modulus will be a good proxy here as the amount of energy stored in the outer layers of the fibre scale as R4.

A further opportunity to improve suspension performance is to utilise fibres with higher stress. aLIGO operates at 800MPa in the thin section which results in a violin mode of 500Hz and bounce/roll modes of 9Hz/13Hz respectively. The bounce/roll modes currently require some damping for control and it would be useful to study techniques to lower these modes. One such possibility is to increase the fibre stress. aLIGO currently operates around a factor 7-8 below the ultimate tensile stress, so an increase to 1.4GPa would mean operating within a factor of 3-4 of the ultimate tensile stress. This is still a comfortable operating point for a material such as fused silica which does not yield. However, robustness tests need to be performed in order to ensure that the higher stress can be developed into an engineered solution. We would propose tests of higher stress suspensions and a system, operating at 1GPa, has already been hanging at LIGO Hanford for over 1 year. Further tests at even higher stresses will prove the robustness. Operating a 1.4GPa for a 1.2m long suspension would result in a violin mode of 400Hz, and a bounce/roll mode of 5Hz/8Hz respectively. Such higher stress fibres can be retrofitted into the current QUAD suspension, requiring minimal change in the suspension, or into upgrades such as A+ with either longer/heavier suspensions.

---

[1]Increasing the suspension length brings the added benefit of reducing thermal noise in the vertical direction, which couples to the longitudinal direction due to the Earth curvature. This is of particular relevance to CE, given its greater length.

3.1.5   Discussion

For each of the potential improvements to Advanced LIGO we consider a factor of two reduction in the corresponding noise term. Each noise term contributes significantly at certain frequencies (see Fig. 6). But alone, none is sufficiently dominant to make more than a 30% change in the BNS or BBH range (see Table 2). **A large improvement in inspiral range is only realized when at least squeezing and coating thermal noise improvements are implemented simultaneously**.

Fig. 5 conveys the relative importance of each potential upgrade, when evaluating the benefit of each improvement separately—*assuming all other improvements have already been made.* For example, the quantum noise curve shows the BNS range as function of the measured squeezing at high frequency for an interferometer in which coating thermal noise and suspension thermal noise have been reduced by a factor of two (or $\sim 6\,\mathrm{dB}$) and the mass of the mirrors has been increased by a factor of two (all with respect to Advanced LIGO). Quantum noise and coating thermal noise are shown to have the largest effect on the BNS range up to $6\,\mathrm{dB}$ improvement. Beyond this point, the BNS range for quantum noise does not increase monotonically with the level of detected squeezing. This is similar to Advanced LIGO as shown in Fig. 4. On the other hand, a $4\,\mathrm{km}$ long filter cavity is now significantly more effective, since radiation pressure has become more dominant at lower frequencies. The maximum achievable BNS range is 20% higher with respect to a short filter cavity—bringing the maximum range to $580\,\mathrm{Mpc}$ for $6\,\mathrm{dB}$ of detected high-frequency squeezing.

Table 2: BNS and BBH ranges for an Advanced LIGO interferometer in which combinations of the main limiting noise sources have been reduced in the manner described in the text. A plausible incremental progression of upgrades is highlighted in blue: *(i)* quantum noise reduction through squeezed light injection, *(ii)* a factor of two reduction in coating thermal noise, *(iii)* a factor of two increase in the mirror mass, and *(iv)* a factor of two reduction in suspension thermal noise.

Improved quantity				Range	
Quantum	Coating thermal	Mirror mass	Suspension thermal	BNS [Mpc]	BBH [Gpc]
—	—	—	—	220	1.3
•	—	—	—	280	1.5
—	•	—	—	280	1.7
—	—	•	—	260	1.6
—	—	—	•	220	1.3
•	•	—	—	400	2.3
•	—	•	—	320	1.9
•	—	—	•	280	1.6
—	•	•	—	350	2.3
—	•	—	•	280	1.7
—	—	•	•	270	1.7
•	•	•	—	470	2.9
•	•	—	•	410	2.3
•	—	•	•	320	1.9
—	•	•	•	350	2.3
•	•	•	•	480	3.0
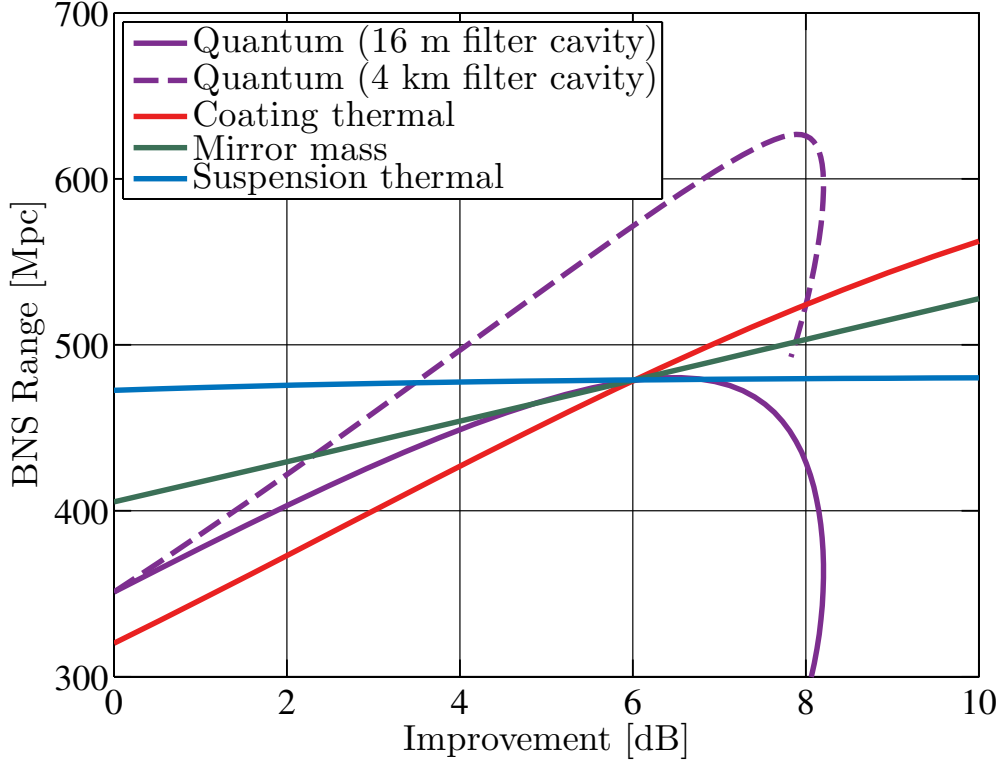
Figure 5: BNS range as a function of individual improvements. For the quantum noise the horizontal axis depicts the measured squeezing at high frequency, for the mirror mass the increase in mass, for the coating thermal noise and for the suspension thermal noise it shows the reduction factor. For each trace the remaining parameters are held fixed at their higher sensitivity. The four continuous curves intersect at the 6 dB point, where they all yield a factor of two improvement. For this configuration a longer filter cavity is significantly more effective (dashed curve).

Mitigating suspension thermal noise offers relatively modest gains in astrophysical output compared to the other approaches. By extension, this indicates that improvements in noise sources such as seismic noise, which is also influential at very low frequencies, but less so than suspension thermal noise, will be even less impressive. Newtonian noise (a.k.a. "gravity gradient noise"), however, can dominate over suspension thermal noise in times of high seismic activity, and mitigation of this noise source will be needed to provide consistently high quality data.

For the BNS and BBH systems used to define our figures of merit the sensitivity around 100 Hz is of utmost importance. However, the astrophysical impact of Advanced LIGO will likely not be limited to the detection of compact binaries. Many interesting sources emit gravitational waves in the 300-3000 Hz band; examples include supernovae, rapidly rotating neutron stars, and the merger phase of binary systems with one or two neutron stars. Sensitivity in this frequency range is, however, entirely dominated by quantum shot noise and thus is insensitive to all of the modifications discussed above except squeezed light injection.
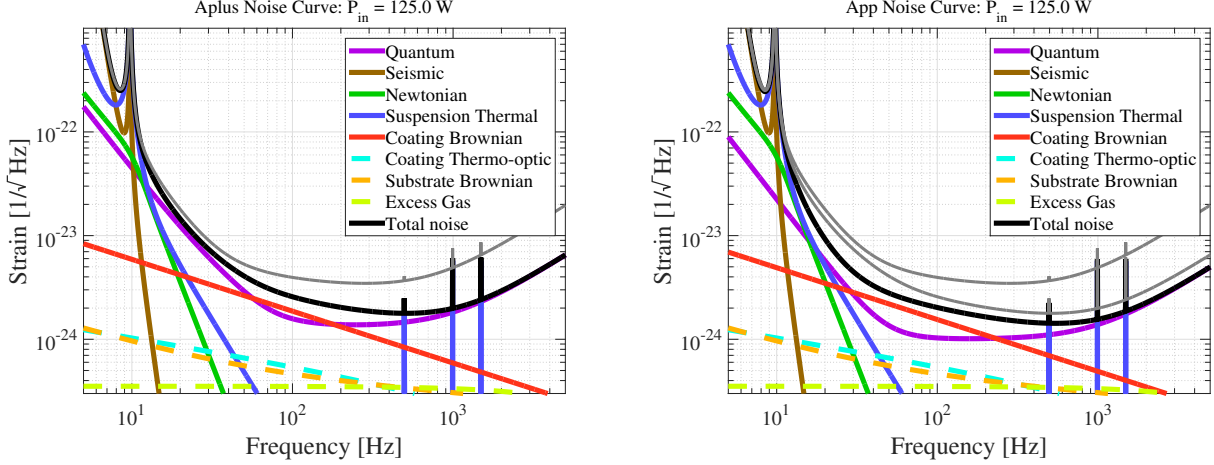
Figure 6: Strain sensitivity of "nominal" A+ (left, 320 Mpc) and "optimistic" A+ (right, 460 Mpc). The left curve uses a 16 m filter cavity and 6 dB of measured squeezing at high frequency, along with a factor of 2 lower loss in the coating high index layer relative to aLIGO (i.e., a loss angle of 10^{-4}). The right curve uses a 4 km filter cavity and 8 dB of measured squeezing at high frequency, with a factor of 4 lower loss in the coating high index layer relative to aLIGO (i.e., a loss angle of 5×10^{-5}). The Advanced LIGO sensitivity curve is show in gray for reference in both plots, while the "nominal" A+ curve is also shown on the "optimistic" plot.

3.1.6 Overview of Research and Development for A+

The following list summarizes the R&D expected to be useful for the aLIGO upgrades discussed above, along with more minor improvements which are not directly related to the interferometer design.

- **Coatings Thermal Noise Reduction:** Coating thermal noise reduction research is in progress on the aLIGO type coatings and this should be continued. The time scale for A+ is short, and IBS coatings are likely the only viable candidate for producing a mature coating technology. Looking farther into the future, however, Voyager and Cosmic Explorer designs will both benefit from an improved coating solution (e.g., crystalline coatings or amorphous silicon coatings).
- **Frequency Dependent Squeezing:** Quantum noise reduction R&D is discussed in section 4.2.1. In order to maximize the benefit from squeezing, it is crucial to minimize the losses between the squeezed light source and the gravitational wave photodetector in transmission to the output mode-cleaner (OMC). This requires developing ultra-low loss Faraday isolators, large diodes with high quantum efficiency, and a high throughput OMC. Moreover, at the interface between a squeezed light source and the interferometer, there are problems of alignment control (discussed in 3.4.2) and mode matching. Squeezing drives stringent mode-matching requirements which can only be met by a system capable of on-the-fly optimization. This will require a sensing scheme capable of measuring the mode-matching and feeding back to in-vacuum optics which can change the beam parameters. The mode overlaps of interest are those between the squeezed light source, the filter cavity, the interferometer, and the output mode cleaner (OMC).

- **Newtonian Noise Subtraction:** All future detectors will benefit from Newtonian Noise Subtraction using seismometer arrays. While this may not be critical for A+, Newtonian Noise coupling predictions vary, as does the seismic environment, making this a important form of risk reduction for both aLIGO and A+.

- **Seismic Isolation Systems:** All three stages of development envisioned here (A+, Voyager and Cosmic Explorer) take advantage of the active Internal Seismic Isolation (ISI) system developed for aLIGO. Although the ISI is designed to support a payload of multiple aLIGO suspensions, detailed mass budgets will be necessary to confirm their fitness. In any case, ISI performance can benefit from improved **vertical inertial sensor** development, and improved position sensors. These upgrades are **not** intended to decrease in-band seismic noise, but rather to reduce the RMS motion of the ISI platform and minimize noise injection at the suspension resonances (in the 0.2 - 1Hz band).

- **Auxiliary Optics:** Stray light control will need to be reevaluated for A+ due to its increased sensitivity. Arm Length Stabilization (ALS) system may need to be redesigned to reduce complexity, possibly by injecting 532 nm lasers from the corner station.

- **Optical Coating Quality:** Study of the three sources of optical loss related to the coatings (coating thickness non-uniformity which leads to figure error, prompt scattering from micro-roughness and scattering from "inclusions" or "defects" in the coatings) will be necessary for A+ to succeed. This is due to the increased sensitivity of the instrument, making scattered light a bigger problem.

- **Charge Mitigation:** Charges on the test-masses are a potentially limiting noise source for aLIGO and future upgrades. Both as risk reduction for aLIGO, and to allow for the improved sensitivity of A+, research related to minimizing charging of (or removing charge from) the test-masses is of interest.

- **Lasers:** The A+ design does not require higher power than aLIGO, but improvements in the PSL design which minimize noise couplings will be very advantageous.

3.2 Voyager

In January of 2012 the LIGO Scientific Collaboration (LSC) Instrument Science Working Groups held a workshop to begin studying designs for third generation interferometers to be installed at the existing LIGO sites. Subsequent studies of 3 straw-man designs (known as the Red, Green and Blue designs) showed that all of the designs shared many common requirements, some of which are anticipated in the A+ design described in the previous section. The most promising of the 3 straw-man designs has been dubbed "Voyager", and adopted as the target of a the next major upgrade to the existing facilities.

While not indented to exclude other options, a straw-man design for Voyager is used to understand potential benefits and expenses involved in upgrading beyond A+. The Voyager straw-man design mitigates limiting noises of aLIGO by replacing the glass mirrors and suspensions with silicon parts, and operating a detector at cryogenic temperature of 123 K. The Voyager noise budget and the corresponding sensitivity described in this section are shown in Figure ??.

The main design features of the proposed cryogenic Voyager design are

- **Large cryogenic Silicon mirror:** In order to obtain broadband improvement of the sensitivity, 200 kg Silicon mirrors at the operating temperature of 123 K are considered.

- **Silicon cryogenic suspension:** Silicon ribbons (and perhaps blade springs) in the final stage suspension at 123 K are employed.

- **Suspensions:** The Voyager design will require new quadruple suspension systems (SUS) designed to support heavier test masses. In addition to supporting a heavier mass, the redesign efforts should also fix any features found to hinder aLIGO operation (e.g., bounce and roll mode damping, violin mode actuation, gas damping noise, etc.).

- **Newtonian noise:** Newtonian noise subtraction with seismometer arrays is included in the Voyager design, which assumes a factor of 10 suppression.

- **High power 2000 nm laser:** 2000 nm wavelength lasers operating at 200 W are employed. Arm cavity powers will reach 3 MW.

- **Coating Thermal Noise:** The beam spot size is increased by $\sim 25\%$ relative to the aLIGO size to avoid optical stability issues and the baseline coating is assumed to be amorphous silicon / amorphous silica.

- **Quantum noise:** Squeezed light injection (10 dB) and a 300 m filter cavity for frequency dependent squeeze angle is assumed.

This configuration and its challenges are described in detail in T1400226. The move to the longer wavelength, motivated by the need for higher thermal conductivity to transport heat away from the optics, along with cryogenic operation offer the wide range of interesting research areas, listed below. **Note that while the wavelength is specified as 2000 nm herein, wavelengths of 1.8-2.1 μm are being considered.** The final choice of wavelength will depend on the material properties of silicon, the availability of stable high-power lasers, and the quantum efficiency of photodetectors, among other things.

3.3   Cosmic Explorer: New Facility

The current facilities, while extraordinary in their capabilities, present significant limitations to gravitational wave astrophysics. In particular, the length of the detectors is well below the optimal value of about 50 km, and the L-shaped vacuum enclosure only allows for the detection of one polarization of gravitational wave signal. A longer, triangular detector would relieve both of these constraints; making an order of magnitude improvement in sensitivity possible, and allowing for both gravitational wave polarizations to be measured with a single detector.

The sensitivity curves presented in figure 9 are computed for a 40 km long detector using A+ technology (CE1) and Voyager technology (CE2). The astrophysical range of such a detector is shown in figure 8. Note that due to the detector's sensitivity to signals from most
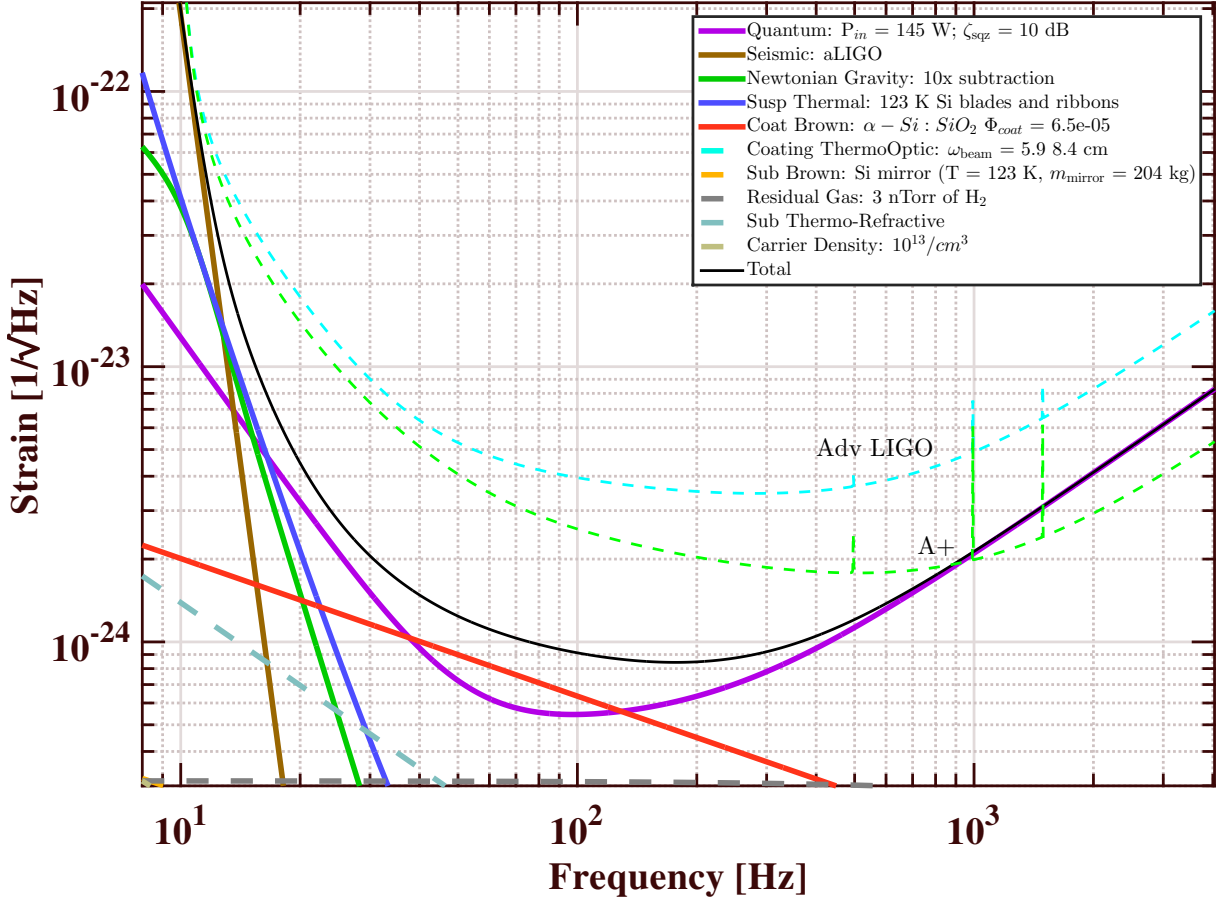
Figure 7: Strain Sensitivity of LIGO Voyager. $200\,\mathrm{kg}$ silicon test masses at $123\,\mathrm{K}$, and $3\,\mathrm{MW}$ of arm cavity power. See https://dcc.ligo.org/LIGO-T1400226 for more details.

of the visible universe, it is necessary to express the range of such an instrument in terms of redshift at the detection horizon.

The designs used to create the CE sensitivity curves in figure 9 make use of existing technology, or well defined extrapolations of existing technology, as a means of computing a *lower limit* to what can be done in a new facility. This should not be interpreted as a design target: LIGO Cosmic Explorer will make use of the best technology available in time for the final design process. This will certainly incorporate the results of Voyager R&D as well as other technological developments that occur in the intervening years (see figure 2). The design concept presented here should drive and not limit research into detector technologies and topologies useful in a very long baseline facility.

Comparison Table 3 shows the comparison of the key parameters of the three detector designs (A+, Voyager amd Cosmic Explorer). Figure **??** shows the comparison of the CE sensitivity curves to the Einstein Telescope sensitivity, and nominal aLIGO.

IFO Cases	aLIGO	A+	Voyager	CE (pess)	CE
Arm Length [km]	4	4	4	40	40
Mirror Mass [kg]	40	80	200	320	320
Mirror Material	Silica	Silica	Silicon	Silica	Silicon
Mirror Temp [K]	295	295	123	295	123
Sus Temp [K]	295	295	123	295	123
Sus Fiber	60cm SiO2	60cm SiO2	60 cm Si	1.2m SiO2	1.2m Si
Fiber Type	Fiber	Fiber	Ribbon	Fiber	Ribbon
Input Power [W]	125	125	140	150	220
Arm Power [kW]	710	1150	3000	1400	2000
Wavelength [nm]	1064	1064	2000	1064	1550
NN Suppression	1	1	10	10	10
Beam Size [cm]	5.5 / 6.2	5.5 / 6.2	5.8 / 8.4	12 / 12	14 / 14
SQZ Factor [dB]	0	6	8	10	10
F. C. Length [m]	none	16	300	4000	4000

Table 3: Baseline parameters for aLIGO and the other configurations

3.4 Interferometer Sensing and Control

The Interferometer Sensing and Control (ISC) consists of three areas (LSC, ASC, and TCS). In addition to these, general remarks about the control systems and the interferometer simulations are made in the AIC context.

The dominant issue of ISC is to maintain IFO stability while not introducing control noise. The following is an overview of the three subsystems:

Length Sensing and Control (LSC): The LSC manages the interference conditions of the fundamental mode in the interferometer in order to maintain a high sensitivity to GWs. The longitudinal distances between the mirrors are adjusted so that they fulfill particular interference conditions.

Alignment Sensing and Control (ASC): The ASC primarily controls the 1st-order optical modes in the interferometer by adjusting the angular orientation of the mirrors. In addition to the LSC, this system is also necessary to maintain interferometer sensitivity. Although the angular motion of the mirrors are locally stabilized by the vibration isolation and the suspension systems, the global control is necessary in order to realize stable interferometer operation.

Thermal Compensation System (TCS): The TCS controls the higher-order modes in the interferometer. The importance of the TCS, and our understanding of it, has been increasing with increasing circulating power in first generation detectors and their enhancements. The sensing of thermal aberrations, which lead to higher-order mode production and instability of interferometer control, is discussed below while the TCS actuators are described in Section 3.4.3.

Horizon and 10, 50 and 75 % confidence levels
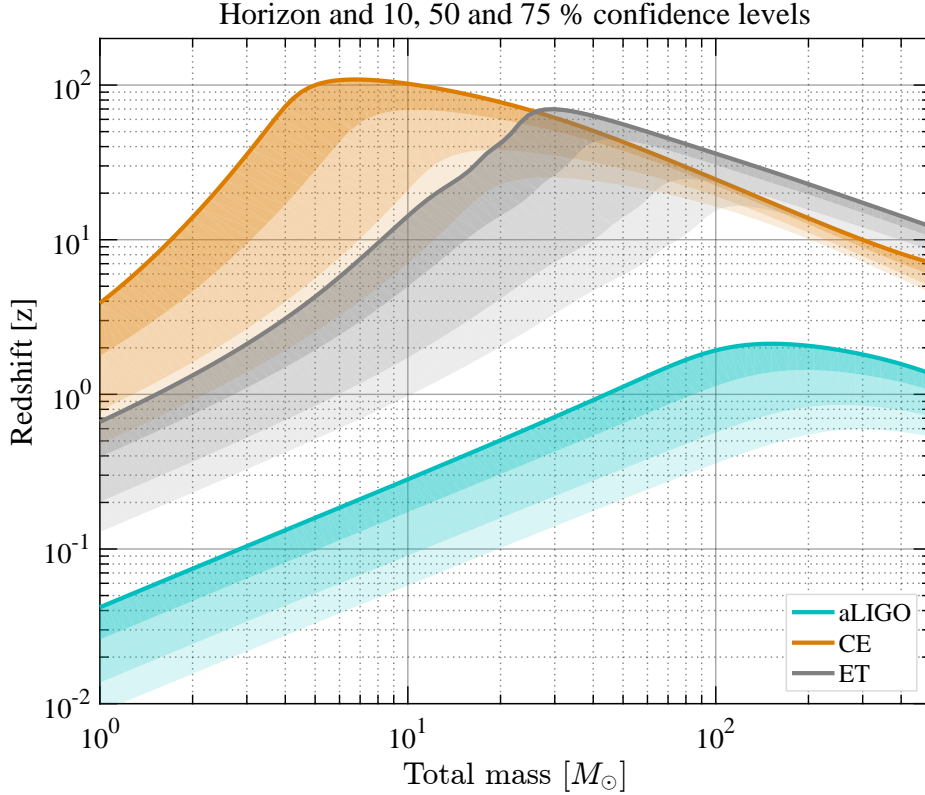
Figure 8: Astrophysical reach of Cosmic Explorer for equal-mass (non-spinning) compact binary inspiral systems. The maximum observable distance is shown as a function of the total intrinsic mass of the system. Baring a large number of primordial black holes, at redshifts larger than $z \simeq 10$ there will be few sources. Thus a horizon of $z > 20$ for a given mass should be taken to indicate that essentially *all* compact binary coalescence in the universe will be observable by a network of similar detectors, many with a high signal to noise ratio. Similar curves for the Einstein Telescope are shown for comparison (see figure 9 for relevant sensitivity curves). A Hubble constant of 67.9 km/s/Mpc and a ΛCDM model of expansion was assumed.

3.4.1 Length Sensing and Control

The Advanced LIGO interferometers consist of five coupled cavities that must resonate simultaneously to reach the operating point. The LSC receives the length sensing signals from the photodiodes and sends them to the actuators on the suspensions so that those five degrees of freedom stay at the operating point. Between the sensing and the actuation, the signals are processed by servo filters so that stable feedback control of each loop is established. The LSC system for the Voyager and Cosmic Explorer detectors will also rest on the above technologies.

The aLIGO LSC employs a combination of RF heterodyne detection and DC readout [26]. This RF sensing scheme comprises the Pound-Drever-Hall technique, Schnupp modulation,
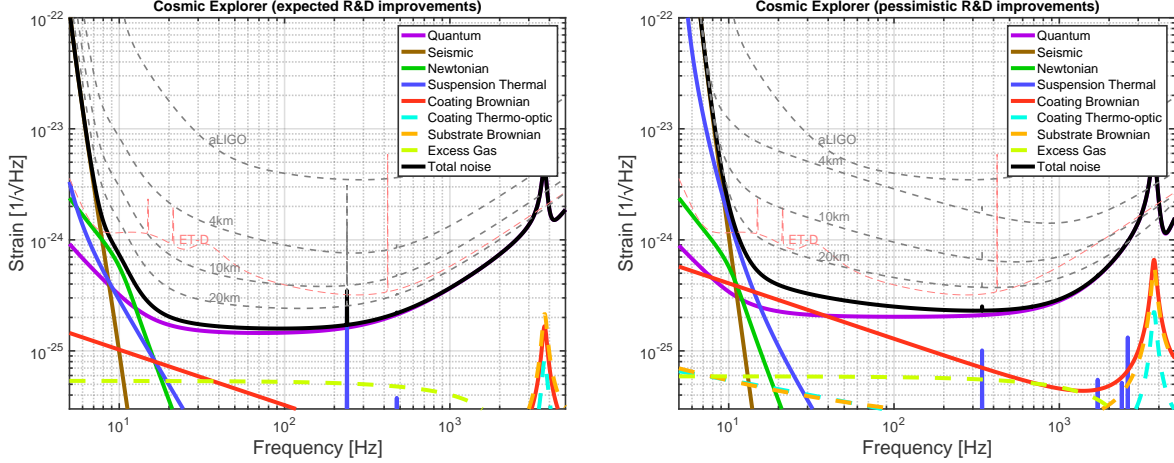
Figure 9: Cosmic Explorer based on Voyager technology (left) has a BNS range of 4.2 Gpc (comoving) and will be able to detect more than 10% of BNS mergers at $z = 5$. A more pessimistic CE design (right), based largely on A+ under the very conservative assumption that little improvement is made in coating technology in the next 20 years, serves as a lower bound to the performance of a new facility (BNS range of 3 Gpc and 10% detection at $z = 2$). Binary black hole mergers like GW150914 will be detectable with high SNR out $z \sim 20$. Sensitivity curves for shorter interferometers using similar technology are shown in grey, with coating thermal noise becoming strongly dominant for short detectors. The aLIGO and ET-D sensitivity curves are shown for reference.

and third harmonic demodulation technique [27] as a baseline design. The DC readout scheme provides sensing of the GW signal with shot noise performance superior to that of RF detection, along with more immunity to laser noises when combined with an Output Mode Cleaner (OMC). DC readout also clears the way for the use of squeezed light injection to reduce quantum noise (see section 4).

These sensing techniques have been independently demonstrated by the Enhanced LIGO [5, 28] and GEO600 [29, 30] interferometers, and other prototype interferometers [31, 32, 33]. The task for the aLIGO interferometer commissioning team is to integrate these well known techniques and find any hidden issues. As a scale model of the full aLIGO interferometers, the Caltech 40m prototype plays an important role in this effort by giving us a first look at potential problems.

An example of an upcoming ISC challenge is the filter cavity which will be required for filtering squeezed light before it enters the interferometer. This cavity will require length control via a carrier frequency which is not the same as the carrier light circulating in the interferometer (to avoid polluting the squeezed state with scattered photons). The filter cavity will also present an alignment control problem similar to the input mode-cleaner. Similarly, the phase of squeezed light source itself must be controlled with respect to the interferometer.

For LIGO Cosmic Explorer, the idea of the Suspension Point Interferometer [34] may also be investigated as it could be a practical solution to mitigate the vibrational noise caused by the heat link of the cryogenic cooling system.

Lock acquisition   A new feature of the aLIGO LSC is the use of independent laser sources in the Arm Length Stabilization (ALS) system [35, 36, 37]. This system enable us to lock the long arm cavities in a deterministic way with the guidance of auxiliary beams injected from the end mirrors.

Advanced LIGO will achieve lock using two single arm interferometers to control the arm cavity mirrors independently of the Michelson and signal recycling cavities, known as Arm Length Stabilization (ALS). The arm cavity locking uses frequency-doubled lasers at each end station, with each laser frequency referenced to the master laser in the vertex.

It may be possible to significantly improve the robustness of the ALS system by injecting the frequency doubled laser beams from the vertex.

High power photo-detection   Unlike previous generations of interferometers, the Advanced LIGO, Voyager, and LIGO Cosmic Explorer interferometers will detect substantial amounts of DC photocurrent at signal frequencies as low as 10 Hz. In this region, photodiodes are subject to excess 1/f noise that degrades their performance. Research to characterize, understand, and improve upon photodiodes will be necessary to detect the signals from high power interferometers.

In addition to the DC photocurrent, the RF power received by the RF detectors will also increase. Increasing the SNR in the RF detectors will directly reduce the auxiliary controls noise (a limit in nearly all GW interferometers) and so needs to be explored carefully.

Output Mode-Cleaner   Future interferometers use high finesse mode cleaning cavities to prepare the input laser beam for use in the interferometer and to ensure that the output photodetectors sense only the interferometer's fundamental spatial mode.

The mode matching between the interferometer and the OMC is particularly critical for future interferometers in which loses will be critical, as discussed in the next paragraph. Output mode matching presents a particular difficulty as it varies with the interferometer thermal state. Current research explores the use of deformable mirrors for adaptive mode matching, together with "Bull's Eye" wavefront sensing for measurement [38].

Balanced Homodyne Detection for DARM   To measure high levels of squeezing, allow for a tunable homodyne readout angle, and to avoid a variety of technical noises it would be advantageous to move away from DC readout for the interferometer's primary output (DARM). Balanced homodyne readout, standard practice in tabletop squeezing experiments, offers many advantages over DC readout (see P1100202, P1300184 and P1500091).

3.4.2   Alignment Sensing and Control

Sidles-Sigg instability   High circulating power in a kilometer-scale Fabry-Perot cavity can lead to an alignment instability in which a radiation pressure driven anti-spring overcomes the mechanical restoring force of the cavity's suspended optics (Sidles-Sigg instability) [22]. The Advanced LIGO interferometers were designed to avoid instability, but this is still a

potential threat for the Voyager/Cosmic Explorer detectors. Essentially, higher power leads to greater instability which can only be suppressed with high-bandwidth active alignment control. As the bandwidth of the ASC loops approaches the gravitational-wave band of the detector, noise from the alignment control signals is introduced into the detection band and can spoil the interferometer sensitivity. The investigations to mitigate this instability should be carried out in both practical and innovative aspects: reduction of the control noise level of the ASC system and exploration of any new scheme to directly suppress the instability (e.g., optical trapping of alignment degrees of freedom).

Towards ASC of Voyager/Cosmic Explorer detectors As the optical system incorporates more components, the Alignment Control System gets increasingly complicated. Already in current interferometers, we will be required to develop new techniques to control the alignment of the OMC [39], the squeezed light source, and the filter cavities, in addition to the already complicated ASC of the main interferometer.

The higher power operation of the interferometer in future detectors will involve coupling of the higher order modes into the field content at the dark port. This coupling will depend on the angular motion of the mirrors and will make the ASC requirements more stringent. To address the issue, deep investigation of the interferometer behavior with simulation is required in the design phase.

Historically, the control noise of the ASC system has consistently been one of the main limiting technical noises in the low frequency band for all interferometric gravitational wave detectors. As the band of gravitational-wave detection moves down, and the bandwidth of alignment control increases, both for suppressing higher-order modes and optical instability, the ASC problem becomes increasingly difficult.

3.4.3 Thermal aberration sensing and control

Mitigation It will be necessary to apply thermal compensation methods to stabilize the recycling cavities, due to thermal lensing in the input mirror substrates, and to maintain the radii of curvature of the test masses against thermo-elastic distortion effects resulting from circulating light absorbed in the mirror coatings. Both bulk and spatially-resolved compensation will be required [40].

One method to maintain a uniform temperature profile is by coating the barrel of the optic with a thin layer (a few microns) of a metal, or other thermal conductor, with high IR emissivity (e.g., gold). This technique is planned for the Advanced LIGO compensation plates, and it may be possible to expand it to other important optics, possibly including the test masses. Coating the barrel of optics has implications for other aspects of the design including thermal noise, charge mitigation, and parametric instabilities [41].

Another method for maintaining thermal uniformity is a scanning (or, more generally, a directed-beam) thermal compensation system that can vary the compensation profile in real time. Such systems can, in principal, offer precise thermal compensation, but come at the cost of additional control systems and related noises [42]. This will require research on carbon dioxide lasers, to reduce noise and possibly boost power, and on low-noise sensing

and actuation. A variety of techniques for beam direction (galvo mirrors, crossed AOMs, MEMs) will need to be investigated.

Local radiant heaters are used in interferometers to provide bulk curvature corrections to mirrors without injecting displacement noise (e.g., the aLIGO ring-heaters). These must have a uniform heating pattern at the mirror to minimize astigmatism. Future work on radiant heaters will improve the heaters' radiant uniformity and introduce tailored non-uniformities to account for non-axisymmetric features of the interferometer optics. Other future research would make the heaters more physically robust, and minimize their electrostatic interaction with the test masses [43].

Thermal aberrations can be corrected not only by adding heat to the mirror to flatten the heat pattern caused by absorbed interferometer light, but also by directly removing the heat from the absorbed interferometer light itself, through radiative cooling to a nearby cold surface. Such a technique has been proven in principle but not developed into a useful technique for high power interferometry.

Wavefront modeling The development of realistic models of the performance of the interferometers is also crucial to achieving the performance goals of Advanced LIGO and its upgrades. FFT-based simulation tools are currently used for setting requirements optical surfaces, coatings, apertures, etc., as well as for for investigating thermal effects [44]. Although FFT-based modeling is in principle more powerful than modal models based on sets of Hermite- or Laguerre-Gauss modes, the modal model codes are faster, and the results are easier to understand. Consequently, it is important to continue the development and support of modal models capable of including thermal loading in interferometers.

Wavefront diagnostics Each of the mirrors in Advanced LIGO will have slightly different absorption characteristics and therefore will react differently when subjected to laser powers projected for Advanced LIGO (see T1100250-v2 [45]) It is useful to develop methods that allow for remote monitoring of the condition of a test mass or beam splitters using optical wavefront sensing methods. On-axis and off-axis Hartmann wavefront sensing have been developed for measuring the absorption-induced wavefront distortion in the test masses and beam splitter. The measured noise limited sensitivity of the Hartmann sensor itself is $\lambda/15,000$, and experiments have measured wavefront changes smaller than $\lambda/3000$ [46]. When applied to off-axis tomographic measurements, the current measured accuracy is $\lambda/120$, limited by factors other than the Hartmann sensor itself [47]. Further research is aimed at improving this performance. Avenues for improvement include simple and stable injection schemes for Hartmann probe beams into working interferometers and incoherent probe beam sources with high power and low noise.

In addition to the Hartmann style sensors, we may use phase cameras (essentially multi-pixel RF Wavefront Sensors). These could be used to implement real-time wavefront correction. Primitive phase cameras have been used in iLIGO and iVirgo, but there were problems due to the scanning induced backscatter. Future phase cameras should allow for wavefront sensing of individual sidebands simultaneously without any moving parts.

3.4.4   General Control Issues

Fast data acquisition   Currently the data acquisition rate of LIGO CDS is limited to a sampling rate of typically 16 kHz to 64 kHz. For some specific purposes high speed data acquisition will add convenience for comissioning. In the first phase this can be a ring buffer to store the data for (for example) ∼10 min to catch lock acquisition/lost events or fast transient noise of laser intensity/frequency.

Adaptive Noise Cancellation   Adaptive noise cancellation techniques will be widely used in the Advanced LIGO interferometers and the future detectors. Basically, noise cancellation based on Wiener filters eliminates the noise in a target signal correlated to witness channels.

This family of techniques has a wide area of application such as seismic noise reduction, Newtonian noise subtraction, and magnetic/acoustic noise cancellation. Residual coupling of auxiliary LSC degrees of freedom to the main GW signals, which presented a sensitivity limit in the initial and Enhanced LIGO interferometers, may also be reduced by adaptive noise cancellation.

Up to now, a basic scheme with linear adaptive noise cancellation is being tested on the CDS system at the 40 m prototype [48]. This technique has also been applied to seismic noise subtraction during Enhanced LIGO [48]. In the future, in addition to the linear noise subtraction, subtraction of bilinear noise should also be investigated as it may prove useful in removing a variety of noise sources from the GW signal.

Automatic Optimization   As the interferometer configuration gets more complicated, the difficulty of optimizing system parameters increases significantly. For example, we have to deal with the different range and frequency dependence of the multiple sensors and actuators at each stage of the suspension and isolation system, as opposed to the single pendulum suspensions use in iLIGO. Optimization of hierarchical control will depend on the noise level of the interferometer, which may change in time, making the traditional approach of by-hand optimization untenable.

Many of the optimization procedures in the future interferometers will need to be automated within the interferometer control system, and some may need to be dynamically adjusted. This approach should be applied in Advanced LIGO and expanded in the future detectors with continuous effort toward automatic optimization or "machine learning". New involvement and collaboration with researchers of this particular field is encouraged.

Modern control   Along with adaptive noise cancellation and automatic optimization, other applications of modern control theory to interferometer gravitational wave detectors should be considered.

Feedback control of interferometer gravitational wave detectors has mostly relied on the classical control theory up to now. The classical control theory, developed in the 1950s, is still effective as one of the approaches for control applications. However, control theory has continued over the intervening 60 years and significant improvements to the classical

approach are available. Modern control theory, offers various possibilities to improve the interferometer control.

An example application of modern control theory is the modal-damping work done on the aLIGO suspensions at MIT [49]. The challenge faced in suspension control, and also elsewhere in aLIGO and similar detectors, is that of combining multiple sensor signals with a variety of noise levels and response functions to provide a controller which is effective in the control band while minimizing noise in the gravitational-wave detection band. The currently employed approach of classical controls requires experts to spend considerable time diagonalizing the system and constructing near-optimal (really just "good enough") filters for each degree of freedom of the system.

These technologies can be first investigated by simulation and then applied to prototype facilities. Once effectiveness of these advanced control is demonstrated, it can be implemented to the aLIGO interferometers in order to accelerate the interferometer optimization.

Virtual Interferometer The flexibility of the Advanced LIGO CDS system allows, for the first time, the beginnings of the "Virtual Interferometer".

Basically, the future detectors should have a computer facility which enables us to login and run the control system for the test of operating and diagnosing tests without having the actual detector equipment. At the beginning this can only be a tool for the commissioning and development, as seen in the "Simulated Plant" concept being tested at the 40m prototype [50], but eventually can provide various realtime test of the interferometer behavior by cooperative interaction with the other simulation tools. This should include the test of the online data production for mock data challenges.

3.4.5 Interferometer modeling / simulations

Interferometric gravitational-wave detectors are sufficiently complicated optical systems that detailed modeling is required for design and performance studies. At present, a variety of simulation tools exist for addressing the various problems encountered in interferometric GW detectors.

As mentioned previously in section 3.4.3, simulations which use the FFT for propagating paraxial beams can be used to make detailed predictions about the impact of optical phase errors (surface roughness, phase distortions, etc.) and finite aperture sizes. FFT simulations are, however, too slow to simulation interferometer dynamics, and are therefore only used to find steady-state solutions.

For understanding interferometer dynamics over a wide range of conditions which don't allow for linearization (e.g., not only at the operating point), time-domain simulation is the most appropriate tool. This type of simulation is important for lock acquisition studies and existing tools fill the need for most optical configurations [51]. However, like FFT simulations, despite considerable optimization effort time-domain simulations are slow and able to simulation only the lowest transverse-spatial modes.

For control system development, where we can assume that we are at a stable operating point

and linearize around that point, frequency domain simulations prove an invaluable tool. With the development of advanced detectors with more than 100 kW of power circulating in the arm cavities, radiation pressure effects have come to play an important role in interferometer dynamics (both for LSC and ASC, as mentioned above). Advanced LIGO control system development has depended on the Optickle simulation engine, which has been packaged for LSC design in Looptickle and later Lentickle, and for ASC design as Pickle.

In addition to control system development, frequency domain simulation tools like Optickle, are also used to compute limitations to interferometer sensitivity due to fundamental noise sources (e.g., quantum noise) and technical noises (e.g., auxiliary length degree of freedom control noise). Recent expansion of the Optickle to include the non-linear optics used in squeezed light sources allows for more complete modeling of aLIGO and future detectors.

The configuration level simulation, discussed in section 4.6, operates at a higher level in that the response of a given optical configuration is symbolically computed and parameterized [52]. These symbolic computations can be compared with the more detailed numerical results given by frequency domain codes. While inappropriate for detailed simulation of the optical plant, this approach is very effective for optimizing plant parameters and even selecting among a variety of optical configurations. Further development of the GWINC configuration level simulation to accommodate the variety of optical configurations under consideration for future detectors will aid in downselection and optimization.

To date these simulations have focused on the core of the interferometer, the optics, and have largely neglected the surrounding mechanical systems. A missing piece in detector simulation is a comprehensive mechanical simulation tool for the vibration isolation and suspension design which includes the capability to handle a variety of mechanical systems and the ability to compute of thermal noise for any given configuration.

In addition development of the various of simulation tools, future detector design and study will benefit greatly from a dedicated effort to organize and document these tools. At present, each simulation tool has a different user interface and while there are many similarities in the parameters required, the format in which these parameters are presented differs from one tool to the next. This divergence of parameter formats and lack of high level organization in the simulation effort inevitably slows progress toward the development of future detectors.

Modelling thermal distortions and radiation pressure during commissioning Advanced LIGO and future detectors will operate at higher light power so that thermal distortions of the optics and the change of the mirror suspension response due to radiation pressure will play a dominant role. In particular the transfer functions of any displacement signal into the detection ports will show the optical spring effects and higher-order mode resonances. Thus to model noise coupling of auxiliary degrees of freedom or auxiliary optics system into the gravitational wave channel we require models that include thermal effects and radiation pressure at the same time. For the rapid development of the control systems and noise mitigation strategies during the detector commissioning it is desirable that such simulation software is a fast, flexible and easy to use tool.

4 Quantum Noise Limits

4.1 Introduction

The 2nd generation detectors, which are now being pushed towards design sensitivity (Advanced LIGO) or being assembled (Advanced Virgo, and KAGRA), are expected to be limited by quantum noise over nearly the entire GW band (10 - 10000 Hz). By quantum noise, we refer to the quantum uncertainty of the electro-magnetic field at Fourier (sideband) frequencies in the GW detection band which beat with the laser field to produce shot noise (quantum measurement noise) and radiation pressure noise (quantum back-action noise). By modifying the sideband spectrum of the quantum-noise phase-space distribution regimes dominated by shot noise and regimes dominated by radiation pressure noise can be reduced (squeezed) simultaneously.

To upgrade those detectors it is essential to reduce the quantum noise. In this section techniques are discussed that go beyond scaling-up the carrier light power and the test masses, which reduce the effect of quantum noise in a 'classical' way. There are several 'nonclassical' configurations that have been proposed within the community [53, 54]. They generally fall into the following three categories:

1. Injection of squeezed vacuum states of light into the signal output port [55, 56];

2. Using coherent feedback to modify the dynamics of the test masses, e.g. the optical spring effect associated with the detuned signal recycling [57];

3. Reading out a quantity that is proportional to the test mass speed at low frequencies [58, 59, 60, 61, 62].

They all require, to a certain extent, introducing additional optics and increasing the complexity of the detectors. Injection of squeezed vacuum states of light has been realized in GEO 600 and was tested in one of the LIGO detectors. In both cases only the shot noise was targeted, since radiation pressure noise was not an issue. This will change in all future GW detectors. They will require filter cavities to avoid radiation pressure noise that is increased due to shot noise squeezing.

Modifying the dynamics of the test masses turns the detector into an opto-mechanical measurement device that uses dynamical back-action between test mass position and radiation pressure of light. In case of detuned signal recycling damping an opto-mechanical instability occurs that needs to be damped.

Changing the detector such that test mass speed is measured instead of test mass position reduces radiation pressure noise at low frequencies and can be realized in various ways. 'Variational readout' [58, 63] uses a frequency dependent readout quadrature thereby making use of ponderomotive squeezing; 'injection of multiple carrier light fields' allows the independent measurement of the radiation pressure driven test mass motion,[64, 65]; and a 'speed meter topology' such as the Sagnac interferometer achieves this goal in the most straight forward way, without filter cavities and without multiple carrier light.

The three categories are not mutually exclusive and can be combined in different ways. In particular the injection of squeezed states can be combined efficiently with all other concepts. Squeezed state injection, in its simplest form, is the only concept that has been used to upgrade an operating GW detector. GEO 600 has been using squeezed light for the reduction of shot noise since 2010 [6]. This configuration, completed by filter cavities for the generation of frequency dependent squeezing and the mitigation of radiation pressure noise, is thus a potential technique for A+ and Voyager and beyond. All other configurations are potentially implementable on LIGO Cosmic Explorer but are too immature to be considered for A+ or Voyager. Intensive research and development is needed.

The following sections focus on those technqiues which modify quantum noise, independent of the interferometer topology. General enhancements of the signal to quantum noise ratio due to the topology are discussed in section 4.6.

4.2 Crystal based squeezed light sources

Great progress has been made over the last 10 years in the generation of vacuum squeezed light.

1. Both ANU and AEI, using cavity enhanced optical parametric down-conversion (PDC), also called sub-threshold optical parametric oscillation (OPO) have measured squeezing of around 10 dB down to 10 Hz at 1064 nm. The AEI has observed greater than 12 dB at MHz frequencies at both 1064 nm and 1550 nm. Recently, the AEI together with the ILP Hamburg observed 15 dB of squeezing at 1064 nm at MHz frequencies [66].

2. GEO 600 has been operated now for many months [6] at a time regularly observing more then 3.5 dB sensitivity improvement with a highest value above 4 dB.

3. An ANU designed squeezer was installed on the LIGO H1 detector operating in the S6 configuration. Sensitivity enhancement was observed above 200 Hz with 2.1 dB improvement above a few hundred Hertz. Importantly, no excess noise was seen below 200 Hz and no additional glitching was found.

4. Photodiodes with quantum efficiency in excess of 0.99 are now available [66].

Any absorption/scattering between the squeezed state generator and detection reduces the level of squeezing. Starting with a suitable source of squeezed light, Table 10 presents a comprehensive list of potential loss sources along with levels required to observe 6 dB, 10 dB and 15 dB of quantum noise reduction. The final column of the table presents the numbers achieved during the H1 squeezing test. The numbers are presented in terms of efficiencies (= (1 - minus) loss as a percentage). A filter cavity (see section 4.6.1) is needed to achieve broadband quantum noise suppression or to at least reduce the squeezing ellipse to a coherent state at frequencies where shot noise does not dominate.

10 dB and eventually 15 dB quantum noise suppression will require significant effort to reduce Faraday isolator loss (cf. section 7.1.2), increase OMC transmission and tweak PD

	Loss source	H1 experiment	Near term goal (6dB)	Longer term goal (10 dB)	Dreaming(15dB)
1	OPO escape efficiency	96%	98%	99%	99.8%
2	Injection path optics	80%	99.7%	99.7%	99.99%
3	viewport	99.8%	99.8%	99.8%	99.99%
4	3 faraday passes	94%, 94%, unknown	97% each (aLIGO input Faradays)	99% each	99.7 % each
7	RF pick off beamsplitter (beam for ISCT4)	98.8%	99%	99.5%	99.8%
5	Reflection off of Signal recycling cavity@100 Hz	arm cavity and michelson =98%	97.5%(Tsrm=35%)	99.2% (Tsrm=50%)	99.5%
6	Circulator for filter cavity	NA	98%	99.5%	99.8%
8	Squeezer mode matching to OMC	71% (inferred from total)	96%	98%	99.7%
10	OMC transmission	82%	97%	99.5%	99.7%
11	QE of PDs		99%	99.7%	99.99%
	Total efficiency (escape * detection)	40-45%	77.6%	91.3%	97.4%
	Total phase noise allowable		17mrad	7 mrad	2.5 mrad
	Measured squeezing (dB)		6	10	15.25

For numbers in the H1 column- red numbers were measured during the experiment, numbers in black were made before installing components or estimates of losses that were too small compared to the total to measure accurately with the uncertainty in our measurements.

Figure 10: Table 11 Maximum acceptable losses to achieve 6 dB, 10 dB and 15 dB of observed quantum enhancement. From Dwyer [67]
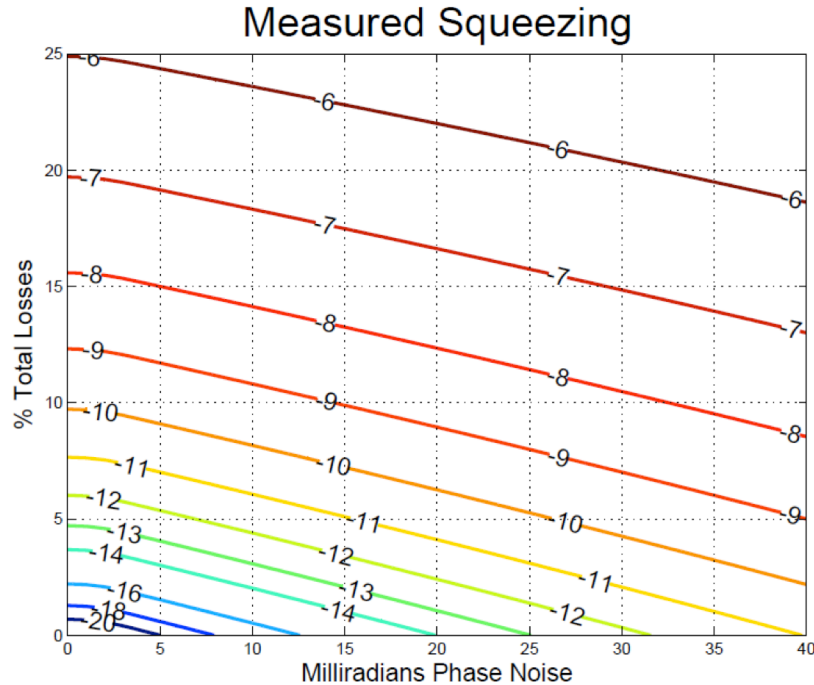
Figure 11: Measured squeezing for different values of total losses (the product of escape efficiency and detection efficiency) and total phase noise. For each value of phase noise, the non linear gain in the OPO is optimized to maximize the measured squeezing, but the nonlinear gain is capped at 90, (pump power at 80% of threshold). Operating the OPO closer to threshold doesnt improve the measured squeezing very much, but could make stable operation of the squeezer difficult. From Dwyer [67]

quantum efficiency. An escape efficiency of 99% is required. Currently the ANU squeezer operates with an escape efficiency of 98.5%.

As the level of squeezing is increased the requirement on stability of the squeeze phase angle is increased. As the phase angle rotates away from the optimum squeezing quadrature the level of squeezing available for quantum noise reduction is reduced. In the presence of phase fluctuations in the squeeze angle the average squeezing level is reduced. The effect gets worse as the ratio of the major to minor axes of the squeezed ellipse increases ie as the level of squeezing increases. The tolerance on phase noise will therefore decrease as total losses decrease. This is depicted in Fig. 11 where measured squeezing loci are plotted for different values of total loss and total phase noise.

An additional issue is backscattering. In the sub-100 Hz frequency range, interferometers and squeezers are particularly sensitive to scattered light. If scattered light from the interferometer seeds the squeezer noise will be generated. Scattered light reflected back off the squeezer which re-enters the made mode of the interferometer will add noise to the measurement. Effects can be mitigated by adding Faraday isolators or by using a squeezing geometry which has a level of immunity to backscatter.

4.2.1 Optical Loss in Filter Cavities

The filter cavity concept is outlined in 4.6.1. Also see AIC.

Optical losses might become more important when squeezing is used, or when internal ponderomotive squeezing is employed for sensitivity improvement (e.g. in schemes with output filtering).

The effect of losses is further amplified if back-action evasion is required, in which case the signal strength in the quadrature being detected is significantly less than conventional situations. A rule of thumb for this limitation is available from Kimble et al. [58], where we have

$$\sqrt{S_h/S_h^{\text{SQL}}} \geq (e^{-2q}\mathcal{E})^{-1/4} \tag{1}$$

where $\mathcal{E}$ is the power loss, and e^{-2q} is the power squeezing factor. Assuming $\mathcal{E}$ to be 0.01, and 10 dB squeezing, we have a SQL-beating limit of 0.18.

For a given filter bandwidth γ_{filter} (to be determined by the needs of input/output filtering), when realized by a cavity of length L, the total loss $\mathcal{E}$ is determined by

$$\mathcal{E} = \frac{4\epsilon}{T} = \frac{\epsilon c}{\gamma_{\text{filter}} L} \tag{2}$$

where T is the input-mirror power transmissivity [related to bandwidth by $\gamma_{\text{filter}} = Tc/(4L)$] and ϵ is the loss per round-trip. It is therefore the ratio ϵ/L that determines the goodness of the filter. Since the per-round-trip loss ϵ depends on the beam spot size, which in turn depends on L, an optimization is need to find out the optimal length and design of filter cavities [68].

Figure 13 shows the effect of round-trip loss on the degradation of squeezing for a filter cavity with 22 Hz detuning and bandwidth. The colors correspond to the quantum-noise spectral
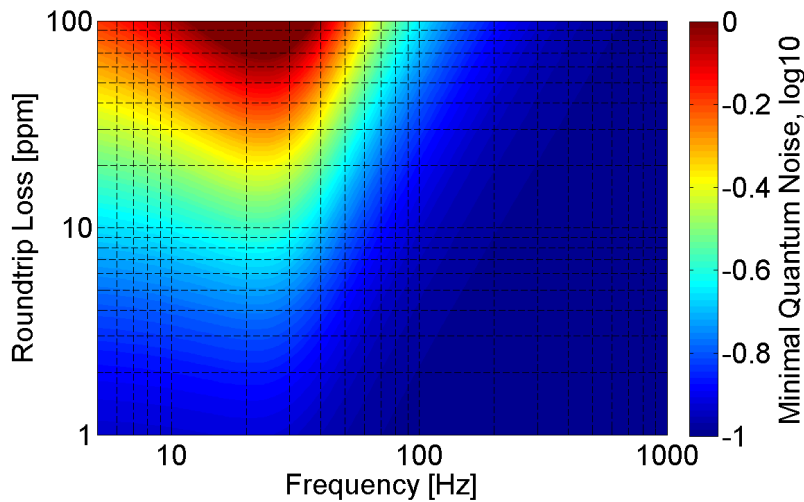
Figure 12: Degradation of 10 dB external squeezing reflected from a 300 m filter cavity as function of round-trip loss (in addition to input transmission) and frequency.

density along the minor axis of the noise ellipse relative to coherent vacuum noise. It can

be seen that round-trip loss over 50 ppm degrades the squeezing to a level comparable to coherent vacuum around frequencies near the filter resonance. Here and in the following, round-trip loss are considered excluding the transmission of the input mirror. The input transmission is comparatively large (about 550 ppm for the filter calculation of Fig. 13) and does not directly contribute to squeezing degradation. Round-trip loss is dominated by optical scatter loss from imperfect mirrors in combination with finite aperture size. The goal is to minimize scatter loss.

Scatter loss in cavities is determined by properties of the individual mirrors such as mirror size, mirror curvature, mirror surface abberations and defects, and by the optical path length of the cavity. Scatter loss in cavities is not fully understood yet. A concerted effort of high-finesse cavity experiments, scattering measurements, numerical simulations and theoretical work is required to form a consistent picture between loss models and observations. Practically speaking, ultra-low losses (around 1 ppm) have been achieved on the mirrors of fixed cavities [69, 70]. However, the lowest loss measured on the large, test-mass-sized beams are more usually in the 50-100 ppm range. FFT simulations have shown that the loss for large beams is dominated by the large scale figure error of the substrate, while the losses for small beams are dominated by point defects in the coatings. Since the low frequency performance of the QND schemes so strongly depends on the loss for intermediate sized (∼mm) beams, it is vitally important to develop ultra-low loss mirrors for this beam size. The modern polishing technology is already good enough.

Additional more specific problems that need to be investigated include small-angle scatter loss in cavities, coherent loss versus incoherent loss, and round-trip loss as a function of cavity aspect ratio. Coherent scatter loss designates the effect when the spatial pattern of higher-order modes resonating inside the cavity matches the pattern of light scattered from a mirror. In this case scattered light can build up resonantly provided that the overall loss in these higher-order modes is not too high. In general, higher-order modes experience more loss since they describe a wider spatial intensity distribution that directs additional light power beyond the mirror aperture compared to the target mode of the cavity, which is usually the Gaussian shaped TEM_{00} mode. For this reason it is also necessary to understand how much round-trip loss is influenced by the cavity aperture, or better by the cavity aspect ratio, which is the aperture divided by the cavity length. Coherent scatter loss can potentially lead to a significant increase of the total scatter loss, and it is no more describable by simple perturbative scatter models.

Losses in mirrors are also addressed in the Optics section 5.

4.3 A+

For A+ we propose the injection of frequency dependent squeezing at 1064 nm and a measured shot-noise squeezing of of up to 6 dB. A list of loss contribution that allows for 6 dB of squeezing is given. This list is input for other groups, in particular to "optics" and "AIC". From Table 10 it is likely that 6 dB is achievable. Reaching the design performance of the aLIGO input Faradays and the aLIGO OMC, careful modematching and using now available photodiodes with quantum efficiency (QE) > 99% should see 6 dB shot noise reduction using currently available squeezers.

From Table 10 we see that 6 dB noise reduction with a total efficency of 76.7% (losses less than 23controlled to better than 17 mrad. This is regularly achieved in small scale laboratory demonstrations. Operation of the squeezer in vacuum should enable thos to achived in A+, but this is yet to be demonsrtated.

R&D experimental tests include control system development for frequency dependent squeezing,sourcce and characterize low loss Faraday Isolators, mode-matching efficiency, Brillouin scattering, and phase noise.

4.4 Voyager

For Voyager we propose the injection of frequency dependent squeezing at 1550 nm and a measured shot-noise squeezing of up to 10 dB. A list of loss contribution that allows for 10 dB of squeezing is given Table 10. We see that the total efficiency required is 91.3% requiring phase noise to be controlled to better than 4.4 mrad. Achieving the levels of stability will likely require operating the squeezer inside the vacuum envelope. In vacuum operation has yet to be demonstrated. Smaller and more compact designs of squeezed light sources will also help to reduce phase noise.

R&D experimental tests: development of an audioband squeezed source of greater than 12 dB from 10Hz to10 kHz at 1550 nm; control system development for frequency dependent squeezing at 1550 nm, sourcing and characterize low loss Faraday Isolators at 1550 nm, mode-matching efficiency, Brillouin scattering, and phase noise. Basically the state of the art for 1064 nm needs to be achieved at 1550 nm. High levels of squeezing at 1550 nm have been demonstrated at the AEI, but not in the audioband.
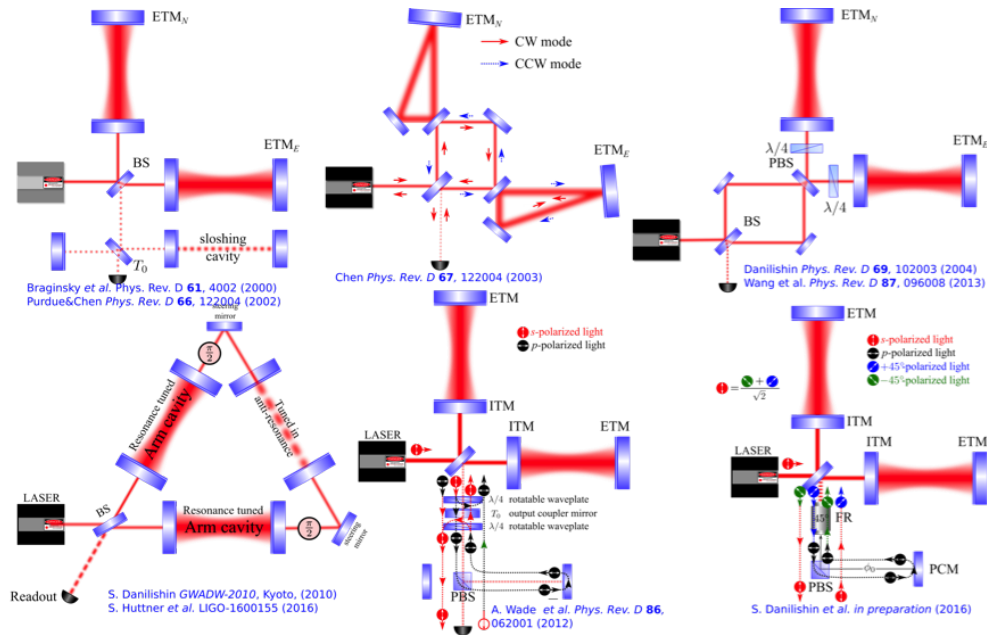
Figure 13: Different Incarnations of speed meters.

References: [1] Huttner, S.H. et al Candidates for a possible third-generation gravitational wave detector: comparison of ring-Sagnac and sloshing-Sagnac speedmeter interferometers

(LIGO-P1600155)

[2] Voronchev, N. V.; Tarabrin, S. P. and Danilishin, S. L. Broadband detuned Sagnac interferometer for future generation gravitational wave astronomy ArXiv e-prints, 2015, http://arxiv.org/abs/1503.01062

[3] Helge Mueller Ebhardt PhD thesis

4.5   LIGO Cosmic Explorer

The longer term goal of 15 dB observed quantum noise reduction is extremely ambitious. From Table 10 we see that the total efficiency required is 97.4% requiring phase noise to be controlled to better than 2.5 mrad! Loss tolerances on the isolators, OMC, modematching etc far exceed anything currently achieved. The most successful technique for generating high levels of low frequency, vacuum squeezed, light uses optical parametric oscillation (OPO). The current limitation arises from optical intra-cavity loss in the OPO cavity. Intra-cavity loss (separate from escape efficiency) is dominated by scattering from optical surfaces and absorption of the nonlinear crystal. Research and development into improved crystal fabrication technique, optical coatings and polishing, as well as particulate minimisation is needed. Further, improved temperature stability (preferably optically sensed) and positioning of the crystal interaction region is needed for phase matching and dual-wavelength dispersion compensation respectively. This will aid in accessing greater levels of squeezing. Finally, pump intensity stabilization will be needed.

Given the timeline for LIGO Cosmic Explorer the full list of quantum noise reduction concepts should be explored in addition to frequency depdendent squeezing and need to be extensively researched. The next section summarizes the currently proposed concepts.

Recently, a variety of new configurations featuring speedmeter characteristics have been invented (see Figure below). Some of these concepts offer on top of the improved quantum noise and relaxed requirements for filter cavities, also the possibility to reduce coating thermal noise [1] and the introduction of negative inertia [2, 3]. Individual design studies are required to evaluate the technical challenges, infrastructure requirements and various benefits of these configurations.

4.6   Review of Quantum Noise Manipulation techniques and Issues.

4.6.1   Frequency-dependent squeezing angle (input filtering)

The first scheme is 'frequency-dependent squeezing' (as discussed in the previous sections). This term refers to a broadband spectrum of squeezed vacuum states for which the squeeze angle is frequency dependent and optimized for the cancelation of back-action noise and for achieving the optimum signal to noise ratio. The frequency dependence of the squeeze angle can be achieved by reflecting off the squeezing spectrum from a detuned narrow band cavity. There might be other ways how the same frequency dependence can effectively be achieved. Research on alternatives might be very valuable for future gravitational-wave detectors.
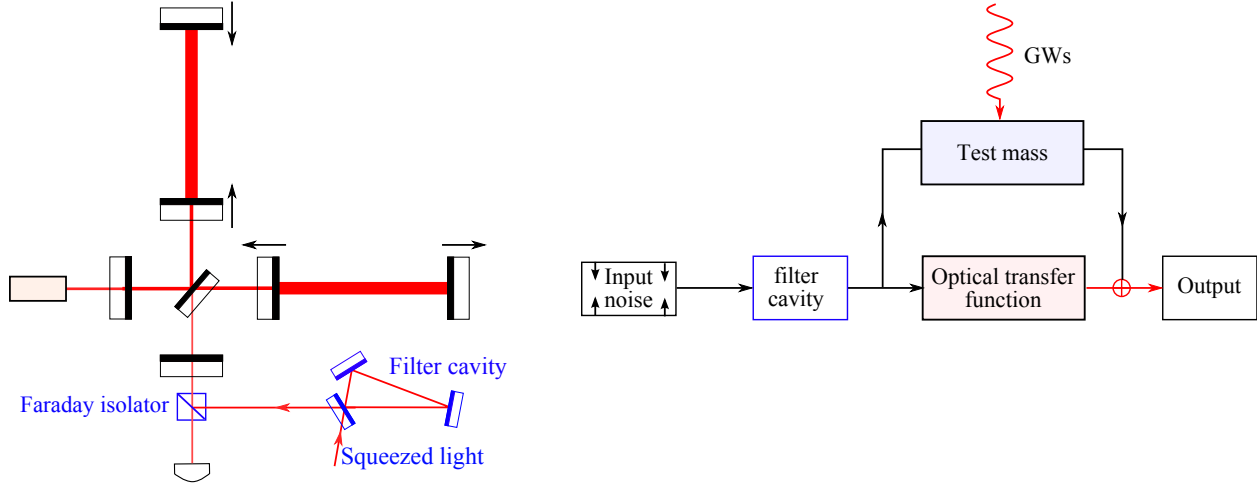
Figure 14: Schematics showing the frequency-dependent squeezing scheme (left) and its associated flow chart (right).

As shown schematically in Fig. 14, it utilizes an optical (filter) cavity to rotate the amplitude and phase quadratures, or equivalently the squeezing angle, in a frequency-dependent way. If the parameters of the filter cavity is appropriately specified, one can rotate the squeezing angle such that the quantum noise spectrum is reduced by an overall factor that is equal to squeezing factor.
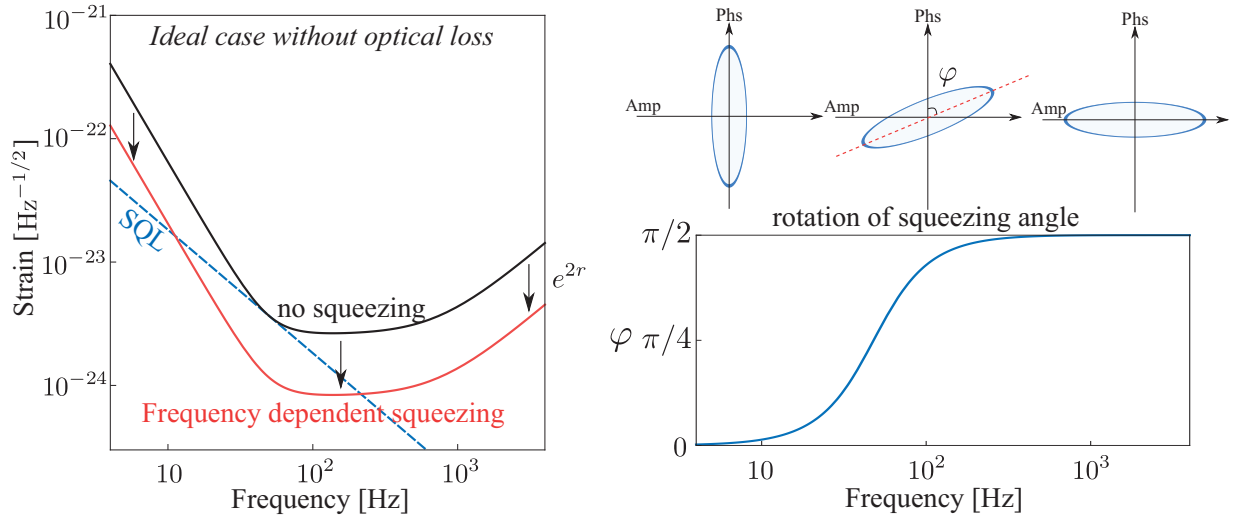
Figure 15: Noise spectrum for frequency-dependent squeezing (left) and rotation of the squeezing angle (right).

For illustration, in Fig. 15, we show the resulting noise spectrum in *the ideal case without optical loss*. As we can see, the squeezing angle rotates in such a way that at low frequencies the fluctuation in the amplitude quadrature is squeezed—thus reducing the radiation-pressure noise, while at high frequencies the phase quadrature is squeezed—thus reducing the shot noise. In order to achieve the desired rotation of squeezing angle, the filter cavity needs to have a bandwidth that is comparable to the detection bandwidth—this indicates a high-
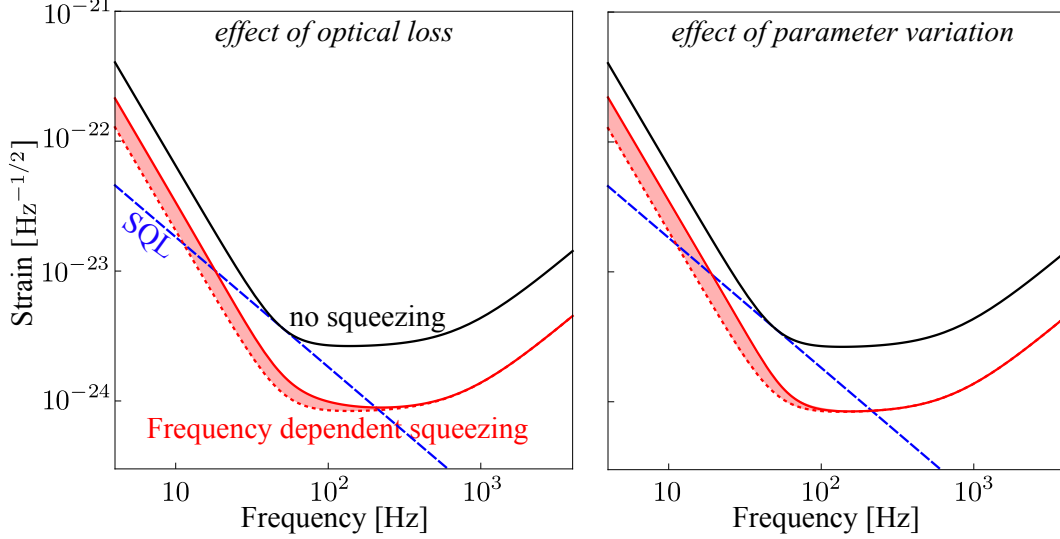
Figure 16: The effect of optical loss (left) and the parameter variation of the filter cavity (right) for input filtering. The shaded regions illustrate the degradation in sensitivity. Here we have assumed the total optical loss of 20% (round-trip loss multiplied by the number of bounces inside the cavity) and parameter variations of 10%.

finesse cavity is necessary if the cavity length is short. The specification for the filter cavity can almost be analytically calculated by using the method outlined in [61].

In reality, the optical loss will affect the performance of input filtering, as shown in the left panel of Fig. 16. Additionally, parameters of the filter cavity, in particular, the transmissivity of the mirrors and the detuning, cannot be exactly set to the optimal value, and their variation will influence the sensitivity in a similar manner to the optical loss, as illustrated in the right panel of Fig. 16.

4.6.2 Frequency dependent readout phase (output filtering)

A close related counterpart to the input filtering is the variational readout, and as shown schematically in Fig. 17, it uses an optical cavity to filter the detector output which allows one to measure different optical quadratures at different frequencies. The filter cavity has the same functionality as in the case of the frequency-dependent squeezing—the only difference is that it rotates the optical quadratures of the output instead of input. In the ideal case, this scheme can coherently cancel the radiation-pressure noise at low-frequencies, and give rise to a shot-noise only sensitivity [58]. In Fig. 18, we show the resulting noise spectrum in the ideal lossless case. In reality, due to the presence of optical loss and parameter variation of the filter cavity, such a cancelation cannot be perfect, as illustrated in Fig. 19.

As this technique leads to reduced signal (but increased signal/quantum noise) at low frequencies it is far more sensitive to optical losses compared with input filtering.
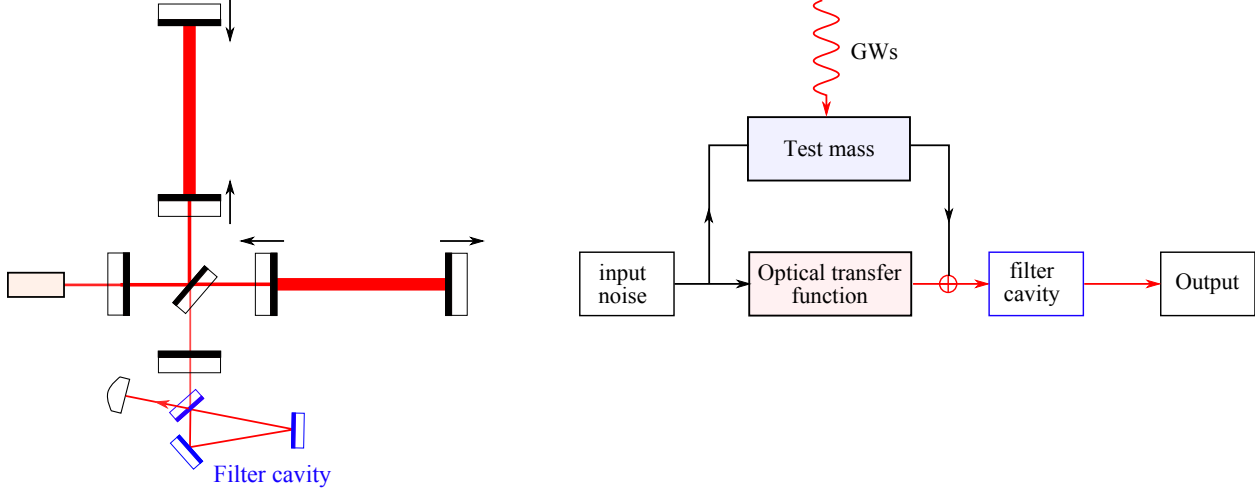
Figure 17: Schematics showing the frequency dependent (or variational) readout scheme (left) and its associated flow chart (right).
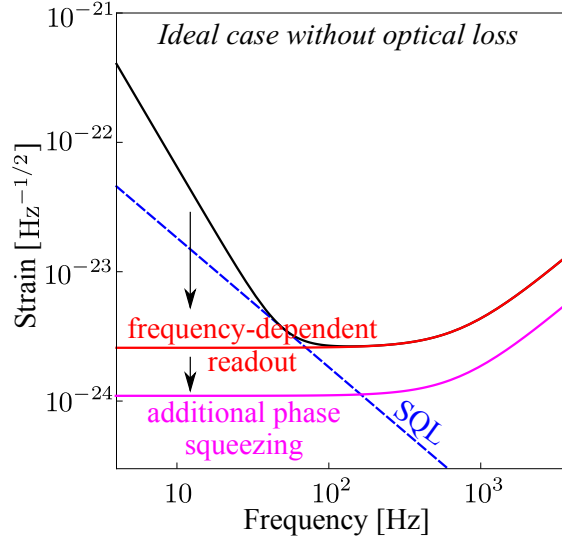
Figure 18: The noise spectrum for the frequency-dependent readout scheme.

4.6.3 Long signal-recycling cavity

In this subsection, we will discuss the long signal-recycling cavity scheme. As shown in Fig. 20, the signal recycling mirror is moved further away from the beam splitter compared with the aLIGO configuration. In the usual case when the beam splitter and the signal-recycling mirror are close to each other, the signal-recycling cavity is relatively short (order of 10 meters) and one can ignore the phase shift difference between different sidebands with frequency Ω ranging from 10 - 10000 Hz, namely $\Omega L_{\mathrm{sr}}/c \approx 0$ with L_{sr} being the signal-recycling cavity length. We can therefore treat the signal-recycling cavity as an effective compound mirror with complex transmissivity and reflectivity, which is the approach applied in Ref. [71]. With a long signal-recycling cavity, however, $\Omega L_{\mathrm{sr}}/c$ is not negligible and different sidebands pick up different phase shifts. After taking into account this fact, one can then apply the standard procedure to derive the input-output relation for this scheme. The final
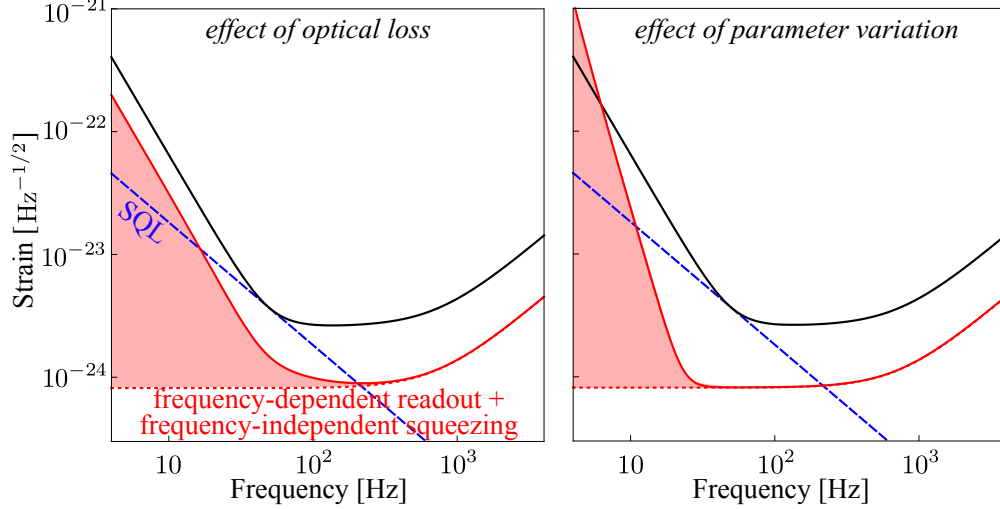
Figure 19: The effect of optical loss (left) and parameter variation of the filter cavity (right) for frequency-dependent readout (output filtering). Similar to Fig. 16, we have used a total optical loss of 20%. In contrast, the parameter variation is chosen to be only 10^{-4} in order to produce reasonable sensitivity, as it is much more sensitive than input filtering.

expression is quite lengthy and not illuminating, and we will not show it here. One can evaluate its noise spectrum numerically.

4.6.4 Twin signal-recycling

Twin signal recycling (TSR) refers to detuned signal recycling in which upper *and* lower signal sidebands are resonantly enhanced simultaneously providing a spectral density which is reduced by up to a factor of two [72]. TSR requires a an additional signal recycling mirror, most likely in a long-baseline arrangement. Squeezed states, however, can be used without setting up another long baseline filter cavity [73].

4.6.5 Speed meter

Here we describe the speed meter configuration. The motivation for it arises from the perspective of viewing the gravitational-wave detector as a quantum measurement device. Normally, we measure the test mass position at different times to infer the gravitational-wave signal. However, position is not a conserved dynamical quantity of the test mass which is treated as a free mass in the theoretical model. According to the quantum measurement theory [74], such a measurement process will inevitably introduce additional back action and perturb the test mass motion. In the context here, the back action is the radiation-pressure noise. In order to evade the back action, one needs to measure the conserved dynamical quantity of the test mass—the momentum or the energy. Since the momentum is proportional to the speed, that is why speed meter is ideal for measuring gravitational wave with no radiation-pressure noise [59].

There are several speed-meter configurations, e.g., the Sagnac interferometer [62] and a recent proposed scheme by using different polarizations [75]. In Fig. 22, we show one particular
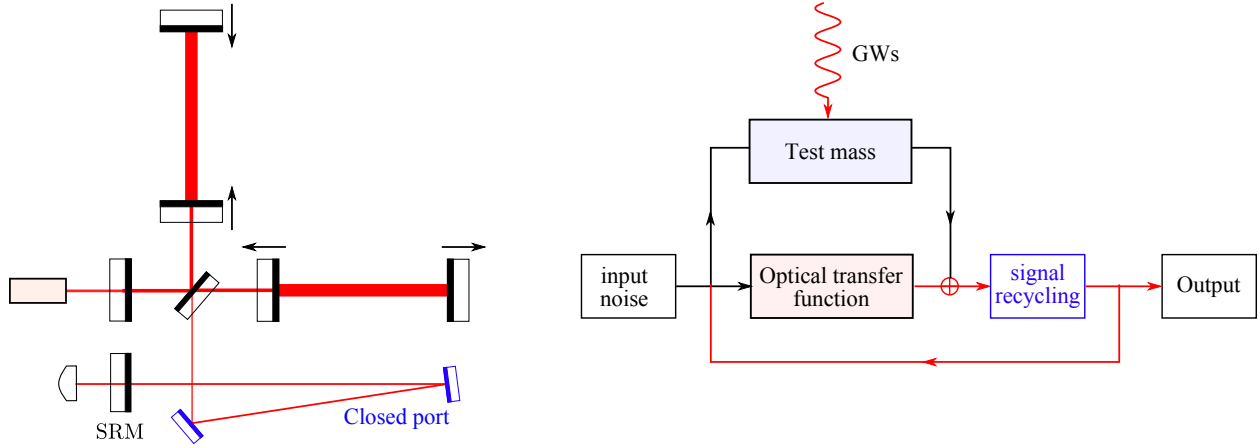
Figure 20: Schematics showing the long signal-recycling cavity scheme (left) and its associated flow chart (right). The signal-recycling mirror coherently reflects back the signal, forming a feedback loop as indicated in the flow chart.
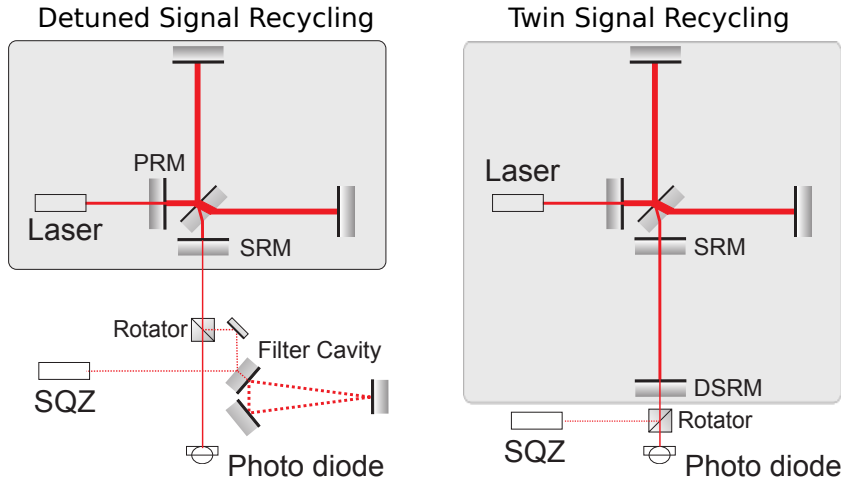
Figure 21: (Color online) Top left (shaded): Topology of the current gravitational wave detector GEO 600. The mirror in the laser input port (PRM) realizes so-called power-recycling. The signal-recycling mirror (SRM) in the output port establishes a carrier light detuned single-sideband signal recycling cavity. Bottom left: Extension for a broadband shot-noise reduction utilizing squeezed states. Right: Topology, proposed here. Two optically coupled cavities are formed with the help of an additional mirror DSRM. Their resonance doublet enables detuned dual-signal-recycling resulting in lower shot noise. Squeezed states can be used without additional filter cavity.

variant of them, which is proposed in Ref. [61]. It uses a sloshing cavity. We can gain a qualitative understanding of how such a scheme allows us to measure the speed of the test mass. Basically, the information of test mass position at an early moment is stored in the sloshing cavity, and it coherently superposes (but with a minus sign due to the phase shift in the tuned cavity) with the output of the interferometer which contains the current test mass position. The sloshing happens at a frequency that is comparable to the detection frequency, and the superposed output is, therefore, equal to the derivative of the test-mass
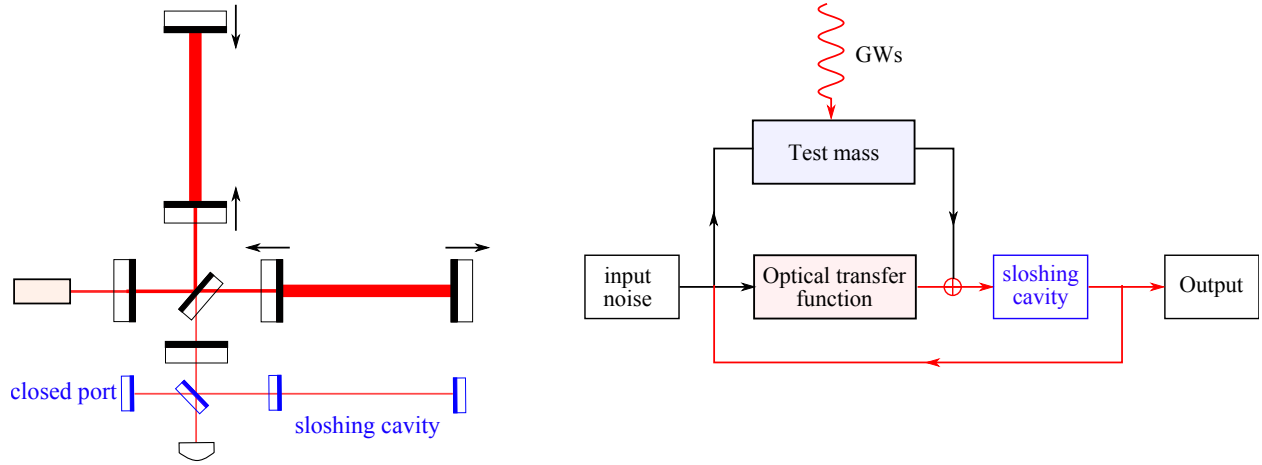
Figure 22: Schematics showing the speed-meter configuration (left) and its flow chart (right).

position, i.e., the speed.

This corresponding noise spectrum is shown in Fig. 23. The low-frequency spectrum has the same slope as the standard quantum limit, which is a unique feature of speed meter. When the optical is high enough, we can surpass the standard quantum limit.
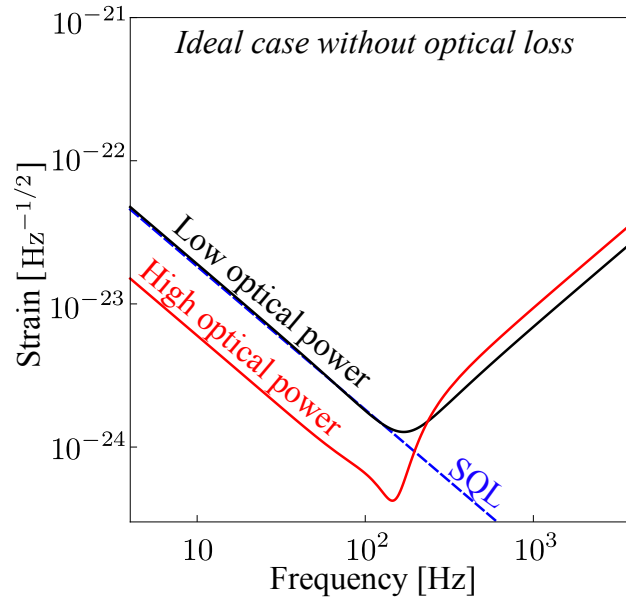
Figure 23: Plot showing the noise spectrum for the speed-meter configuration for two different optical powers.

One important characteristic frequency for this type of speed meter is the sloshing frequency ω_s, and it is defined as

$$\omega_s = \frac{c}{2}\sqrt{\frac{T_s}{L\,L_s}}, \tag{3}$$

where T_s is the power transmissivity for the front mirror of the sloshing cavity and L_s is the cavity length. To achieve a speed response in the detection band, this sloshing frequency

needs to be around 100Hz. For a 4km arm cavity—$L = 4000$ and 100m sloshing cavity—$L_s = 100$, it requires the transmittance of the sloshing mirror to be

$$T_s \approx 30 \, \text{ppm}. \tag{4}$$

This puts a rather tight constraint on the optical loss of the sloshing cavity. To release such a constraint on the optical loss, we can use the fact that ω_s only depends on the ratio between the transmissivity of the sloshing mirror and the cavity length and we can therefore increase the cavity length.

In addition, it seems that no filter cavity is needed for speed meter configuration, as the radiation pressure noise at low frequencies is cancelled. However, such a cancellation is achieved by choosing the homodyne detection angle that is deviated from the phase quadrature, therefore decreasing sensitivity at high frequencies. The deviation is proportional to the optical power. With frequency-dependent squeezing, we can reduce the effective optical power seen by the test mass, which allows us to measure the quadrature closer to the phase one, and thus enhance the high-frequency sensitivity. Similarly, the frequency dependent readout allows us to cancel the low-frequency radiation pressure noise without sacrificing the high-frequency sensitivity by rotating the readout quadrature to the phase one at high frequencies.

Similar to output filtering, this technique leads to reduced signal (but increased signal/quantum noise) at low frequencies so it is far more sensitive to optical losses compared with input filtering.

4.6.6 Multiple-Carrier Fields
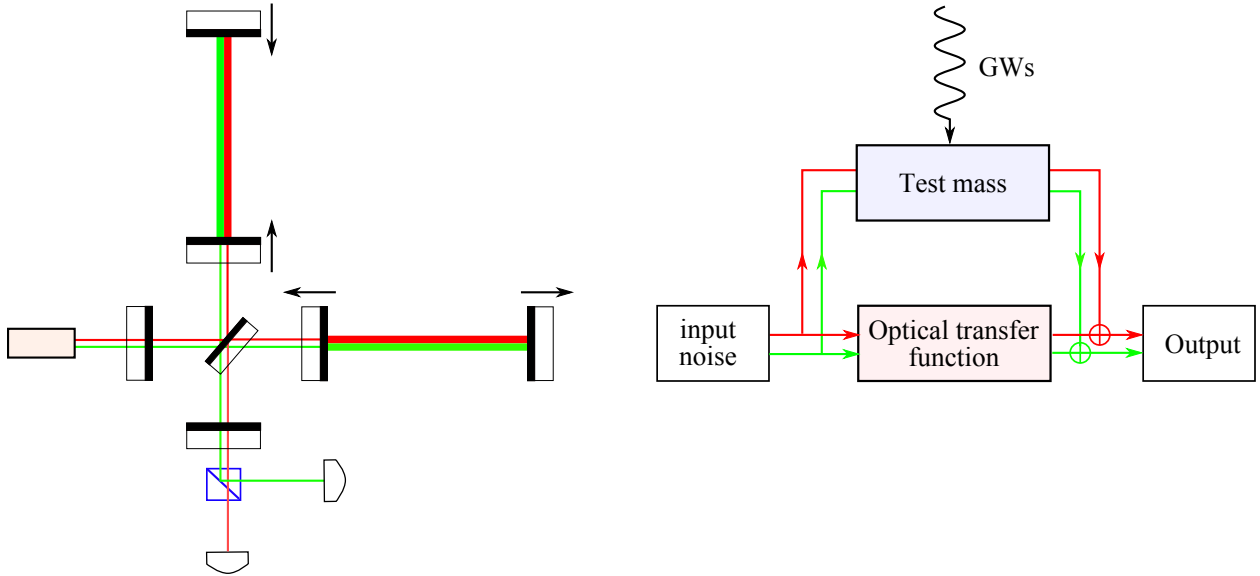
Figure 24: Schematics showing the dual-carrier scheme (left) and its flow chart (right).

Here, we introduce the multiple carrier light scheme, and in particular, we will focus on the dual-carrier case as shown schematically in Fig. 24. The additional carrier light provides us

another readout channel. As these two carriers can have a very large frequency separation, we can in principle design the optics in such a way that they have different optical power and see different detune and bandwidth. In addition, they can be independently measured at the output. This allows us to gain a lot flexibilities and almost provides multiple interferometers but within the same set of optics.

These two optical fields are not completely independent, and they are coupled to each other as both act on the test masses via radiation pressure and sense the test-mass motion (shown pictorially by the flow chart in Fig. 24). Since the frequency separation between them is much lager than the detection band, these two fields can be measured independently. To achieve the optimal sensitivity, we need to combine them with the optimal filters. In [64], the authors have shown the procedure for obtaining the optimal sensitivity and the associated optimal filters in the general case with multiple carriers.

4.6.7 Local Readout
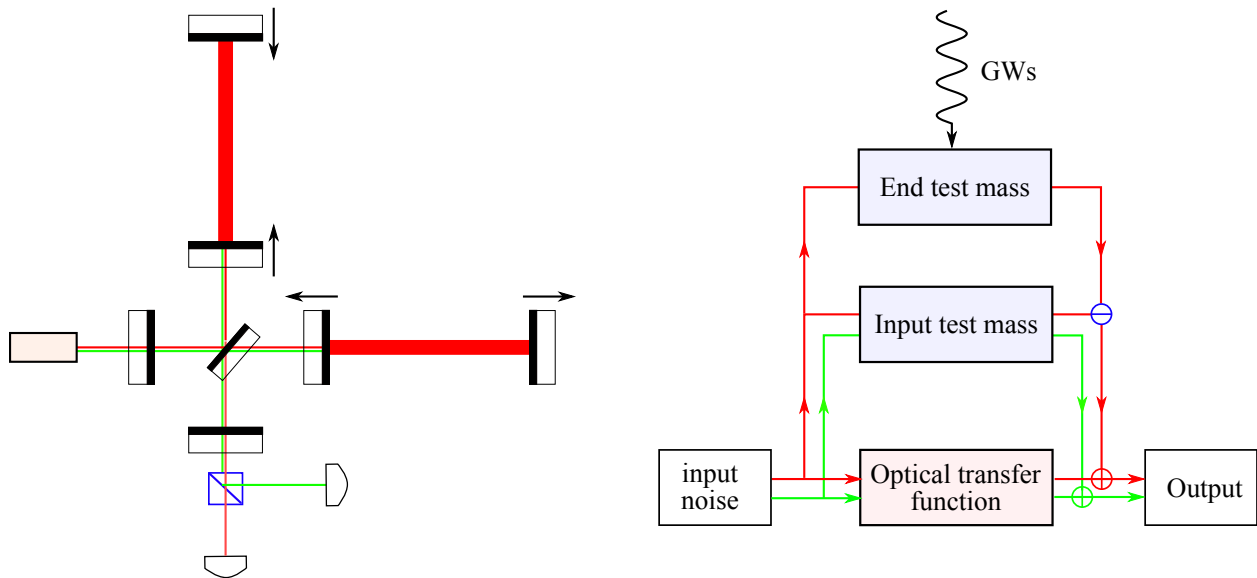
Figure 25: Diagram of the local-readout topology (left) and the resulting feedback loops (right).

The local-readout scheme is shown schematically in Fig. 25. It is actually a special case of the dual-carrier scheme mentioned in the previous subsection—the second carrier light is only resonant in the power-recycling cavity and is anti-resonant in arm cavity (barely enters the arm cavity). Why we single this scheme out of the general dual-carrier scheme and give it a special name is more or less due to a historic reason. This scheme was first proposed in Ref. [65] and was motivated by trying to enhance the low-frequency sensitivity of a detuned signal-recycling interferometer, which is not as good as the tuned signal-recycling due to the optical-spring effect. The name—"local readout"—originates from the fact that the second carrier only measures the motion of the input test mass (ITM) which is *local* motion in the proper frame of the beam splitter and does not contain gravitational-wave signal. One might ask: "how can we recover the detector sensitivity if the second carrier measures something that does not contain the signal?" Interestingly, even though no signal is

measured by the second carrier, it measures the radiation-pressure noise of ITM introduced by the first carrier which has a much higher optical power due to the amplification of the arm cavity, as shown schematically by the flow chart of Fig. 25. By combining the outputs of two carriers optimally, we can cancel some part of the radiation-pressure noise and enhance the sensitivity—the local-readout scheme can therefore be viewed as a noise-cancelation scheme. The cancelation efficiency is only limited by the radiation-pressure noise of the second carrier.

To evaluate the sensitivity for this scheme rigorously, one has to treat the input test mass (ITM) and end test mass (ETM) individually, instead of assuming a single reduced mass as we usually do for those schemes mentioned earlier. One can refer to [65] for details.

4.7   Numerical Optimization and Comparison

To find out the possible candidate that is feasible for upgrading the sensitivity of aLIGO, we made a systematic comparison of those configurations mentioned in the previous section, and the results are reported in the LIGO document [76]. Here we will just show the main result and one can refer to the document for more detail.

The final optimization result critically depends on the cost function. In the literature, optimizations have been carried out by using a cost function that is source-oriented—trying to maximize the signal-to-noise ratio for particular astrophysical sources. Here we apply a rather different cost function that tries to maximize the *broadband* improvement over aLIGO. This follows the same philosophy of designing aLIGO which aims at a factor of 10 broadband improvement over initial LIGO.

For optimization, we also take into account the various classical noise sources (to be distinguished from the quantum noise). In particular, we consider Brownian thermal noise in the mirror suspensions [77, 78], seismic vibrations propagating to the mirror [79], terrestrial gravitational fluctuations [80, 81], and Brownian thermal fluctuations of the mirror (and mirror coating) surface [16, 82].

The results of the numerical optimization are shown in Figs. 26 and 27, where we plot the total noise spectra (the quantum noise + the classical noises) for different configurations with frequency dependent squeezing (input filtering) and frequency dependent readout (output filtering), respectively. In producing Fig. 26, we assume a moderate reduction in the thermal noise and the same mass and optical power as those for aLIGO. In producing Fig. 27, we assume a more optimistic reduction in the thermal noise, the mirror mass to be 150 kg and the maximum arm cavity power to be 3 MW.

As we can see, by adding just one filter cavity to the signal-recycled interferometer (aLIGO topology), we can already obtain a broadband improvement over aLIGO. Limited by thermal noise at low frequencies, the difference among these configurations is not very prominent. This leads us to the conclusion that adding one input filter cavity to aLIGO seems to be the most feasible approach for upgrading in the near term, due to its simplicity compared with other schemes. If the low-frequency thermal noise can be reduced in the future, the speed meter and the multiple-carrier scheme can provide significant low-frequency enhancement of the sensitivity. This extra enhancement will, for some low enough thermal noise, be enough to compensate for the extra complexity.
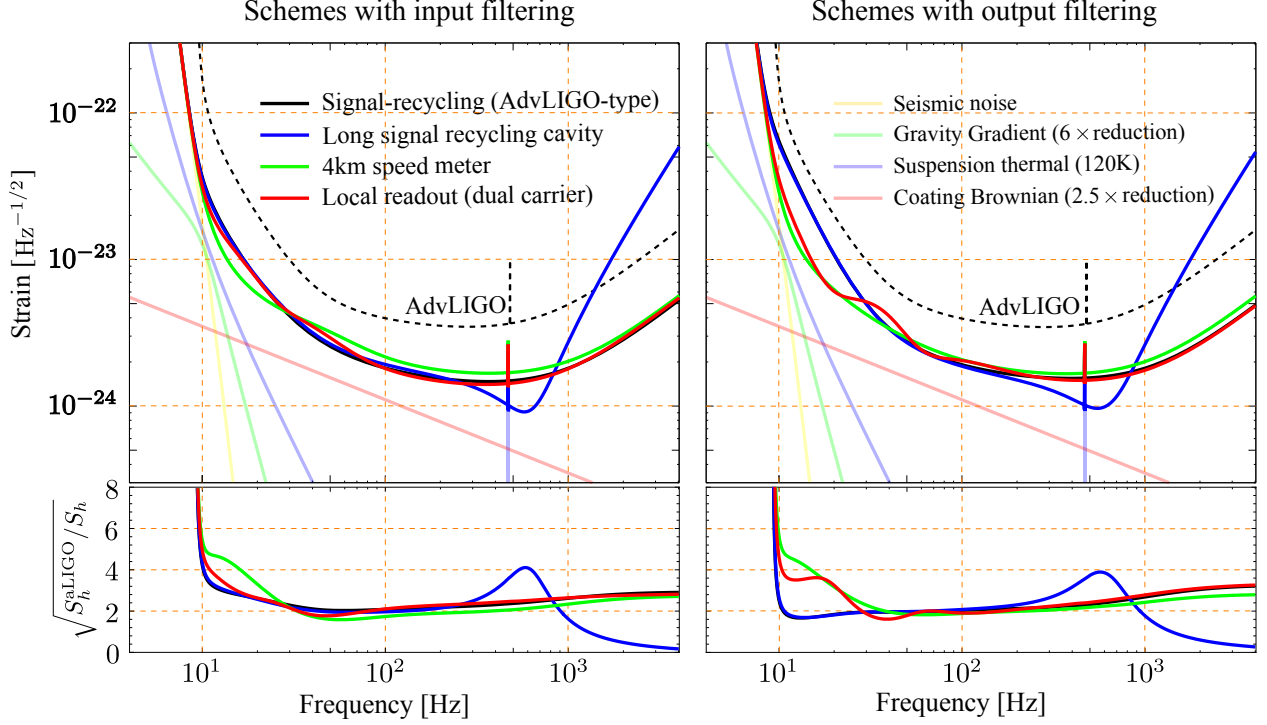
Figure 26: The optimized total noise spectrum for different schemes assuming a moderate improvement of the thermal noise compared with aLIGO baseline design. The lower panels show the linear strain sensitivity improvement over aLIGO.

4.8 Time-Dependent Interferometer Configurations

4.8.1 Time allocations for steady-state operation with different configurations

LIGO aims at several distinct astrophysical populations. The above optimization works in general towards a baseline configuration that optimizes the overall sensitivity for all sources. However, if each particular population is targeted, one might obtain somewhat different optimizations. It would be interesting to ask: is it better to run the interferometer through a sequence of configurations, staying a certain fraction of the total observational time at each configuration, or to run the interferometer at a generic, "one-configuration-fits-all" mode.

The answer of course depends on how optimal one can gain for each particular source compared with the baseline, how much one loses for the other sources that are not optimized for — and how likely each particular source is present, in the first place.

As an example, compared with the baseline configuration, O, we have two alternative configurations A and B. Suppose for configuration A we have a relative sensitivity 1.5 for events of type a, but $1/1.5$ for those of type b, while for configuration B, we have the opposite, $1/1.5$ for a, but 1.5 for b. If we use A half the time and B half the time, assuming that the durations we keep our interferometer running at each configuration is much longer than the durations of the signals of either type, the the mean event rate for both types of events can be estimated as 1.83 times the baseline event rate, a rather dramatic improvement — regardless of the intrinsic rates of a and b. If intrinsic rates for a and b could be estimated, we might further improve rate of detection — or bias towards the rarer type of events — by
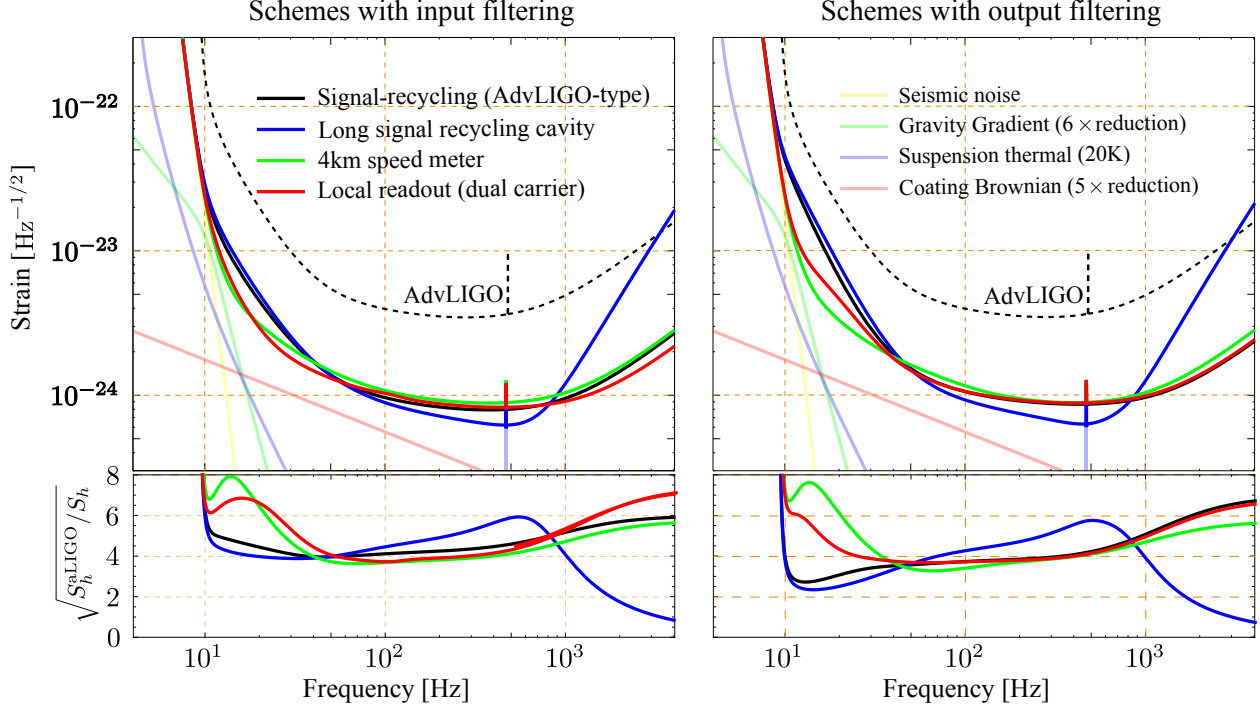
Figure 27: Optimization results for different schemes assuming more substantial thermal noise improvements, increasing the mirror mass from 40 to 150 kg, and increasing the arm cavity power from 800 to 3000 kW.

adjusting the fraction of time we assign to A and B.

This simple example teaches us that if sizeable improvement of sensitivity is possible for a particular population, we might not want to keep a "one-configuration-fits-all" strategy, but instead should aggressively look for that type of sources by allocating preferences.

4.8.2   Triggered switch of configurations

The interferometers may also switch between two configurations when triggered by the possible arrival of a particular signal. For example, if restricted to frequency-independent input squeezing, a trade-off is made between sensitivities at low and high frequencies by adjusting the angle of the squeezing ellipse.

Instead, it may be possible to set the low-frequency-enhanced configuration as the default configuration, which is most sensitive to the early stage of compact binary coalescence. If an event trigger is obtained from this configuration, the control system can promptly switch to the high-frequency-enhanced configuration to gather more statistics for the merger phase. Although this type of scheme makes sense in an intuitive, quasi-static sense, detailed modelling of the transient behavior of the interferometer is required to further estimate if this can be done in practice.

4.8.3   Variable Reflectivity Signal Mirror

The signal recycling mirror can be replaced with a Fabry-Perot cavity. This tuneable cavity will change the effective reflectivity of the signal mirror and allow for a tuneable finesse for the signal cavity in addition to the usual signal cavity detuning phase. This can be realized either by an etalon, or by a Michelson interferometer, as has been demonstrated at the ANU [83] as well as with the concept of squeezed-light-input twin-signal-recycling [73]. This option is also naturally combined with the concept of a long signal recycling cavity. Combined with tuning of SR cavity, such a configuration can dynamically modify the interferometer response with changes in incoming GW signal

4.8.4   Intracavity Readout scheme

This refers to configurations in which the gravitational wave signal is detected when a second carrier field (or some other sensing device) is used to measure the motion of a particular set of mirrors in their local inertial frames (see Ref. [84] and references therein). The word "intracavity" is used because it is assumed that the first carrier field does not generate useful output signals for readout.

The "local readout scheme" mentioned in the previous subsection can be regarded as an example of a mixture of intra- and extra-cavity readout. At high frequencies, the interferometer is dominated by extra-cavity readout, while at lower frequencies, it is dominated by intra-cavity readout. In the local readout example above, one may find it useful to use an alternate wavelength laser: the second wavelength can be made to have a very high finesse in the recycling cavities only, so as to maintain a high phase sensitivity for the ITM motion.

4.9   Development of quantum radiation pressure dominated and QND apparatus

Before any of these ideas can be considered for LIGO Cosmic Explorer, a major experimental R&D and prototyping effort is required. To date no experiment has observed quantum radiation pressure noise on gm-scale let alone kg-scale mirrors, let alone reached the 'naive' standard quantum limit. Efforts to demonstrate QND interferometry are crucial to understanding what is achievable, to learn about problems which could mask such phenomena and how to beat such limits.

To date there are major activities planned or underway at the AEI 10 m prototype; MIT; the University of Tokyo and LSU. The Glasgow 10m, the Gingin Facility and the ANU have embarked on testing optical spring dynamics. More effort is needed toward observing QRP noise. The first serious effort to demonstrate a quantum speed meter is under construction at the University of Glasgow. As such experiments run up against excess noise sources and thermal noise they will inform activities across other working groups. More effort is needed.

Obviously, without QRP noise and SQL limited apparatus, no direct tests of these ideas can be performed. However, measuring transfer functions, demonstrating low loss manipulation of squeezed states and variational readouts can be performed with shot noise limited systems. Plans are underway for such an experiment at MIT and AEI. More effort is needed.
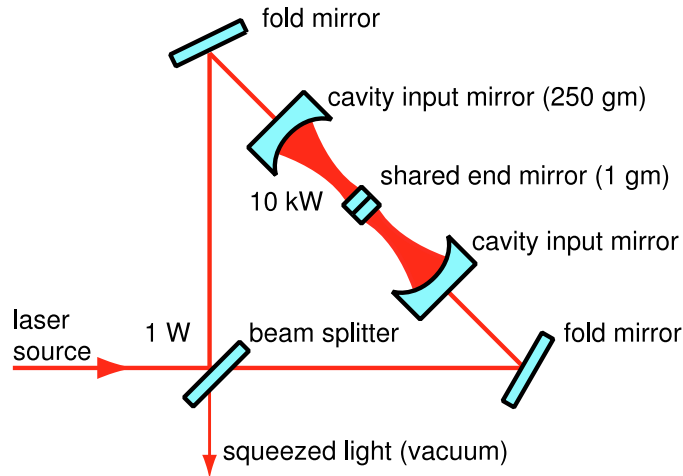
Figure 28: Ponderomotive Squeezer, taken from Corbitt et al. [86]

4.10 Development of other signal-to-quantum-noise enhancement techniques

4.10.1 Ponderomotive Squeezing

Squeezed light can be produced by mirror motion under radiation pressure — this is called ponderomotive or opto-mechanical squeezing. Although to date it has been more difficult than generating squeezing with nonlinear crystals, it may become more reliable and more flexible in the future. A Ponderomotive Squeezing experiment has been going on at MIT [85]. See Fig. 28 for a sample configuration.

4.10.2 Intra-cavity squeezing and white-light cavity

Independent of the injection of externally produced squeezed light, intra-(signal-recycling) cavity squeezing might result in an additional signal to quantum noise improvement. Intra-cavity squeezing also modifies the signal-to-bandwidth product in a non-trivial way, from which the sensitivity of signal-recycled gravitational-wave detectors could benefit. Theoretical as well as experimental work is required to research and develop appropriate schemes based on crystal squeezers. It was theoretically shown that negative dispersion can result in a white light cavity without significantly adding quantum noise [87, 88]. A suitable medium that provides negative dispersion are atomic media, but they introduce an additional constrain on the wavelength a gravitational-wave detector can be operated at. It should be investigated whether solid state optical systems at suitable wavelengths can also provide the same property.

4.10.3 Induced Transparency

Electromagnetically induced transparency (EIT) in an atomic vapors or opto-mechanically induced transparency (OMIT) can slow down light, possibly improving high finesse optical filters [89]. With enough slowing, one can almost eliminate the need for long filter cavities. This research needs to be pushed into a direction that does not introduce an unrealistic

constrain on the gravitational-wave detector wavelength [90].

4.10.4   Atom Interferometry

There is the general question of whether atom interferometry offers a competitive topology for a third generation detector. Whilst this research area is not a fundamental activity of the LSC we should keep a watching brief on this technology and provide scientific support and advice when and where we can.

5 Optics

The Optics Working Group (OWG) of the LSC pursues research related to the development and implementation of optical components for ground-based gravitational wave detectors. This includes work on optical components being installed in Advanced LIGO, to better understand their behavior during commissioning and operation, possible upgrades to subsystems of Advanced LIGO including core optics, input optics, and auxiliary optics, and longer term research into ways around significant limitations in current detectors to be implemented in future generations of interferometers.

The OWGs work can broadly be divided into the following categories.

Mirror coating research   The high-reflection (HR) coatings on the test masses must satisfy a number of performance criteria including low absorption, low scatter, high uniformity, high reflectivity at two wavelengths, low mechanical loss, and low thermo-optic noise. Of these, mechanical loss and optical absorption provide the greatest sensitivity limits, and thus the most significant opportunity to improve performance.

The majority of coating research is focused on understanding and reducing the thermal noise arising from the HR coatings because it is a leading noise source in Advanced LIGO's central frequency range and a major design hurdle for all future detectors. However the anti-reflective (AR) coatings also present some challenges.

Coating research encompasses the following areas:

- **Materials Investigations:** Measurements of the physical characteristics (Mechanical loss, Thermo-optic loss, Young's modulus, optical absorption etc) for coating material candidates for A+ LIGO and LIGO Voyager. This research includes investigations of how these characteristics change through processing, composition, temperature, etc.

- **Structural Measurements and Modeling:** Research to determine the coating structure by measuring or modeling the distribution of atoms and bond congurations, which can then be used to identify correlations to mechanical loss and other material properties. These investigations aim to understand the mechanisms of coating mechanical loss, and identify ways of reducing its effect through a materials-by-design process.

- **Direct Thermal Noise Measurements:** Use of precision interferometry to directly measure thermal noise from coatings made from new materials, techniques, designs, etc. to verify predictions coming out of material investigations. This is an important step to both test predictions and test coating performance before use in actual gravitational wave detectors.

Mirror substrate research   Mirror substrate research encompasses the following broad areas:

- **Substrate Material Properties:** The mirror substrates for gravitational wave detectors must meet many requirements including low mechanical loss, low optical absorption, low scatter losses and appropriate figure. While previous experience with fused silica substrates is directly relevant for A+ LIGO, the proposed change to silicon substrates for LIGO Voyager requires significantly more research and development. The proposed change from silica to silicon substrates for Voyager is largely driven by the increase in mechanical loss of fused silica at cryogenic temperatures. In addition, silicon mirrors will experience less thermal lensing for the same laser power, potentially allowing the use of higher powers in the arm cavities with silicon mirrors. Silicon is not transparent at 1064 nm, so a change in interferometer laser wavelength, possibly to 1550 nm or higher, would also be required. Low optical absorption is important in a cryogenically-cooled mirror to minimise the heat load and allow the required operating temperature to be maintained. In addition, other optical effects in silicon need to be considered, including two-photon absorption and noise associated with both intrinsic and generated free carriers. n

- **Parametric instabilities:** The build-up of parametric instabilities in the arm cavities related to the high laser power levels are a potential problem from high optical power in Advanced LIGO and beyond, with parametric instability already having been observed in the Livingston aLIGO detector. These undesirable effects result from exchange of energy between light stored in cavities and acoustic modes of the mirror which define the cavities, and can result in high excitation of particular acoustic modes of the mirrors, leading to control problems and in extreme cases loss of lock of the interferometer. Research focuses on understanding parametric instabilities and developing methods of reducing the effects.

- **Charging research:** There are various mechanisms by which the mirrors in an interferometer can become charged, and interaction between charges on the mirror and charges on nearby surfaces can generate force noise on the mirror. In addition, charging may lead to interferometer control problems through interactions with the electrostatic drives. Charging research focuses on measurements of charge noise and identification and testing of methods for charge mitigation.

5.1 Advanced LIGO Risk Reduction

Risk reducation for Advanced LIGO continues to be an important area of work. For the OWG, it is particularly important to ensure that the thermal noise and optical performance of the aLIGO mirror coatings is fully understood. Understanding the variations in coating mechanical loss measured on different substrates, and how this relates to direct thermal noise measurements on test mirrors and to the magnitude of thermal noise expected in the aLIGO mirrors, will be critical for understanding the thermal noise performance of the aLIGO detectors. Similarly, a full understanding of the scattering characteristics of the aLIGO coatings is required to assist with fully characterizing scatter loss, and potential related noise sources, in the detectors.

5.2 A+ LIGO

5.2.1   Mirror coating research

Coating thermal noise is related to several properties of the coating including the mechanical loss, the Young's modulus and the thickness, and to the radius of the interferometer laser beam and the temperature of the mirror. For A+ LIGO, a number of different techniques are expected to be capable of providing some reduction in coating thermal noise, including using a larger beam radius, optimising coating designs (including composition, layer thicknesses and possible exploitation of differences in the loss angle associated with shear and bulk motion) and possible reductions in mechanical loss via optimising doping,annealing or via the use of promising alternative coating materials. It seems likely that a combination of a number of these techniques may be used to produce the best possible coating for the A+ LIGO detectors.

5.2.2   Coating Research: Increased Laser Beam Radius

The use of a larger laser beam radius in the interferometer (along with the use of appropriately larger mirrors) is one of the most obvious methods for reducing coating thermal noise. However, the use of larger mirrors will have a significant impact on the mirror suspensions and seismic isolation systems, so detailed trade-off studies in collaboration with the suspensions working group are required. In addition, detailed discussions with coating vendors are required to determine how much development is required to enable coatings of the required uniformity to be deposited on larger optics.

5.2.3   Coating Research: Mechanical Loss

For room temperature mirrors at 1064 nm, the coatings with highest optical quality are ion beam sputtered (IBS) amorphous coatings, where the high index material is typically a metal oxide (ie. Ta_2O_5 or TiO_2) and the low index material is usually silica.

The thermal noise due to the mirror coatings can be calculated from the coating mechanical loss using the Levin method [91]. Two methods are currently employed to measured the mechanical loss. The first method measures the loss via ringdown of small coated cantilever samples over the temperature range of $0 - 300$ K. These measurements map out the Debye loss peaks and determine the activation energy of the loss mechanism. This knowledge can then be used as a constraint in models of the coating structure (see Section 5.2.7) By accurately modeling the coating structure, one may be able to identify the microscopic causes of internal friction and design coatings with minimal loss. Thus, while temperature dependent coating loss measurements are also of interest for cryogenic coatings for LIGO Voyager, these measurements are also relevant to understanding loss mechanisms in room temperature coatings for A+ LIGO.

The second method measures the mechanical loss of coated thin silica disks at room temperature over a wide frequency range (typically $3 - 20$ kHz). The frequency dependence allows separation of the bulk, surface and thermoelastic losses. Characterizing the mechanical loss at a wide range of frequencies and temperatures is valuable both as a search for new materials and to better understand the causes of thermal noise in amorphous thin film oxides.

The high index materials that have been explored include: tantala, titania, niobia, hafnia,

and zirconia. Silicon nitride, Si_3N_4, also may be promising. Low index materials include silica and alumina. As applied, the high index materials have losses ranging from 3 – 7 $\times 10^{-4}$.

The loss in the silica coating layers, while several times less than the high-index layer, is not negligible. For coating geometries, the loss in silica is dominated by surface and stress-induced losses. The latter loss can be minimized through a slow annealing process. However, this process typically destroys a multilayer coating by either crystallization of the high index material or adhesion failure due to differential thermal expansion. Thus the loss in the silica layers will depend on the geometry and thermal history of the multilayer coating. The loss in alumina is dominated by thermoelastic loss and is not currently suitable for room temperature coatings.

The most commonly used model for loss in these glassy materials [92] assumes an asymmetric, double-well bond potential formed by two nearly degenerate bond states. In silica, for example, the O bond potential has an angular dependence that is described by nested, asymmetric potentials [93], where the activation energy depends on the atomic distribution. In this model, one may minimize the loss by either removing the potential's double-well (ie. doping to change the bond potential) or by removing the asymmetry (ie. annealing to allow the material to assume its lowest energy state).

Doping Doping can reduce the mechanical loss by favorably changing the bond potential and by stabilizing the matrix against crystallization. For example, doping the tantala layers with titania has been shown to reduce mechanical loss by about 40%. This reduction allowed titania-doped tantala/silica to be selected for the Advanced LIGO coatings. Silica-doped titania has shown promise for reduced thermal noise, and was considered a fallback coating for Advanced LIGO. A trinary alloy of titania/tantala/silica as the high index material may allow for benefits from each material. Silica, while effective at stabilizing high-index materials and thus allowing for higher annealing temperatures, also reduces the index of refraction, thus requiring thicker coating layers. Effective medium theory may be of use in modeling alloys and doping, and comparing Q measurements to predictions of effective medium theory are an important next step in verifying this approach.

The use of dopants in tantala, titania, hafnia and zirconia are being explored as a means of understanding and reducing the mechanical dissipation. While it is crucial that any new material also satisfy the stringent optical requirements of LIGO interferometers, there are advantages of initially just pursuing lower mechanical loss.

Shear and bulk loss angles Amorphous materials, including fused silica, tantala, titania doped tantala, and other oxides under consideration as coating materials have two independent elastic moduli, and thus two independent loss angles. Recent work at Caltech by Yanbei Chen's group suggests that it should be possible to design coatings with reduced Brownian thermal noise by having the thermal noise generated by different loss angles partially cancel out. Whether this is practical or significant depends on the values of the loss angles for the coating materials, which can only be determined experimentally. Measurement of torsional and bulk mechanical losses of coating materials will provide necessary input for these designs.

Annealing Ion beam sputtering forms coatings with high compressive stress, and comparatively high mechanical loss and absorption. Annealing these coatings will reduce the stress and correspondingly reduce the absorption and mechanical loss. Typically the annealing temperature is limited by either the crystallization temperature for the high index material or shear failure from the differential expansion of the coating layers. If these failure mechanisms can be avoided, annealing could potentially provide significant improvements in mechanical loss and absorption.

The mechanical loss in silica coatings have be reduce by about $8\times$ through high temperature annealing. In addition a zirconia/silica coating has been demonstrated to survive a 1000° C annealing without shear failure. Annealing has also been shown to reduce the absorption in zirconia coatings by a factor of several. Work is currently underway to use doping to stabilize the coatings against crystallization, which leads to unacceptable scatter. Silica doping suppresses crystallite growth during annealing in Titania [94], Hafnia and Zirconia [95]. Coating designs to withstand high temperature annealing could see significant improvements in their absorption and their mechanical loss. Planar layered composites consisting of alternating nm-scale Titania (or Hafnia) and Silica (or Alumina) layers can be annealed to much higher temperatures compared to (un-doped) materials [96], [97]. Recent results have suggested that heat-treatment of zirconia-doped tantala coatings can significantly reduce the mechanical loss, and heat-treatment at temperatures up to 800°C is possible without crystallisation occuring. Further measurements and repeat coating runs are required to fully characterise this material. It is interesting to note that zirconia was also identified as an interesting dopant by atomic modelling work carried out within the LSC. This work showed that titania doping increased the felxibility of ring-structures found in the coating, and suggested that zirconia doping would increase the flexibility further, possibly resulting in lower mechanical loss [G1300379]. The strategy of using a doped material consisting of the correct proportions of two high-index materials to stabilise against crystallisation appears promising and should be further investigated with other material combinations.

Elevated temperature deposition Deposition of amorphous silicon coatings onto heated substrates can reduce the mechanical loss by orders of magnitude [97], possibly due to the material forming a more ordered amorphous state referred to as an 'ideal glass'. Evidence suggests that a larger loss reduction is possible with elevated temperature deposition than with post-deposition annealing, possibly due to the coating atoms have more freedom to move during the deposition process. Since post-deposition annealing is already known to reduce the mechanical loss of oxide coatings such as silica and tantala, deposition at elevated temperatures may also be a promising technique for significantly reducing the loss of these materials. Alternative methods of providing more energy to the coating atoms as they are deposited on the substrate may also be of interest, for example the use of ion-assisted deposition where a secondary ion-source is used to bombard the substrate with an ion beam during coating deposition.

Interface Effects Early experiments on loss in Initial LIGO's tantala/silica mirror coatings [98] demonstrated that the loss was primarily due to the tantala layers. No significant loss could be attributed to the coating interfaces. Measurements conducted at LMA on the

Advanced LIGO coating initially indicated some excess loss associated with the coating interfaces, but that conclusion was not borne out in subsequent measurements. Nevertheless, for any proposed change in coating material a study of interface losses should be conducted. [99].

5.2.4   Coating Research: Coating Design

nm-Layered Composites   Planar layered composites consisting of nm-scale alternating films of Titania and Silica are increasingly stable against crystallization, as the (Titania) layers thickness is reduced [96]. These composites behave as homogeneous materials as regards their optical and viscoelastic properties, for which simple and accurate modeling is available. Crystallization inhibition up to very high annealing temperature has been also observed in nm-layered Hafnia-Alumina composites [97].

Optimized Coatings   Since the thermal noise in the coatings typically scales as the total thickness of the more lossy material, reducing this thickness while maintaining the optical properties will reduce thermal noise. Constrained numerical optimization codes have been shown to produce high reflectivity coatings while reducing the volume of high index materials by as much as 20%. Thermo-optic noise from thermoelastic and thermorefractive effects is included in this optimization. The mechanical loss of the low index (silica) material takes on a larger role for thickness optimized coatings, as optimization typically makes the high index (titania- tantala) contribution equal to the low index. Such an optimized design was proposed for use in Advanced LIGO [100], [101]. Greater understanding of mechanical loss in thin film silica and/or other low index materials is crucial to exploiting the full potential of this optimization. Thickness optimization should be generalized to incorporate the dopant concentrations (which affect both the optical and viscoelastic properties of the materials) in the parameters to be optimized, in the perspective of designing minimal noise coatings based on doped (or nm-layered) mixtures.

Designing coatings that take advantage of different loss angles for bulk and torsional motion will be important once numerical values are found. This optimization will need to be done while including thickness effects on Brownian thermal noise as well as thermo-optic noise.

Multi-material coatings   The use of multi-material coatings to take advantage of the properties of different materials has been proposed [102, 103]. In particular, it may be possible to exploit the fact that most of the incident light intensity is reflected by the first few bi-layers of a coating, potentially allowing coating materials with higher optical absorption, but lower mechanical loss, to be used in the lower layers of a coating stack without significantly increasing the total absorption of the coating stack. It should be noted that multi-material coating designs, coupled with the low optical absorption observed in amorphous silicon coatings deposited using a novel ion-beam sputtering process at the University of the West of Scotland, may potentially allow the use of amorphous silicon layers in mirror coatings for use at 1064 nm for A+. Amorphous silicon is an attractive coating material due to its low mechanical loss and high refractive index: see section 5.3.1 for more details.

5.2.5 Coating Research: Optical Properties

Optical Absorption Absorption of light in the coatings will result in thermoelastic distortion of the optics and will ultimately limit the circulating light power in the interferometer. When coupled to the bulk absorption in the input test masses, this leads to significant surface deformation of the test masses and bulk thermal lensing in the input test masses. Coating absorptions as low as 0.3 ppm have been reported in undoped silica/tantala coatings, while titania-doped tantala and silica-doped titania coatings have been shown to have absorption at or below 0.5 ppm. Further improvements beyond this level will make thermal compensation easier for A+ LIGO, and detailed studies of absorption are essential for any coating materials considered for use in current or future detectors.

Studies aimed at understanding and improving coating mechanical loss may involve working with coatings with relatively high absorption during a research phase e.g. to understand why a particular dopant affects the mechanical loss. Further research into the absorption of anti-reflection coatings is also required, as these coatings consistently have a higher absorption (up to 10 ppm) than high-reflectivity coatings (typically below 1 ppm).

Optical Loss from Scattering In order to maintain the highest optical power in future detectors, it is important to minimize the optical scatter. Scatterometer measurements should be conducted for proposed coatings and new coating materials. Studies of the dependence of scatter on coating materials and manufacturing are important in determining the lowest possible scatter.

Realizing more sophisticated quantum non-demolition (QND) topologies also requires extreme low-loss optical systems as is explained in section 4.2.1 for the case of filter cavities. One of the important sources of optical loss is scattering from mirror-surface abberations. These are traditionally investigated by measuring the angular distribution of scattered light (i.e. measurements of the bidirectional scattering distribution function (BSDF)), or scanning the surface with lasers and integrating the scattered light in spheres. As much as these measurements are important to link scattering from mirrors with losses in optical systems like cavities, they do not give direct information about the cause of scattering.

Scatter loss in (future) optical systems with sizes up to a few hundreds of meters will likely be dominated by point-defect scattering as the quality of substrate polishing has advanced to a level that makes residual surface-roughness scatter loss negligible in most cases. These conclusions are based on numerous simulations and partially on scattering measurements in first-generation GW detectors. Even though it is believed that very low-loss systems can be realized in the near future with scatter loss around 10 ppm per mirror, the question is how much further loss can be decreased. Loss estimates play a major role when deciding between the various candidate QND configurations for future GW detectors. Whereas input filters (see section 4.6.1) are relatively robust against optical loss, output filters (see section 4.6.2) that can potentially eliminate all back-action quantum noise are known to be highly susceptible to loss. A few ppm loss per mirror typically destroys the entire advantage that output filters have over input filters (eventually making them even worse in performance). Similar problems are encountered with alternative QND schemes.

Assuming that point-like defects residing in the mirror coatings are the dominant source

of scatter loss, one has to investigate individual defects for their material compositions, morphologies, and structures. The answers can be used to understand the origin of the defects with the goal to improve the coating process. Various analysis methods are available. Defect morphology can be studied optically or with force microscopy depending on defect size. Defect materials can be investigated spectroscopically. The analyses should progress from larger to smaller defects since the larger defects dominate the point-defect scatter even if they are significantly less numerous.

5.2.6 Coating Research: Other Coating Properties

Thermo-optic Noise Thermo-optic noise is the change in the optical thickness of a coating due to temperature fluctuations. Thermo-optic noise depends on both thermo-refractive (dn/dT) and thermo-elastic (dL/dT) effects in coatings, which partially cancel from the -dn/dL term. Measurements of dn/dT and dL/dT for coating materials are important to quantified and minimize the thermo-optic noise for Advanced LIGO and for any future detectors.

Measurement of the thermal expansion coefficient of coating materials is also essential to allow the level of thermo-elastic noise to be predicted and, if possible, partially canceled with thermo-refractive noise through careful coating design. Measurement of thermal expansion coefficients at cryogenic temperatures is also valuable for future low temperature detectors.

Young's Modulus and Stress The Young's modulus of a coating is required both for the analysis of mechanical loss measurements and for calculations of the level of coating thermal noise. It is therefore important to obtain accurate values of Young's modulus for every coating, and post-deposition coating treatment, studied. Residual stress in coatings is likely to be an important property, and there is interesting evidence suggesting that stress can alter mechanical loss of coatings, particularly in silicon nitride. Therefore studies of the effects of residual stress on the loss and of methods of altering the stress in particular coatings are of interest. The use of several measurement techniques can be beneficial in these studies, as each technique has different systematic errors and, for example, different sensitivity to the properties of the coating substrate material. In addition to measuring these properties at room temperature, where possible the capability to measure the temperature dependence of these properties should be developed.

A Young's modulus and dissipation measurement method with sub nanometer spatial and depth resolution developed by Konrad Samwer shows that the Young' modulus in glasses has a position dependent spread as wide as 30% (and the local loss factor is also poorly defined), that the spread is reduced with annealing, while crystals have constant Young's modulus everywhere. It has also been shown that fused silica, which is the glass with the lowest known mechanical loss, has a substantially narrower Young's modulus spread than other glasses. The method can either explore small shallow volumes, or wider and deeper volumes, up to several hundreds of atomic spacings in dimension. The capability of this method to scan the Young's modulus with sub nanometric resolution offers a new way to explore the uniformity of our coatings, as a function of annealing, and perhaps shine some light on some loss mechanisms.

Uniformity It has also proved challenging to maintain coating thickness uniformity across the large face of Advanced LIGO optics. Non-uniformity in thicknesses leads to non-uniformity of transmission and scatter of light out of the cavity mode to other optical modes. This also leads to limits on optical power and squeezing, as the higher spatial frequency scatter discussed in the previous paragraph. Even larger optics are possible in future detectors, making maintaining coating uniformity even more challenging and thus an important research topic. The limitation on obtainable uniformity can come from metrology limitations, so improved metrology is an important research direction. An additional research direction is to explore corrective coatings, which place additional coating material onto a coated optic after uniformity measurements have been made.

Production Variables Variations in the loss of nominally identical coatings from different vendors have been observed, suggesting that the precise deposition parameters may be important in determining the loss. Thus more detailed measurements of the effects of parameters such as ion energy, sputtering ion, oxygen pressure and thermal treatment may be valuable. While ion beam sputtering produces the lowest optical loss coatings, the mechanical loss of coatings deposited by other techniques has not been extensively studied. Studies of coatings deposited by different techniques (e.g. magnetron sputtering, e-beam evaporation, atomic layer deposition) may enhance understanding of the relationship between loss and structure in these materials.

Coating layer thickness may also prove an important variable in determining amorphous material properties, especially mechanical loss. There are suggestions that very thin, much less than a wavelength, layers may have improved mechanical loss. This may be related to stress and/or annealing properties of thin coatings. If this effect can be confirmed and understood, it is possible to design high reflective coatings with much lower thermal noise using known materials like tantala and silica.

5.2.7 Coating Research: Structural Studies

There is currently little understanding of the mechanical loss mechanisms in amorphous coatings, although it seems likely that the loss mechanism is related to the local atomic structure and may involve transitions of two-level systems as is believed to be the case in fused silica. The mechanical loss of tantala in particular has been found to be strongly affected by treatments such as doping and post deposition heat-treatment, which cause both structural and chemical changes to occur in the material. Identifying the mechanical loss mechanisms in the coatings is a crucial step in developing improved techniques for reducing coating loss. Investigating the atomic structure of the coating materials to identify the mechanisms of mechanical loss, in an effort to identify ways of reducing its effect, form an important area in coatings research.

Experimental structure investigation Experimental structural measurements of coating materials, such as electron diffraction and reduced density function (RDF) analysis, are currently being used investigate the local atomic structure of the coating materials. These measurements have identified the first correlation between changes in the mechanical loss of

titania doped tantala coatings and certain changes in the atomic structure measured from the coating RDFs, when varying the level of titania doping. Extended X-ray Absorption Fine Structure (EXAFS) provides detailed measurements of local order around specific atomic species in the coating structure, such as tantalum and titanium. In addition, using X-ray Diffraction to generate RDFs gives the possibility to study changes in the atomic structure between the surface and bulk of the material. Nuclear Magnetic Resonance (NMR) spectroscopy is also being used to study the local atomic co-ordination around oxygen, through ^{17}O enrichment of the coatings. Methods of studying medium range order (1- 5 nm) in coating materials, such as Fluctuation Electron Microscopy (FEM), are being used to establish correlations with mechanical loss that may be more evident over a larger local structure range, especially in the case of post-deposition heat-treatment. The combined effort of these complementary experimental techniques to study the coating atomic structure provides a powerful tool to probe the correlations to, and mechanisms of, mechanical loss.

Atomic modeling Atomic modeling based on the experimental measurements is being carried out using a combination of Reverse Monte Carlo methods and Density Functional Theory. This results in detailed models of the coating atomic structure in which the distribution of parameters such as bond angles and nearest neighbor distances can be analyzed. There is also an effort underway to produce theoretical atomic models of coatings, which are being used to identify possible mechanical loss mechanisms. Silica is thought to be the best material to begin with, as there is fairly extensive literature on atomic modeling of silica and the cause of the mechanical loss is fairly well understood. Developing models of tantala and titania doped tantala is also a priority going forward. Atomic modeling of the coatings has the potential to provide a materials-by-design based approach to coatings development, where coatings can be purposively designed with lower mechanical loss.

5.2.8   Coating Research: Direct Thermal Noise Measurements

Direct measurements of thermal noise are of interest to compare with the predictions obtained from mechanical loss measurements and to test the improving theories of coating thermal noise.

Fixed Spacer Cavities Coating thermal noise measurements are now being carried out using fixed spacer cavities, which are limited by coating thermal noise over a wide frequency band and are significantly easier to operate than a suspended mirror system. These systems will use standard size (1 inch diameter) substrates and can provide a convenient test-bed for the development of low thermal noise optics.

AEI 10 meter prototype The 10 meter prototype interferometer at the Albert Einstein Institute in Hannover Germany will be able to directly measure coating thermal noise. In addition to testing Khalili cavities as a means of reducing coating thermal noise, it will have the ability to change the size of the laser spot on the mirrors. This will allow for a direct test of spot size dependence, which is an important driver of the desire for larger optics in future detectors.

5.2.9   Mirror substrate research

Fused Silica   Experiments to measure mechanical loss in silica versus annealing parameters, including ramp down and dwell times have lead to improvements in the substrate thermal noise. In order for the fused silica thermal noise to pose a problem in the future, the thermal noise of the coating would have to be reduced by more than an order of magnitude. This makes silica substrate mechanical loss studies a lower priority than coating mechanical loss.

5.2.10   Mirror Substrate Research: Parametric Instabilities

The build-up of parametric instabilities in the arm cavities related to the high laser power levels are a potential problem from high optical power in Advanced LIGO and beyond. These undesirable effects result from exchange of energy between light stored in cavities and acoustic modes of the mirror which define the cavities. At high optical powers, the radiation pressure force of scattered high order optical cavity modes can couple strongly to the mechanical modes of the test masses, resulting in a parametric instability. High excitation of the mirror's acoustic modes can result in difficulties in the controls engineering and at very high amplitudes can lead to loss of lock. Unfortunately, the requirements for high sensitivity are commensurate with the conditions under which parametric instability occurs. These include high optical power and low mechanical loss materials in the mirrors.

Using finite element methods, it is possible to start developing a quantitative understanding of this problem by modeling the modes and parametric gain for different test mass configurations, as well as investigate methods for mitigating the instabilities. In order to make a realistic estimate for the parametric gain, it is necessary to also include the full field calculations of the dual-recycled interferometer [104].

Measurements on suspended test masses are needed to obtain realistic, as-built, test mass Q values to establish the net gain for the instabilities. Adding tuned mass dampers to the barrel of the test masses (LASTI-MIT) and/or using feedback to the electro-static drive also show promise for controlling parametric instability. In addition, spatially-resolved radiation pressure feedback on the mirror surfaces is being contemplated (Gingin-UWA). Outstanding questions include whether these approaches are compatible with high sensitivity, including low shot noise, low thermal noise, and realizable controls.

Small scale suspended test mass experiments are also underway to study parametric instability. The larger scale experiments will be useful in testing noise performance of various parametric instability suppression schemes, the small scale experiments will be useful to validate the theory of parametric instability and for proof-of-principle test of suppression schemes. The small scale experiments using millimeter scale test masses in a tabletop configuration using coupled cavities and/or specially designed near-concentric cavities can be done using a standard NPRO laser and standard 1 inch optics. The small scale resonator experiment at UWA has reached the threshold of parametric instability. These experiments are valuable but because of its applicability to Advanced LIGO and A+ LIGO, the emphasis of parametric instability research should be on suppression schemes.

Modelling   [106, 107, 108] already showed that 3MI signal gain had extreme sensitivity
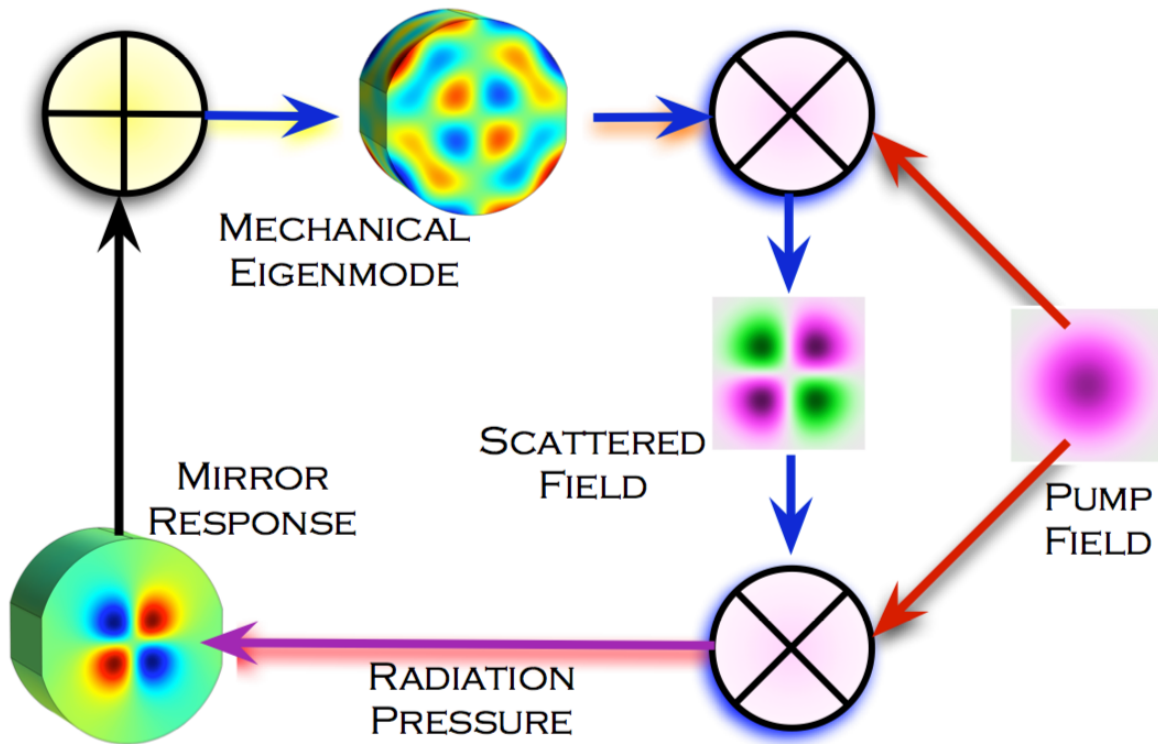
Figure 29: Schematic diagram of the parametric instability mechanism [105]

to metrology errors. This result carried the message that 3MI monitoring could be very sensitive, but its usefulness was not recognized because the main concern at the time was to suppress the few interactions for which the parametric gain could exceed unity as these represent parametric instability. Using selected modes with gain between 10e-1 and 10e-3 that have been shown experimentally to be easily observed with excellent signal to noise ratio, we would be able to monitor the interferometer global state variations. Because of the complexity of the information that the 3MI provides, further efforts in modelling and experimental research is required to make the 3MI to be a practical monitoring tool.

5.2.11 Mirror Substrate Research: Charging

There is a wide range of charging research currently underway in the LSC groups. A viable solution to the charging problem for Advanced LIGO exists and additional backup scenarios are under further development. This work is performed in conjunction with the Suspensions Working Group.

Surface charge may build up on the test masses through a variety of mechanisms, including contact with dust (particularly during pump down) and/or the earthquake limit stops, removal of First Contact used to keep the optic clean during transport and handling, as well as cosmic ray showers. There is evidence from initial LIGO that charging of the optics has occurred and noise has visibly increased from hitting earthquake stops. There are several

mechanisms by which the interaction between changes on the optic and charges on nearby surfaces can generate force noise on the optic. One noise mechanism is that a static charge distribution on either the optic or the earthquake stop will couple motion of the earthquake stop into forces on the optic [T080214].

Another mechanism is the noise caused by time-varying charge distributions on the optic (or the earthquake stop) resulting in time-varying forces on the optic. Gaussian noise from this mechanism can be described by a Markov process [T960137]. The result depends on the magnitude of the deposited charge and the correlation time of the deposited charge, with a smaller actuating noise for correlation times far from the reciprocal of the frequency at which the noise is being measured. These correlation times are being measured using scanning Kelvin probes operated in vacuum which measure the magnitude and distribution of surface charges and their rate of motion across a sample. Current results indicate that the correlation times depend on the type of silica, but can be very long for very clean samples, leading to current estimates that this need not be a significant noise source for Advanced LIGO. Continuing work will focus on examining a variety of silica types, different cleaning and handling methods (including ways of applying and removing First Contact), and optics with a variety of coatings (which will be characterized as they are developed in the coating research program). Understanding what sensitivity limits might come from charging and how this may depend on cleaning and handling is crucial for Advanced LIGO. Depending on results, it may prove an important area of research for upgrades.

Charge may also interact with the electro-static drive to be used in Advanced LIGO causing noise or reduced effectiveness of the drive. Modeling has been started to study this, and experimental work at LASTI at MIT has begun to better understand the role of charge with the electro-static drive. There have also been two experimental verifications of a charging contribution from dielectric polarization of the fused silica [G1200853, P1000077]. Further experimental and theoretical work is planned on polarization noise. Calculations have also been carried out to estimate the force noise that might be expected from Coulomb interactions between charge accumulations on the test mass and various components in the suspension system. The earthquake stops being the closest to the test mass surfaces are of greatest concern for most issues with charge on the optic [T080214].

Charge mitigation investigations The primary solution to mitigating charge in the advanced detectors involves blowing nitrogen gas across needles at 4kV AC, which ionizes the gas externally to the vacuum chamber [G1000383, T1000135, T1100332]. The nitrogen ions, which comprise both polarities, travel through an aperture and into the vacuum tank. As this is essentially a thermally driven process, with charge on the optic attracting the appropriate polarity of ion to provide neutralization, it is unlikely that any damage to the HR coatings will occur, although tests are currently underway to assess this issue. A prototype system has been demonstrated at MIT and work is ongoing to test this technique on the monolithic noise prototype at LASTI. The discharge procedure would require approximately 1 day of downtime for the detector. In addition to the above technique, alternative discharge strategies are also being developed.

Shining UV light on in situ optics has been investigated as a way to mitigate charge buildup. This involves testing UV LEDs, developing AC driver electronics, and performing experi-

ments to determine if the UV can cause harm to the optics or their coatings. Coated optics are tested by subjecting them to UV light for days to weeks at a time, then are re-measured for optical absorption and mechanical loss. Results on tantala/silica optics indicate that UV can cause increased optical absorption and thus this method is not deemed suitable for aLIGO. An interesting variation of this technique utilizes the fact that charging events arising from contact with earthquake stops will deposit charge in this local region. Furthermore, there are a number of interesting coating materials for future upgrades to aLIGO and 3rd generation detectors, including Al-GaP, AlGaAs, hafnia, zirconia, and others, that might allow for UV charge control, and this line of research is currently being considered.

Experimental work on low energy ions as a way to mitigate charge without the need for UV exposure has also been extensively studied. These ions can be brought into contact with the charged optic through either a partially directional gun or from a low pressure vent of the entire vacuum chamber. UV light is also being explored as a way to generate low energy ions, somewhat combining these two approaches. Work on utilizing a DC glow discharge to generate both polarities of charge carriers in Argon has also been shown to mitigate charge on the surface of fused silica [P1100033]. The technique uses a Faraday cup to maintain a neutral flow of ions which can be used to flow over the surface of the optic. Although tests do not show any absorption change at the level 50 ppm, the possibility of performing further tests in the Stanford photo-thermal common path interferometer are being considered to verify this approach. Any DC glow discharge technique is likely to be considered a backup to the above ionisation technique.

There are other ideas being developed to measure charge and eliminate it as a problem for LIGO optics. Developing and testing finite conductivity coatings is also an important area of research. Here, the influence of charge on the coating surface will be reduced by having a lightly conductive coating under the dielectric stack, which will support a compensating image charge plane. This will mitigate the effect of surface charges interacting with nearby support structures, particularly the earthquake stops. The conductive coating can then be effectively grounded by UV photoemission conduction, between the optic and support structures. Work is ongoing on conductive ion beam sputtered layers composed of alumina doped zinc oxide (AZO), and measuring the relationship between electrical conductivity, optical absorption, and mechanical loss. A "UV electron photoemission wireless conduction" system has been developed, and tests verify that it can ground the test mass to less than a 10 V potential. The UV source will consist of UV GaAs LED's and photoelectrons will be generated from the earthquake stops and from the facing surfaces on the side of the test masses. To reduce potential disturbances, no bias and or active controls will be used. Similarly, we have developed an electric field measurement system that meets following requirements: (i) compatible with integration into the earthquake stops (ii) capable of measuring the potential of the test mass opposite the earthquake stops to an accuracy of equal to or better than 10 V. Further tests on the prototype aLIGO suspension will be pursued.

Charge noise measurements It would also be useful to directly measure noise from charging, to confirm both the Weiss Markov-process noise model and the parameters found from the Kelvin probe work. Torsion balances, which have been used for laboratory gravity experiments and to test noise models of LISA, offer another possibility to verify Markov

noise from charges. Torsion balances are well suited to this since they reach their highest sensitivity at frequencies where Markov charge noise is expected to be large. For charge studies, the torsion pendulum will need to be made entirely of an insulator, likely fused silica, which is a departure from previous experience. The LSC group at the University of Washington, which has experience with torsion pendulums through LISA and other research programs, has performed studies of charging noise [G1000367]. Additional torsion balance experiments are also being developed at University of Glasgow [G1100714] and Moscow State University. In Glasgow, a torsion bob comprising fused silica discs is being utilized to study charge motion on the surface of fused silica and the level of charge deposition when fused silica surfaces come into contact. A Kelvin probe located within the vacuum tank also allows the correlation time to be measured. Initial results suggest that the Weiss theory does give an accurate estimation to the level of charge noise [G1300213, P1300078]. Further tests are planned with zinc oxide coatings which have the possibility of providing well defined characteristic correlation times, thus allowing the level of charge noise to be varied in a reproducible way. Research at Moscow State University is focusing on the exploration of noise associated with dielectric polarization induced when an electrostatic drive (ESD) is operated near a fused silica test mass [G1200166]. The experimental setup includes a monolithic torsion oscillator with frequency of 63 Hz fabricated entirely from fused silica.

5.3   LIGO Voyager

The proposed move to silicon mirrors operating at 120,K and at 1550 nm will require further research into silicon as an optical material, continued development of suitable low thermal noise coatings and measurement of a wide range of properties of these coatings at low temperature. Many of the research areas and techniques mentioned in the previous section are relevant to LIGO Voyager, but applied to different materials and with many of the measurements required to be carried out at low temperature.

5.3.1   Mirror coating research: Mechanical Loss

The thermal noise of a system depends on the level of thermal energy and the amount of dissipation. For many optical coating materials, the mechanical loss actually increases at cryogenic temperatures. Thus using coatings designed for room temperature at cryogenic temperatures will see less improvement in the thermal noise than one might naïvely assume. Thus the shift to cryogenics will require the development of new mirror coatings.

Crystalline Coatings   Single-crystalline coatings grown by molecular beam epitaxy are of signficant interest as a possible alternative to current amorphous coatings. This is likely to be of particular relevance for low-temperature detectors, as the cryogenic dissipation peaks observed in current silica and tantala coatings are thought to be related to the amorphous structure of the materials. There are multiple crystalline coatings under investigation within the LSC; among them are aluminum gallium arsenide, AlGaAs, and aluminum gallium phosphide, AlGaP. General factors which require investigation for crystalline coatings include adhesion to substrates at cryogenic temperatures, scattering, and fabrication on curved mirror substrates.

Aluminum Gallium Arsenide, AlGaAs GaAs:AlGaAs coatings[18] have been studied as free-standing micromechanical resonators for use in quantum optomechanical experiments, and have been shown to have very low mechanical losses (as low as 4.5×10^{-6}) at cryogenic temperature. In addition, good optical properties have been demonstrated, with the lowest optical absorption measured to be approximately 10 ppm. However, these coatings are grown on GaAs substrates, and would require to be transferred and bonded onto appropriate mirror substrates for use in gravitational wave detectors. The method of epitaxial lift-off is well established, and has been demonstrated for AlGaAs coatings on flat substrates up to 150 mm in diameter. The application of this technique to curved mirrors requires some development, and it is essential to study these coatings after transfer to appropriate substrates to evaluate any additional mechanical loss and scatter which may be associated with the bonding process.

Aluminum Gallium Phosphide, AlGaP AlGaP and GaP are lattice-matched to silicon, allowing a reflective coating to be grown directly on to a silicon mirror substrate, eliminating the need for coating transfer and bonding. Initial measurements of the mechanical loss at room temperature were limited by thermoelastic damping in the silicon substrate: however, these measurements did allow an upper limit of approximately $< 2 \times 10^{-4}$ to be placed on the coating loss at room temperature. Continuing to characterize the loss and optical properties of these coatings at cryogenic temperatures is also of very high priority. These coatings are more typically grown on GaP substrates, and thus further development of the techniques for growing these coatings on silicon substrates is desirable [109].

Amorphous Coatings In addition to the proposed design of Voyager to operate at 120 K planned future detectors such as the Einstein Telescope in Europe and KAGRA in Japan will operate at cryogenic temperature to reduce thermal noise. It is therefore essential to fully characterize the performance of coating materials at cryogenic temperatures. In particular, the mechanical loss can be a strong function of temperature and low temperature loss peaks have been observed in silica, tantala and titania-doped tantala coatings. While these loss peaks will lessen the potential reduction in thermal noise obtained from cooling, there is still some benefit to operating these coatings at cryogenic temperature. For example cooling to 20 K would provide a reduction in coating thermal noise by a factor of about 2, rather than the factor of 4 improvement which would be expected if the coating loss was constant with temperature.

Cryogenic mechanical loss measurements of coating materials are also a valuable tool for exploring the microscopic processes responsible for energy dissipation. Identification and analysis of Debye-like loss peaks allows key parameters of the dissipation mechanisms to be calculated and, coupled with atomic modelling and structural measurements, may allow the association of loss peaks with particular types of atomic motion within the coating structure.

There has recently been significant progress in understanding the loss mechanisms in tantala coatings, with analysis of cryogenic loss peaks providing information about the dissipation mechanisms, and structural studies and atomic modeling revealing correlations between structure, doping level and loss. The level of loss in tantala below 100 K is strongly dependent on heat-treatment and doping level, and continued studies to optimize coating composition and post-deposition annealing may yield further improvements in coating thermal noise. The

results are consistent with a model in which transitions of atoms between energetically stable positions are responsible for the loss, and suggest that the atomic structure of the coating is a key factor in determining the loss.

To enable further reductions in coating thermal noise there is an ongoing effort to identify coatings with a lower mechanical loss at cryogenic temperatures. A number of research paths are being pursued, including further improvement of current silica/tantala coatings, the use of alternative coating materials, particularly amorphous silicon high-index layers, tantala doped titania, silica doped hafnia and titania, nm-layered silica/hafnia and silica/titania composites.

For cryogenic coatings, amorphous silicon is a leading candidate for a high index material. Amorphous silicon (a-Si)coatings can have a particularly low mechanical loss, with recent measurements placing a conservative upper limit of 5×10^{-5} on the loss angle of ion-beam sputtered $\alpha - Si$ below 50 K. In addition, the high refractive index of silicon allows thinner coatings with fewer layer pairs. The use of a silicon/silica coating could potentially reduce coating thermal noise by a factor of 2.4 at 20 K compared to a silica/tantala coating. However, the first measurements of optical absorption in these coatings suggest that significant efforts to understand and reduce the absorption may be required. However, the effect of the high absorption could be signifcantly reduced through the use of 'multi-material' coatings 5.3.2, and the use of heat-treatment has been shown to be effective in significantly reducing the absorption of aSi films. Recent work carried out within the LSC has shown that amorphous silicon films deposited using an ion-beam sputtering system with a novel electron cyclotron resonance ion source can have optical absorption a factor of up to 50 lower than other, commercially available ion-beam sputtered aSi coatings. Finally, the absorption of aSi can be a factor of ~7 lower at 2000nm than at 1550nm, so a move to a $\sim$ 2000nm laser could also be useful for enabling the use of aSi coatings.

It has been shown that infusing hydrogen in the silicon coating can significantly reduce the loss, thought to be related to passivating dangling bonds. Studies to test this for ion-beam sputtered coatings and to evaluate the effect of hydrogenation on the optical absorption should therefore be carried out. However, the hydrogen can diffuse out of the silicon, reversing this effect. Nevertheless, the usefulness of dopants to improve the mechanical loss is clear. Recent work also suggests that deopisiton of aSi films at elevated temperature (400°C) can result in signficant reduction of the mechanical loss due to an increase in the structural order of the film. The effect of deposition at elevated temperatures on the optical absorption is therefore an important area of study.

Studies of different deposition methods for aSi are also if interest. In particular, chemical vapor deposition is a more mature technology for aSi deposition than ion-beam sputtering (used, for example, for solar cells) and allows for relatively straightforward tuning of the deposition process including control of doping and stress.

Measurements of hafnia coatings indicate that, even when in a partially poly-crystalline form, this material has a lower loss than tantala at temperatures below 50 K. Preliminary results [110] seem to indicate that amorphous TiO_2 may also be almost exempt from a cryogenic loss peak. Experience with tantala suggests that poly-crystalline structure may significantly increase the loss. One method of preventing crystallization of hafnia films is doping with silica and it has been shown that this does not significantly increase the loss at room temperature.

Silica doping is also effective in stabilizing Titania against crystallization [94]. Layered nm-scale silica-titania (and alumina-hafnia) can also be annealed at high temperatures. Low temperature loss measurements of silica-doped hafnia coatings are underway. Cryogenic loss measurements on Tantala and Silica doped Titania, and nm-layered Hafnia/Silica and Titania/Silica composites are also being planned.

There have been reports on the particularly low cryogenic mechanical loss of stressed amorphous silicon nitride films (LIGO-G1300171 and LIGO-G1400851). The composition of this material is highly process-dependent and is possible to make both high and low refractive index SiN_x films by varying the composition, leading to the possiblitiy of an entirely CVD-grown, SiN_x based HR coating.

Diamond-like carbon (DLC) coatings may also be of interest for further study, as there is evidence in the literature that the loss of this material is very low, with some films having a lower loss than amorphous silicon.

Studies of other possible alternative amorphous coating materials should continue, and where possible the choice of material (or treatment regime e.g. dopant, doping level, heat-treatment) will be informed by the results of structural measurements and modeling. While most of the effort to date has focussed on developing alternative high-index coating materials for use at low temperature, it should be noted that silica coatings also have a cryogenic loss peak of a similar magnitude to that observed in tantala. Thus more studies of possible alternative low-index materials are required. In this connection, silica doped Hafnia (or nm-layered Hafnia-Silica composites) could be an interesting candidate low-index material, with a refractive index of ≈ 1.5. This could be used with Tantala doped titania (or silica doped titania, or nm-layered titania-silica composites) for the high-index material (with refractive index ≈ 2.15), to achieve a contrast comparable to that of the silica/tantala HR coatings presently in use, hopefully featuring much better cryogenic behaviour.

Shear and bulk loss angles   Understanding the mechanical loss angles associated with bulk and shear motion is of interest for any candidate coating for LIGO Voyager, and suitable finite element modeling will be required to support experimental investigations. Extension of this work to crystalline coatings, where separate loss angles are expected to be associated with each crystal axis, is required.

5.3.2   Coating Research: Coating Design

nm-Layered Composites   Planar layered composites consisting of nm-scale alternating films of titania and silica are increasingly stable against crystallization, as the (titania) layers thickness is reduced [96]. These composites behave as homogeneous materials as regards their optical and viscoelastic properties, for which simple and accurate modeling is available. Crystallization inhibition up to very high annealing temperature has been also observed in nm-layered hafnia-alumina composites[97].

Optimized Coatings   Since the thermal noise in the coatings typically scales as the total thickness of the more lossy material (although there are recent reports of mechanical loss be-

ing different in tantala with different thicknesses), reducing this thickness while maintaining the optical properties will reduce thermal noise. Constrained numerical optimization codes have been shown to produce high reflectivity coatings while reducing the volume of high index materials by as much as 20%. Thermo-optic noise from thermoelastic and thermore-fractive effects is included in this optimization. At low temperature, where the loss of the low-index silica layers becomes more significant and may in some cases be greater than the loss of the high-index layers, a very different optimization may be required.

Multi-material coatings The use of multi-material coatings to take advantage of the properties of different materials has been proposed [102, 103]. In particular, it may be possible to exploit the fact that most of the incident light intensity is reflected by the first few bi-layers of a coating, potentially allowing coating materials with higher optical absorption, but lower mechanical loss, to be used in the lower layers of a coating stack without significantly increasing the total absorption of the coating stack. This type of design may allow the use of aSi in the lower part of a coating stack, taking advantage of both the low mechanical loss and high refractive index of this material.

5.3.3   Coating Research: Optical Properties

Optical absorption Measurements of coating absorption at cryogenic temperatures are required for the proposed Voyager design. As with the mechanical loss, the optical absorption can be strongly dependent on doping and annealing. These dependencies should be investigated for any proposed coating in order to minimize both mechanical loss and optical absorption. As noted above, Si is one of the most promising low mechanical loss coatings for use at low temperature, however, the absorption of aSi coatings is currently significantly higher than required, and further development is required.

Optical Loss from Scattering In order to maintain the highest optical power in future detectors, it is important to minimize the optical scatter. Scatterometer measurements should be conducted for proposed coatings and new coating materials. Studies of the dependence of scatter on coating materials and manufacturing parameters are important in determining the lowest possible scatter. Realizing more sophisticated quantum non-demolition (QND) topologies also requires extreme low-loss optical systems as is explained in section 4.2.1 for the case of filter cavities. One of the important sources of optical loss is scattering from mirror-surface aberrations. These are traditionally investigated by measuring the angular distribution of scattered light (i.e. measurements of the bidirectional scattering distribution function (BSDF)), or scanning the surface with lasers and integrating the scattered light in spheres. As much as these measurements are important to link scattering from mirrors with losses in optical systems like cavities, they do not give direct information about the cause of scattering.

Assuming that point-like defects residing in the mirror coatings are the dominant source of scatter loss, one has to investigate individual defects for their material compositions, morphologies, and structures. The answers can be used to understand the origin of the defects with the goal to improve the coating process. Various analysis methods are available.

Defect morphology can be studied optically or with force microscopy depending on defect size. Defect materials can be investigated spectroscopically. The analyses should progress from larger to smaller defects since the larger defects dominate the point-defect scatter even if they are significantly less numerous.

5.3.4 Coating Research: Other Coating Properties

Thermo-optic Noise

Young's Modulus and Stress   The Young's modulus of a coating is required both for the analysis of mechanical loss measurements and for calculations of the level of coating thermal noise. It is therefore important to obtain accurate values of Young's modulus for every coating, and post-deposition coating treatment, studied. Measuring the temperature dependence of Young's modulus will be of particular importance for LIGO Voyager, and this capability should be developed.

Residual stress in coatings is likely to be an important property, and there is interesting evidence suggesting that stress can alter mechanical loss of coatings, particularly in silicon nitride. Therefore studies of the effects of residual stress on the loss and of methods of altering the stress in particular coatings are of interest. The use of several measurement techniques can be beneficial in these studies, as each technique has different systematic errors and, for example, different sensitivity to the properties of the coating substrate material.

Uniformity   As discussed in 5.2.6, coating uniformity is important to avoid transmission and scatter of light out of the cavity mode and into other optical modes and can lead to limits on the optical power and squeezing. With larger optics proposed in Voyager, maintaining coating uniformity will be even more challenging and thus an important research topic. The limitation on obtainable uniformity can come from metrology limitations, so improved metrology is an important research direction. An additional research direction is to explore corrective coatings, which place additional coating material onto a coated optic after uniformity measurements have been made.

Production Variables   Variations in the loss of nominally identical coatings from different vendors have been observed, suggesting that the precise deposition parameters may be important in determining the loss. Thus more detailed measurements of the effects of parameters such as ion energy, sputtering ion, oxygen pressure and thermal treatment may be valuable. While ion beam sputtering produces the lowest optical loss coatings, the mechanical loss of coatings deposited by other techniques has not been extensively studied. Studies of coatings deposited by different techniques (e.g. magnetron sputtering, e-beam evaporation, atomic layer deposition) may enhance understanding of the relationship between loss and structure in these materials.

Coating layer thickness may also prove an important variable in determining amorphous material properties, especially mechanical loss. There are suggestions that very thin, much less than a wavelength, layers may have improved mechanical loss. This may be related

to stress and/or annealing properties of thin coatings. If this effect can be confirmed and understood, it is possible to design high reflective coatings with much lower thermal noise using known materials like tantala and silica.

5.3.5   Coating Research: Structural Studies

There is currently little understanding of the mechanical loss mechanisms in amorphous or crystalline coatings, although it seems likely that in the amorphous case the loss mechanism is related to the local atomic structure and may involve transitions of two-level systems as is believed to be the case in fused silica. Studies of the structure of amorphous coatings, aimed at understanding links between structure, composition, loss and optical properties, are a critical part of the research required to develop coatings suitable for use in LIGO Voyager. The suite of structural investigation and atomic modeling techniques discussed in 5.2.7 will also be applied to interesting candidate materials for Voyager, and used to inform the mechanical loss studies outlined above. Understanding structural defects in crystalline coatings is also likely to be an important area of research.

5.3.6   Coating Research: Direct Thermal Noise Measurements

Direct measurements of thermal noise, as described in 5.2.8, are also of interest on coatings suitable for use in LIGO Voyager. In cases (e.g. crystalline coatings) where thermo-optic noise cancelation is required to get the thermo-elastic or thermo-refractive noise below the Brownian noise, Q measurements alone cannot truly probe the thermal noise limits.

5.3.7   Reduced Coating and Coating Free Optics

Several ideas have been proposed to reduce the mirror thermal noise by reducing the required coating thickness or removing the coating altogether, including:

- Corner cube style retro reflectors

- Brewster angle prism retroreflectors

- Khalili cavities as end mirrors

- Diffraction gratings

While some of these techniques may be more appropriate for consideration for use in LIGO Cosmic Explorer, some of them may provide possible alternative solutions to the coatings for LIGO Voyager. Corner reflectors and Brewster angle mirrors would allow for no coatings to be needed and Khalili cavities would allow for much thinner coatings than conventional mirrors. Experimental work is needed to test some of these concepts for practical limitations. A bench experiment has been done forming a cavity with one Brewster angle mirror and one conventional mirror on fixed suspensions to see if a high finesse cavity can be formed. Follow on work with suspended mirrors will be necessary to evaluate the mechanical stability of such a system. The new prototype interferometer at the AEI in Hannover is slated to test Khalili cavities as a way of reducing coating thermal noise.

Diffraction gratings   All-reflective interferometers using diffraction gratings as optics avoid problems associated with the transmission of large laser powers through optical substrates. Moderately high finesse optical cavities have been demonstrated using small gratings. The challenge will be to scale up the optical aperture to what is required for a large detector. In addition, absorption by the grating surface can distort its surface profile, possibly resulting in changes in the beam profile as well as power-dependent changes in the diffracted beam shape and efficiency. Modeling has been done along with sample produced, but these effects need to be investigated more in depth. Investigations of mechanical loss in gratings are needed to verify thermal noise levels as are direct thermal noise measurements. Demonstration of high reflectance values is also important.

5.3.8   Mirror substrate research

Silicon   The OWG is investigating alternative materials to fused silica for use as test mass substrates for use in low temperature detectors. Both silicon and sapphire potentially offer superior performance at cryogenic temperatures and/or at particular frequency bands. Different substrate materials, operating temperatures, and laser wavelengths may also require and/or allow for different coatings and suspension connection techniques that must also be studied.

Previous research efforts on silicon have largely focused on acquiring and fabricating cylindrical test specimens and investigating their mechanical properties as a function of doping. Studies of silicon properties, including mechanical loss for predicting thermal noise, of different crystal orientations are valuable. In addition, silicon cantilever micro-resonators with resonant frequencies in the sub-kHz range have been fabricated to explore dissipation mechanisms in a regime where thermoelastic effects are significant. Surface loss effects are also emphasized by the large surface-area to volume ratio of the micro-resonators. Preliminary experiments measuring the dissipation have been carried out and reveal disagreement with theoretically predicted loss.

Understanding the optical loss of silicon if used as a transmissive optic at 1550 nm is also a useful area of research. The high thermal conductivity of silicon could significantly reduce the effects of thermal loading of transmissive components if the optical loss is low enough. Understanding the temperature dependence of light absorption along with all other thermo-optic and thermophysical properties is important. Silicon might also be used as the high index material in coatings. Research will be required to develop suitable components if a change in wavelength is considered. Silicon mirrors and suspension elements have an advantage of being conductive thus control of charging effects may be easier to implement. Nonetheless, charging will need to be investigated since doping and especially coatings can influence the charging dynamics.

Investigations of the wavelength dependence of the absorption of silicon is of interest, as it may be beneficial to consier operating at a longer wavelength to reduce or eliminate two-photon absorption effects.

Sapphire   Recent efforts have yielded information about the mechanical and optical properties of sapphire, methods for growing and processing large sapphire blanks, and ways to

achieve high homogeneity, low absorption sapphire. Studies on annealing for improved optical absorption have been extended to elucidate further details of the kinetics of the out-diffusion process. Gathering experimental data at low temperature is important to predict the performance of cryogenic sapphire test masses. The KAGRA project is pioneering this effort. Room temperature sapphire is also a potential mirror substrate for detectors optimized at higher frequencies. Measurements of mechanical properties including mechanical loss as a function of crystal orientation are also important for predicting substrate and coating thermal noise.

5.3.9 Mirror Substrate Research: Parametric Instabilities

As discussed in 5.2.10, parametric instabilities are a potential problem arising from high laser power. These undesirable effects result from exchange of energy between light stored in cavities and acoustic modes of the cavity mirrors. Experimental research and modelling of parametric instabilities, and possible suppression techniques, in silicon mirrors at high power levels will be required.

5.3.10 Mirror Substrate Research: Composite Masses

Increasing the mass of the test masses reduces the influence of both classical and quantum radiation pressure noise. Beyond a certain size, however, it is impractical to fabricate monolithic masses. Using large masses made as a composite of multiple, smaller pieces could circumvent this problem. Non-cylindrical mass distributions could also be used to increase the total mass and total angular moment of inertia without increasing the optical pathlengths within the substrate. The larger translational and angular moments of inertia would reduce the radiation pressure noise and the influence of the Sidles-Sigg instability. Thermal noise issues related to mechanical loss from the interfaces will have to be resolve

5.3.11 Mirror Substrate Research: Charging

The use of semi-conductor silicon optics will require several new areas of research into charging.

- Silicon resistivity at low temperature. Determination of the resistivity and time constants of charge motion on silicon at cryogenic temperatures. At these low temperatures the free carriers begin to freeze out. Work could assess the charge mobility on high purity silicon substrates with resistivity at the level few thousand ohm m with Kelvin probe, 4-terminal measurements and electromechanical oscillators

- Coating charging. R&D is necessary to assess the time constant of charge motion on the surface of coatings necessary for cryogenic detectors. Materials include amorphous silicon and crystalline coatings based on GaAs and GaP. There is further potential to link closely to work of the Optics group via the development of coatings with low mechanical loss and electrical conductivity. Pushing the performance of future detectors to lower frequencies (1-10Hz) will require the assessment of charge noise mechanisms.

These include surface charge with low mobility on the surface of coatings, charge motion in silicon surface/substrates and the interaction of these charges with the electric field of the ESD and nearby grounded hardware.

- Study of discharge mechanisms including (i) utilising He gas rather than N2, (ii) mono/multi layers of gas adsorbed on surfaces (iii) pumping time at low temperature (iv) charging mechanisms.

5.4   LIGO Cosmic Explorer

While optics research targeted at LIGO Cosmic Explorer is rather more speculative and long term, it is clear that research on optical components for future ground-based interferometers must begin well in advance of any complete conceptual design. One important consideration will be the operating temperature of LIGO Cosmic Explorer, and research into the temperature dependence of both the thermal noise and the optical proprieties of coatings and mirror substrates will be critical in informing this choice. Thus all of the research avenues detailed in the previous sections for substrates and coatings for use at room temperature and at cryogenic temperature are potentially of strong relevance for Cosmic Explorer.

It should be noted that some of the promising technologies discussed in the LIGO Voyager section, in particular AlGaP and AlGaAs crystalline coatings, have not yet been demonstrated on the scale required for future gravitational wave detector mirrors. Technical restrictions, such as the maximum available diameter of GaAs substrates on which AlGaAs can be grown, may potentially restrict or prevent the use of these coatings in Voyager. However, on the time-scale of Cosmic Explorer, it seems more likely that some of these technical issues may be overcome. In addition to this, research into improved amorphous coatings should continue to be pursued. As discussed above, some amorphous coatings (e.g. aSi) have already been demonstrated to have mechanical loss factors that are equivalent to or better than those measured for crystalline coatings, and further progress with modeling and theoretical understanding of the properties of these materials may allow both mechanical loss and optical absorption to be optimized. Finally, other concepts for making mirrors without coatings (e.g. waveguide mirrors, consisting of coating-free structured surfaces), or with a much reduced coating thickness, are also of interest and further research into the application of these methods to large-scale interferometer mirrors is of interest.

6   Suspensions and Vibration Isolation Systems

The research of the Suspension and Isolation Working Group (SWG) is aimed at providing the necessary isolation, alignment, and control of the interferometer optics from seismic and mechanical disturbances while simultaneously ensuring that the displacement due to thermal noise of the suspended systems is at a suitably low level. To first order we can divide the research into two broad subdivisions, suspensions and isolation, both of which involve mechanical and control aspects. Suspension research involves study of the mechanical design of the suspensions, the thermo-mechanical properties of the suspension materials and suitable techniques for damping suspension resonances and applying signals for interferometer control. Isolation system research involves mechanical design and active control for isolation and alignment. The overall isolation of the optics comes from the product of the two systems.

The isolation and suspension system for the most sensitive optics in Advanced LIGO is comprised of three sub-systems: the hydraulic external pre-isolator (HEPI) for low frequency alignment and control, a two-stage hybrid active & passive isolation platform designed to give a factor of ~ 1000 attenuation at 10 Hz, and a quadruple pendulum suspension system that provides passive isolation above a few Hz. The final stage of the suspension consists of a 40 kg silica mirror suspended on fused silica fibers to reduce suspension thermal noise.

The R&D for baseline Advanced LIGO isolation and suspension sub-systems is complete. These systems are in operation at the LIGO facilities, and were successful during Advanced LIGO's first Observing run. Upgrades to the Suspension and Seismic Isolation and Alignment System are grouped into four broad categories: In section 6.1 we describe ongoing work on immediate improvements and risk reduction for the baseline Advanced LIGO detector. In section 6.2, we describe the A+ improvements which can improve the baseline sensitivity without substantially altering the existing equipment. In section 6.3 we describe the Voyager R&D which will make more substantial changes and allow us to operate with cooled optics, and finally in section 6.4 we describe the long term work on suspension and isolation systems which build the foundation for the ultimate ground-based gravitational wave detectors.

6.1   Vibration Isolation R&D for Incremental Upgrades to Advanced LIGO

There is ongoing R&D work to provide incremental improvements to Advanced LIGO to improve performance of the aLIGO vibration isolation and suspensions, and improving the duty cycle of the observatories by making the instruments more capable of withstanding high winds and teleseismic earthquakes. This type of work is designed to be easily incorporated with the existing detector systems with minimal disruption of the Observatories. These upgrades include work to add additional environmental sensors and incorporate them into the controls, adding more sophisticated control algorithms to improve performance during unusual environmental conditions, small mechanical changes to damp vibration modes, and relatively modest changes to the facilities.

6.1.1   Tilt/horizontal coupling and advanced seismometers

One of the limits to the performance of seismic isolation systems is the coupling between ground tilt and horizontal motion of the isolation platforms. This is fundamentally caused

by the inability of a horizontal sensor (or a passive horizontal isolation stage) to distinguish between horizontal accelerations and tilts in a gravitational field.

This tilt-horizontal coupling causes a variety of problems and is a basic limit to the performance of the isolation systems at low frequencies (below ∼0.3 Hz) [111]. Seismic motion in the 30-300 mHz region is governed by the microseism, wind and large earthquakes. Excess motion in this band affects the locking of the interferometer and consequently the duty cycle of the observatories. It may also affect noise in the GW band by frequency up-conversion through non-linearities in the interferometer control. The aLIGO HEPI and ISI systems are now limited by the tilt-horizontal coupling at low frequencies, and an external sensor could be easily integrated into the system to reduce amplification of low frequency ground motion.

We are developing sensors to measure the rotational acceleration of the ground or of stages of the seismic isolation system in vacuum, which could be used to remove the rotational component, creating a purely translational horizontal sensor and/ or reduce the rotation of the stages. Several rotational sensors have been investigated in the past [112, 113, 114, 115] and two approaches are currently being pursued. These include:

1. A tiltmeter based on a low-frequency flexure-beam-balance with an optical readout has been developed which looks very promising [116]. Two of these instruments were installed at the LIGO Hanford Observatory and have been shown to reduce tilt-noise in a co-located seismometer by factors of ∼10 below 0.1 Hz under windy conditions. Recent studies suggest that incorporating these sensors into the isolation control system is beneficial to the interferometer, enabling locking under higher wind speeds than before. A compact and UHV-compatible version of this instrument with an interferometric readout is also being developed which is suitable to be mounted directly on the ISI. Such an instrument has the potential to significantly improve the angular control of the ISI and further reduce the low-frequency differential motion of the platforms.

2. Suspending a horizontal seismometer. This approach is distinct from the others in that the seismometer is made to passively reject tilt noise, thus producing a tilt-free horizontal sensor [115].

Work has also been proposed on a variety of other technologies for making gyroscopes. Work on passive ring gyros [114] has concluded, and some investigations into Atomic Spin Gyroscopes has been undertaken [117, 118].

Demonstrations of gyroscopes have shown us that the ground tilts can be measured in our frequency band of interest. The goal now is to measure these ground tilts reliably and with low noise, to distinguish the tilt from ground translation, and to use this information improve the performance of the observatories when the environmental noise from the wind and the microseism are causing trouble for the interferometer control systems.

6.1.2   Wind Mitigation

The largest driver of tilt on the technical slabs at the LIGO Observatories is the wind. In addition to measuring the tilt as described in section 6.1.1, work has recently begun to reduce the wind driven tilt of the buildings. The tilt effects are seen most clearly at the

End Stations where the End Test Masses are located. The Hanford detector currently has difficulties when the wind speed exceeds about 10 meters per second. The wind causes tilting of the slab between at least 10 mHz to 1 Hz. It has been suggested that wind breaks could reduce the force loading on the buildings and thereby reduce the typical tilt of the slabs during windy times [119]. Preliminary work has begun to design and test ways to install wind breaks at the Hanford End Stations. Since the amplitude of the spectrum of ground tilt seems to scale with the square of the wind speed, even modest reductions of the wind speed at the building could potentially have large pay-offs in improved duty cycles of the instrument. This work would be completely complementary to the work on better measurement of the ground tilts. Transforming our large, unmeasured tilts into medium sized and well measured tilts would allow us to reduce the excess motion of the isolation platforms below 100 mHz.

6.1.3 Pier Motion Control

The motion at the top of the HEPI piers is significantly higher than the ground motion, especially in the horizontal direction. A set of solutions have been suggested to address the problem [120]. We have recently shown that the amplification is due to motion of the bending piers and the attachment of the payload to the pier top [121]. The FE model is being updated with new experimental results. These results shed considerable light on an old problem, and enable research on how to address the problem. Solutions to mitigate this motion amplification will be proposed and studied. Both passive (reinforcement, truss, cross beams, cables) and active solutions (feedback shaker on the chamber, active tendons) should be considered.

6.1.4 Control System Enhancements for the Existing System

Advanced LIGO has an impressive array of sensors and a flexible control system. Most of the baseline Advanced LIGO control schemes use local information to control the seismic platforms and Interferometer readouts to control the interferometer lengths and angles. As system integration proceeds, studies need to be conducted to investigate optimal ways to combine all the sensor information to achieve the best interferometer performance. For example, using feedforward to directly cancel the contribution of ground motion signals which appear in the interferometer signal was demonstrated in Enhanced LIGO [122]. Studies on the coherence between various channels from the ground, up through the seismic platforms and suspension systems to the various interferometer readouts should be conducted. When coherent contributions are found, they could be used to inform the development of advanced control techniques to be layered onto the existing controls. Other control improvements have also been suggested such as optimally distributing the control authority between the isolation stages [49] to improve system locking and robustness, and changing the control laws in real time in response to changing environmental conditions [49, 123]. We often experience variations in the local environment arising from many difference sources such as wind at the Hanford Observatory, storms in the gulf of Mexico with cause large microseismic motions, logging near the Livingston Observatory, and teleseismic earthquakes (those far from the Observatories). We can now accurately predict the arrival of the teleseismic waves from these distant earthquakes [124], but can not yet adjust the control parameters to better compensate for the motions.

Another question which needs to be answered is "what in particular limits the upper unity gain frequencies of the isolation control loops for the Advanced LIGO seismic isolation platforms?" A clear understanding of the practical limits could be used to inform a campaign to modify the platforms to achieve better isolation performance, particularly in the 5-40 Hz band. For example, a numerical study has shown that a high frequency blend with a force sensor (even a virtual force sensor) may help to increase significantly the controller bandwidth of the active isolation stages,without compromising the isolation [125, 126]. This technique will be further studied on more elaborate models.

An interesting risk reduction idea would be to develop a fail-operate control system for the seismic isolation platforms. These systems use position sensors, geophones and seismometers in their control loops. While these instruments have very low failure rates, we cannot exclude the possibility that one of them could stop working during operations, thus compromising the functioning of the platform and the interferometer. It is therefore important to study methods to monitor performance of the sensors, actuators, and the mechanical plant to help mark when the behavior of a component begins to degrade, and to identify which component is malfunctioning. A set of basic Matlab scripts have been developed to perform this task [127] but those functions are difficult to use in the observatory environment and can only be used while the interferometer is offline. A realtime estimator system could be developed to continuously compare the expected and actual performance of the system so that diagnostics could be run continuously in the background. In the event of a problem, it is also important to study "emergency control schemes" that would allow the platform to keep operating with a malfunctioning sensor. Feedforward techniques to either compensate for the loss of performance, or possibly reconstruct the lost signal are good candidates. Control schemes accounting for the failure of each type of sensors should be proposed and studied.

There is ongoing research on the controls for the Suspension system. We have recently demonstrated a technique called 'Global Damping' to reduce the sensor noise from the Suspension which couples into the Interferometer [128]. Global damping also reduces the interdependence of damping and IFO length control. This technique could be incorporated into the control system at the Observatory and studies should be done to investigate its utility for the full-scale interferometer.

Testing of adaptive control schemes have be done [49] to automatically adjust the trade-off between damping strength and feedthrough of sensor noise in the GW band. Tests are also planned to study damping methods of the bounce and roll modes within the monolithic section. As described above, studies of how to distribute the control authority (hierarchical control) are underway, both for control of a pendulum chain, and also for offloading pendulum control to the seismic isolation system.

6.1.5   Suspension Design Updates

Upgrades to specific suspension designs are being considered as potential near-term improvements for Advanced LIGO [129]. First, the current size of the beamsplitter optic (37 cm diameter) was established early in the Advanced LIGO design, and is the limiting optical aperture. Retrofitting the detector with a larger beamsplitter optic would enhance optical performance. This will require design changes to the beamsplitter triple suspension itself

and its supporting structure [130, 131]. Also under consideration is the addition of actuation on the beamsplitter optic. Currently global control signals are applied to actuators at the middle mass of the beamsplitter triple suspension. Actuation directly on the optic would allow wider bandwidth operation to improve lock acquisition.

Secondly, noise in the signal recycling cavity (SRC) length coupling into the GW readout may be a greater noise source than we would like. In particular the highest vertical and roll modes (around 28 and 41 Hz) in the small and large HAM triple suspensions (HSTS and HLTS) potentially add noise in the GW band. This noise could be addressed by adding a third stage of cantilever springs at the middle masses of the HSTS and HLTSs, taking the vertical mode below 10 Hz and increasing the overall vertical isolation. Preliminary design work has begun on this possible modification [132]. An alternative, also under consideration, is the addition of passive dampers which would reduce the peaks at the highest vertical and roll modes at the expense of modest increase in thermal noise performance on the wings of the peaks. Their design could be similar to that for the quads, discussed below.

Thirdly some improvements to the test mass quadruple suspensions are also underway. Work by colleagues in the LISA area and subsequent follow-up by LSC groups has shown that enhanced gas damping in small gaps could lead to excess noise in aLIGO suspensions [133, 134, 135]. In the current suspensions there is a small 5 mm gap between the end test mass and end reaction mass to allow sufficient actuation force for cavity locking using electrostatic drive (ESD). A new design of reaction mass has been developed which is donut shaped to reduce the squeezed film damping associated with this small gap. [136]. The outer dimensions and material are the same as the present mass, with a central hole $\approx$ 220 mm in diameter. Since this mass will be lighter than the currently suspended reaction masses, the penultimate reaction mass design requires modification to increase its mass to compensate, so that the existing blades are still correctly loaded. It is anticipated that the new reaction masses may be installed after the second observing run.

Two other developments for the quad suspensions are also underway associated with damping high Q modes. We have developed a non-magnetic damper for the upper intermediate mass blades to suppress the thermal excited motion at the internal modes of the blade [137]. We have also developed passive dampers, so-called BRDs (bounce and roll dampers), to reduce the size of the bounce and roll mode peaks around 10 and 13 Hz associated with compression and extension of the silica fibers between the test mass and penultimate mass [138]. Both types of dampers are currently being installed at LLO and we will see how they perform when the detector comes online again.

6.2   Research and Development for LIGO A+

The LIGO upgrades for A+ will require more substantial changes to the Suspension, Isolation, and Alignment subsystems. Suspensions may be replaced to take heavier test masses, and the beamsplitter may be enlarged if not already done. In addition to the improved isolation from ground motion, improved rejection of thermal noise is also being studied, although the system will remain at room temperature. The seismic isolation systems will remain largely unchanged, but could be improved with higher performance sensors. It may require adjustments to the mounting to allow more space for proposed longer suspensions.

6.2.1 Larger Main Optics

Studies are underway to explore the design of improved suspensions for the 4 main optics (the 'Test Masses') of Advanced LIGO. It has been shown that by increasing the mass from 40 kg to 80 kg, and increasing length of the final suspension fiber to 120 cm, the thermal motion of the optic can be lowered by a factor of 2 from the current design [139]. By using 160 kg test masses and 120 cm long final suspensions, the thermal noise of the suspension can be improved so that it is 3 times better than the current design. However, work needs to be done to optimize the entire suspension design [140] so that it has good overall seismic isolation. Work needs to be done to show how to fit this larger, heavier suspension onto the existing Seismic Isolation Platforms. One possibility is mount the longer suspension to the top of the final stage of the seismic isolation system, rather than the bottom, and interleave the suspension through the isolation system. A second option would be to raise the entire seismic isolation system up on its existing support structure. Since the optical table would need to move up substantially, it is not clear what the performance impact would be and it requires investigation.

6.2.2 Alternative Control Approaches for Larger Suspensions

The design and installation of larger optic suspensions gives an opportunity to revisit the design of the caging, sensing, and control of the pendulum system. One alternative approach is to merge a portion of the suspension cage and the reaction chain [141]. This is a major design change, but could result in improved access and alignment and it would allow all the pendulum DOFs to be sensed and controlled. The reduced the mass of the combined cage and reaction structure would allow a more massive main optic.

6.2.3 Improved OSEMS

The Suspension sensors should be improved. A set of Optical Sensor/ Electromagnetic Motors (OSEMs) are used to provide actuation and local sensing for the Advanced LIGO suspensions. Improved sensors could be used to increase the damping of pendulum modes without compromising the performance, but making practical, low-cost units which have better performance than the existing OSEMs is a challenge. Studies are underway to provide better thermal stability and optical modifications to improve the signal to noise by a factor of two by adding a displacement-doubling prism to the optical system [142]. Another example of an improved sensor is the 'Euclid' interferometric sensors [143] but further development would be required to integrate those onto the existing pendulums and to make the sensors UHV compatible. Improved sensors may be necessary for LIGO A+ detectors.

6.2.4 Studies of the monolithic final stage

Extensive characterization (strength, dimensions, mechanical loss) of fused silica fibers as suspension elements [144, 145], produced using both oxy-hydrogen and laser-based pulling techniques [146], has been done. Welding techniques and silicate bonding techniques including characterization of associated losses [147] has been done, along with extensive exploration on the ear shape and fiber shape.

Several monolithic suspensions have been installed in Advanced LIGO. Integration of the suspensions into the Advanced LIGO interferometers will allow the first measurements of the ultimate noise performance of these systems in the 10 Hz to 40 Hz range. As the interferometer noise is improved, participation of experts will be critical to understanding the interferometer performance.

The first integration of a test mass into the interferometer resulted in 2 incidents of fiber breakage, one caused by an impact by a dropped part, and one caused by large excitations from a computer control system error. Studies of possible mechanisms for the fiber break, and methods to prevent future damage are underway.

Several areas of research could yield enhancements to Advanced LIGO suspensions. Further understanding and characterizing of losses in silica fibers including investigations of non-linear thermoelastic noise and of surface losses could lead to improvements. Changes in fiber neck shape including shorter neck and thicker stock could lead to enhanced thermal noise performance.

Research is also underway to further understand the role of weld loss in addition to techniques to observe and ameliorate stress in the weld regions. Furthermore, an increase in strength of the fibers could allow reduction in cross-section and in vertical bounce frequency, enhancing isolation. Investigations of the silicate bond mechanical loss and strength as a function of time and following temperature treatments are underway to reduce further the loss contribution and optimize ear design. As noted in 3.1.4, increased fiber stress can move the bounce/roll modes below 10 Hz which reduces the requirements on passive or active damping of these modes. A test suspension has been hanging at 1 GPa for 1 year at LIGO Hanford, and a further series of tests at stresses up to 1.5 GPa will verify the robustness of an engineered suspension. Such an upgrade can easily be incorporated into a 60 cm aLIGO QUAD system, or an upgraded longer/heavier system in A+.

6.2.5   Seismic Platform Interferometer

It is also possible to improve the performance below 1 Hz with an auxiliary system which reduces the differential motion and tilt of the various optical tables in the detector. This type of approach has been discussed for many years, and is traditionally called a 'Suspension Point Interferometer' (SPI), i.e., an interferometric sensor which measures between the points which suspend the arm mirrors [34].

The systems under investigation are slightly different; the method involves controlling the relative motion of the optical tables, and hence an alternative name is Seismic Platform Interferometer. The relative motion of the tables for this system will need to be measured in at least 3 degrees of freedom, namely length, pitch, and yaw. This will allow the detectors to be mounted securely to the table, and will also allow the benefits to be shared by multiple suspensions on the same table, a common situation on the HAM optical tables.

A prototype system has been demonstrated at Stanford [148, 149] using a fiber coupled 1.5 micron laser, which uses a Mach-Zender interferometer to measure the inter-platform length motion and an optical lever to measure differential angles. At the AEI 10m prototype, another SPI prototype is under development. It is based on a set of Mach-Zender

interferometers, and use a LISA style phasemeter for readout [150]. The rotational degrees of freedom (DOFs) are sensed via differential wave-front sensing. The target sensitivity is $100\,\mathrm{pm}/\sqrt{\mathrm{Hz}}$ and $1\,\mathrm{nrad}/\sqrt{\mathrm{Hz}}$ at 10 mHz for displacement and rotational DOFs respectively.

Considerable work remains to adapt either of these systems for use with Advanced LIGO (e.g. stable mechanical coupling to stage 1 of the HAM-ISI or stage 0 of the BSC-ISI, reliable UHV compatible fiber coupling, control integration). In addition, were this system to be used for the 4 km arms, then considerable work would be required to achieve the necessary laser frequency stability required to realize a beneficial system.

It should be noted that improved rotational sensing described in Section 6.1.1 and the SPI are complementary approaches to the low-frequency noise issue. It is also important to realize that since the optical tables for Advanced LIGO are controlled in all 6 degrees of freedom, once new SPI or tilt sensors become available, they can be incorporated into the existing control system easily, because the seismic tables will not require modification.

6.2.6   Improved Seismic Sensors

Future improvement of the seismic isolation performance will require the use of a very-low-noise inertial instrument, with noise performance roughly a factor of 100 better than today's GS-13. Such an instrument remains to be designed, built and tested. The requirements for the design of this instrument will include: very low sensitivity to temperature gradients, very low thermal noise, very low sensitivity to environmental and actuator electromagnetic fields, and very low readout sensor noise. Both horizontal and vertical instruments will be necessary for future seismic isolation upgrades. Several improved inertial sensors are now being studied [151, 152].

6.2.7   Mechanical Upconversion: Crackling Noise

Some sources of gravitational waves produce short, impulsive events in an extremely large body of data, and so characterization and reducing "background" transients of technical origin is important. Investigations of non-thermal noise originating in the fused silica fibers has been carried out with no non-thermal noise being seen at modest sensitivity (insufficient to exclude it as a significant noise source for aLIGO). Work has been done to study the noise associated with the violin modes of the silica suspensions in GEO 600 [153]. Further work has started to extend these studies by modeling and analyzing data from O1 and future engineering or science runs to put upper limits on this noise component in Advanced LIGO. Direct experiments to characterize the level of and/or put upper limits at a meaningful sensitivity level to potential non-Gaussian transient events associated with the Advanced LIGO suspension system are challenging. However new ideas for carrying out such experiments are encouraged.

One approach which is being pursued to observe impulsive releases of energy or acoustic emissions ("creak effect") is to strain the element statically while also driving the element through a large amplitude motion at low frequency below the measurement band, while interferometrically measuring the element at high sensitivity in band (above 10 Hz). By large amplitude motion we mean much larger (100∼1000 times) than the out of band motions

estimated through modeling. We will drive the large amplitude low frequency motions in a common mode fashion between two identical devices under test while measuring the noise which will be uncorrelated between the two elements. Experiments of this type are underway to measure or put upper limits on noise from maraging steel cantilever blades [154, 155] and separately from silicate bonds.

6.3 LIGO Voyager

The LIGO Voyager design represents a major shift in the LIGO design with adoption of cryogenic test masses. Investigations of moving to cryogenic temperatures have shown that they can provide significant improvements in the thermal noise, even with test mass temperatures as high as 120 K to 130 K. The LIGO Voyager design is based on the ideas presented in the 'Blue Team' design and incorporates a 150 to 200 kg silicon optic which is radiatively cooled to about 123 K with a cold-shield held at around 77 K. Increasing the mass of the interferometer mirrors will linearly reduce the displacement noise due to radiation pressure noise. Changing the size, mass, temperature, and material for the optic requires many changes across the detector, and especially close collaboration between the Optics Working group (see Section 5) and the Suspension and Isolation Working Group.

This design requires test masses and heat links (either to the mass or to the cooling shield) with excellent thermal and vibration properties. These are likely copper, but might also be silicon or sapphire. Any cold system will require an ultimate heat sink. Current cryocoolers, even those designed for gravitational wave detectors [156] are not free from vibration, and the heat transport properties of heat links are limited. Thus, it is essential that studies of systems with suspension elements of suitable design and dimensions to provide an efficient path for required heat conduction while still maintaining good thermal noise and mechanical isolation performance be carried out, and followed with experimental demonstrations. A possible way to reduce the requirements of the heat links is to shorten them by having flowing liquid nitrogen in pipes within the main vacuum system. Chilling the nitrogen could further reduce the requirements on these heat links.

6.3.1 Experimental Demonstrations of Cooled Optics

Cooling the optics without compromising their vibration performance is a significant challenge, and experimental demonstrations are critical to the long-term engineering success of the progrom. These experiments are now underway [157, 158, 159, 160]. It has recently been realized that the scattered light from the optic will be a significant heat load for the cryogenic shield. It is critical that we demonstrate technology capable of removing the heat from both the absorbed laser power in the optic and the scattered power from the optic which is incident on the cryoshield – while maintaining vibration levels small enough to prevent upconversion of the scattered light returning from the shield back into the interferometer beam.

Another of the challenges to implementing a cryogenic silicon suspension is extracting the required heat in a reasonable amount of time. A purely radiative cooled suspension with a 150 to 200 kg silicon test mass will require cool down periods to 120 K on the order of weeks at best to months at worst. Research is currently underway to investigate the benefits and

feasibility of introducing a cool down period which incorporates aggressive cooling technology that would not be permitted during Observing Runs. Current research is focussing on the methods of convectively cooling the suspension in a dry atmosphere and contacting the suspension stages with a movable cold link [157].

Methods of maintaining room temperature detector infrastructure near the cold suspension stages should be pursued. This issue is particularly relevant for Advanced LIGO hardware that will be reused in a future cryogenic system. Notable components that might be influenced are suspension springs, electronics, and sensors and actuators.

Materials   Investigations of materials suitable for construction of elements of the isolation and suspension systems with good properties for use at cryogenic temperatures should be studied ,e.g. silicon carbide which has excellent stiffness to weight ratio (specific stiffness) and low thermal expansion constant and silicon, which has excellent thermal conduction properties and high specific stiffness.

Passive damping of structures at low temperatures is also an area of concern. Viton is quite lossy at room temperature, and is vacuum compatible, and so is used extensively in Advanced LIGO to help control structural vibrations above 80 Hz. Unfortunately, handbook values [161] indicate that it is not effective at cryogenic temperatures, so investigations into replacements should be undertaken.

Integrated Control of Cryogenic Suspensions   The design and installation of new optic suspensions should be accompanied by a careful design of the caging, sensing, and control of the suspension and final optic. One alternative approach to the Advanced LIGO design is to split the suspension cage into a warm and cold section and to combine the structures of the cold portion of the cage with the cryogenic shield [160].

6.3.2   Low noise cantilever blade springs and improved suspension thermal noise

There are a variety of techniques being explored which could improve the room temperature thermal noise of the suspensions [25]. It is possible to improve dissipation dilution by increasing suspension length or thickening fiber ends to enhance energy distribution (e.g. 5 mm stock rather than 3 mm stock).

Studies are also underway to understand how to lower the first 'bounce' mode of the test mass. Development of fused silica or silicon blade springs which could be incorporated in the final monolithic stage for improved vertical isolation compatible with lower thermal noise is an attractive option to explore for possible upgrades to Advanced LIGO and future interferometers. Sapphire is also a possible material choice. Experiments are already underway to investigate the breaking stress for such materials when used as blades.

6.3.3   Silicon Suspensions

Silicon has attractive thermal and thermo-mechanical properties making it a strong candidate for the suspension elements in future detectors possibly operating at cryogenic temperatures

to reduce thermal noise. It is also conductive which may have advantages for controlling charging effects (discussed elsewhere). Development and measurement of suitable suspension flexure elements, including studies of the optimum material, thermal noise properties, and the geometry and assembly of elements including methods of bonding to test masses are being pursued [139]. Analysis techniques include the use of FEA to study the various contributions to thermal noise such as surface loss and bond loss. Investigation of fabrication techniques, properties of silicon- silicon bonds such as strength and thermal conductivity and thermo-mechanical properties of silicon, for example as a function of doping, are examples of areas which can be addressed.

Suspension elements are being fabricated via two methods (i) laser heated pedestal growth, and (ii) mechanical fabrication from wafers. The laser heated pedestal method is being pursued in both sapphire and silicon. With this technique surface tension is used as the "crucible", resulting in the purest fibers. It is expected that the strength and thermal conductivity of these pristine fibers should be high, and this will be tested once samples are available. Sapphire is an easier material in principle to grow as it absorbs efficiently at 10.6?m, from the CO2 heating laser. Silicon undergoes a "metallic" phase transition resulting in a change in emissivity during melting, and this might prove an interest control problem to maintain the melt temperature. Mechanical etching/machining silicon ribbons has already been used to make short (5 cm) long suspension fibers. This technique has been shown to reduce fiber strength by approximately one order of magnitude (300 MPa) compared to the pristine material (4 GPa). This is likely to be caused by a damage layer. Oxidizing/ wet etching the samples has been shown to improve the strength by a factor of 2, possibly due to healing these damaged layers. We are currently investigating alternative protection coatings such as Diamond Like Carbon (DLC), in addition to thermally-grown oxide coatings and magnetron sputtered silica coating. In addition, the effect of edge polishing the silicon flexures and argon plasma pre-deposition treatment is being investigated.

Attachment techniques A slightly modified version of silicate bonding for silicon-silicon attachment for, e.g., the attachment of interface pieces to silicon test masses is well underway. Strength measurements at both cryogenic and room temperatures of these bonds has shown it is a viable attachment technique and investigations are ongoing to further understand the influence of different parameters on strength like the nature and thickness of the oxide layer required. Bond loss measurements on silicon test masses have also started producing initial results.

Alternative attachment techniques to silicate bonding may be investigated, e.g., to eliminate shear stress in any contact point in the mirror suspensions.

6.4   R&D for LIGO Cosmic Explorer

The baseline concept for Cosmic Explorer is to use the Voyage Technology for the isolation of the optics. The technology envisioned for LIGO Voyager should be of such performance that the direct seismic coupling is below the noise of a cryogenic mass, and that the motion at 10 Hz is dominated by Newtonian Noise, even though local seismic arrays are used to eliminate at least 90% of that noise.

7   Lasers and Auxiliary Systems

The Lasers and Auxiliary Systems working group (LAWG) developed out of the Lasers working group. In addition to all types of *classical* lasers (squeezing is part of the Quantum Noise WG), this group now includes auxiliary systems which encompasses all technologies which are not part of any of the other working groups.

The following sections are organized in terms of the needs and requirements for LAX systems according to the road-map (section 2) It lists the identified technologies and research areas with respect to A+, LIGO Voyager and LIGO Cosmic Explorer and closes with research areas and R&D that is relevant to all envisioned detectors.

7.1   A+

Some small upgrades to aLIGO may be possible between major observing runs, given sufficient technical readiness and scientific payoff. The following section lists R&D areas that need continuous efforts for the A+ time frame.

7.1.1   Advanced LIGO PSL

The development of the aLIGO pre-stabilized laser system (PSL) is finished [162]. A four stage Nd:YVO amplifier system is used to increase the 2 W power of a Nd:YAG non-planar ring-oscillator (NPRO) to 35 W [163]. An injection locked Nd:YAG end-pumped rod system was chosen as the high power oscillator. It was shown that an output power of more than 200 W in a linear polarized single spatial and frequency mode with such an aLIGO laser system [164] can be emitted. The laser has been developed and built by the GEO group in Hannover (Laser Zentrum Hannover (LZH) and Max-Planck-Institut für Gravitationsphysik / Albert-Einstein-Institut AEI). All PSL systems have been installed or are in storage for LIGO India. Although all PSL systems have been running nominally it is becoming clear that such complicated systems can develop problems when being run over long stretches of time and several longevity issues have come up.

The task and goals for A+ are to provide continuing technical support for the PSL system, to address problems that arise from continuous running over long times and to further monitor the long term stability and operating parameters of the laser.

7.1.2   Faraday Isolator in Squeezing Systems

Faraday isolators are required to separate the counter-propagating beam from the incoming beam. The aLIGO Faraday isolators use TGG as the Faraday material. The TGG rotates the polarization angle by an amount proportional to the length of the crystal, the Verdet constant, and to the applied magnetic field. The main issues with the Faraday isolator are beam distortion due to laser heating and subsequent thermal lensing, a reduction of the optical isolation due to depolarization and changes in the temperature dependent Verdet constant. This is further complicated by the fact that the FI is usually placed inside the vacuum chamber following the suspended input optic mode cleaner.

The power handling capabilities of the output Faraday isolator are far less critical. However, the optical losses inside the Faraday would currently limit the amount of usable squeezing. Since squeezing is one of the leading ideas to 3rd generation detectors, any improvement in the optical losses could directly improve the range of these detectors.

Figure 30 shows how the losses in the squeezed beam path are strongly affecting the amount of squeezing detectable in the interferometer and therefore the improvement in the sensitivity. With 10 dB of squeezing injected, for instance, the losses need to be less than 20% in order to be able to detect at least 6 dB of squeezing.
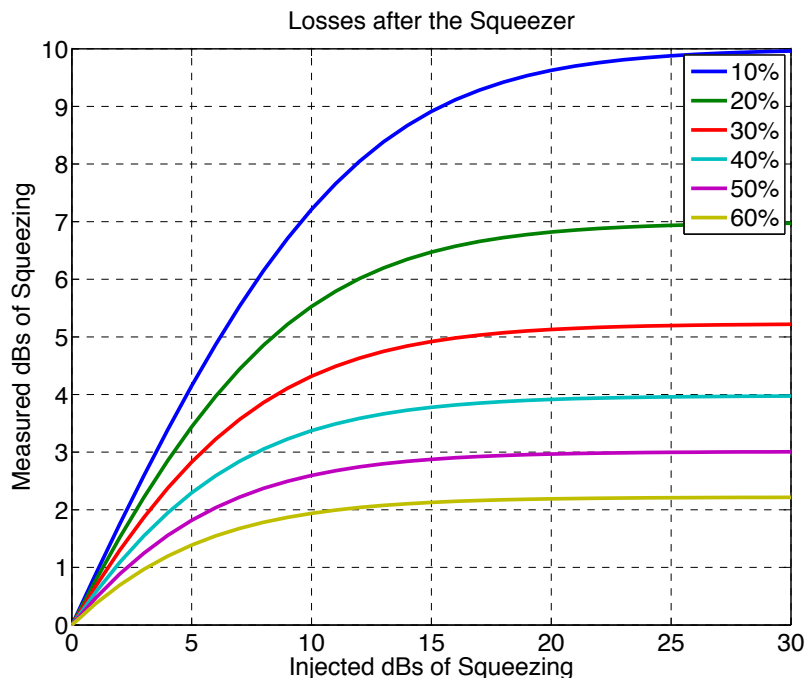
Figure 30: Measured squeezing as function of the injected squeezing for different levels of losses in the squeezed path.

In a typical layout for injecting squeezing in the interferometer the squeezed beam needs to pass through not only the main output Faraday of the IFO (twice), but also at least one additional Faraday to isolate the interferometer from the squeezer and mitigate noise from back scattered light. The losses of the new Advanced LIGO Faraday have been measured to be $\sim$ 4%. Similar measurements in initial LIGO Faradays give losses of 4 - 6%. With the current losses the Faradays themselves will account for about 15% of the losses in the squeezed path. In order to maximize the benefit from the injection of squeezed light, it is important to reduce the losses of a single Faraday to 1 - 2%.

For the main dark port Faraday, it is also important to reduce the amount of light which leaks into the squeezed beam path, as this is a source of noise once it is back scattered back into the IFO from the squeezer source. In the new Advanced LIGO Faraday about 0.5% of the light which passes through the Faraday is reflected by the thin film polarizer. By improving the mechanical design of the Faraday one can hope to reduce this percentage down to $\sim$0.01%.

7.1.3   Laser Stabilization

Power stabilization will probably be the most demanding laser stabilization task in future gravitational wave detectors. Technical power noise on the laser can couple via many paths into the gravitational wave channel: asymmetric arms and radiation pressure noise, deviation from the dark fringe, radiation pressure noise. Advanced LIGO requires a relative intensity noise (RIN) of around $10^{-9}/\sqrt{\text{Hz}}$ in the interferometer input beam. The accurate sensing of the needed 500 mW laser power at that location is difficult and the signal is still contaminated by pointing, polarization, and potentially even frequency noise. Ongoing research is needed to understand these couplings and reach the required stabilities.

7.2   LIGO Voyager

The LIGO Voyager design mitigates limiting noises of aLIGO by allowing moderate changes to the LIGO detectors without affecting the vacuum envelop but with possibly including cryogenic temperatures of 120 K. The following section list R&D related to those improvements.

7.2.1   PSL LIGO Voyager

The road map for the general description in section 2. The designs call for laser wavelengths of 1.5μm and longer to be compatible with silicon optics at cryogenic temperatures. Non cryogenic systems could continue to use fused-silica optics and would require 1μm laser wavelengths. As the final sensitivity depends on the power inside the interferometer the input power can be traded against power recycling gain without affecting the fundamental noise limits. However, the power recycling gain is limited by the optical losses inside the arm cavities as well as the contrast defect at the beam splitter. Typical typical power levels for the lasers required for the next stage are envisioned to reach up to 1 kW.

High power concepts - 1030-1064nm   At this time the Nd doped YAG gain medium is the best choice for 100 W class gravitational wave interferometers. However, in the future if kilowatt class lasers become necessary Yb doped YAG, which operates at 1030 nm, could replace the Nd system because of its higher efficiency, lower quantum defect, better thermal management and potentially longer-lived laser diode pumps. Its main disadvantages are that it is a quasi-3-level system at room temperature and thus more sensitive to increased temperatures within the gain medium, and that it has a much lower pump absorption coefficient. However, at cryogenic temperatures, the quasi-3-level system turns into an efficient 4 level system. The Adelaide group demonstrated already 200 W, with diffraction limited beam quality for all power levels, requiring no thermal compensation, at 1030 nm from a cryogenic Yb:YAG laser using a single zig-zag slab [165].

There is a substantial commercial interest driving the development of both Yb lasers and their pump diodes for very high power applications.

High power concepts: 1550-1650nm   Erbium doped fiber lasers and Er:YAG lasers emit between 1550 and 1600 nm where the absorption in silicon is expected to be very low. Commercially available erbium fiber systems include a master laser and a fiber amplifier and achieve output powers of 10 W in single mode, single frequency operation and higher power levels are expected in the near future.

The GEO group is currently working on the development of a 1550 nm light source with a power level of 50 W while the Adelaide group plans to transfer their cryogenic Yb:YAG technology to a resonantly pumped cryogenic Er:YAG lasers to generate several 100 W of laser power at 1617 nm.

High power concepts - 2μm and longer   To avoid or reduce 2-photon absorption in Silicon wavelengths of 2μm or longer are desirable. Ho:YAG and Tm:YAG lasers are possible candidates but more research is needed to find the most suitable laser medium and to demonstrate the feasibility of a 2μm PSL.

Additional Requirements   Many different applications drive the laser development worldwide and it appears that nearly every year improved laser systems become commercially available. However, there is currently no application which has similar stringent requirements on the temporal and spatial stability as gravitational wave detectors. Hence a specific laser development program for 3$^{\text{rd}}$ generation detectors will be required to design and build a reliable laser with sufficiently low free-running noise, an appropriate spatial beam profile and good controllability. Such a program could include spatial mode filters and adaptive optics to improve and match the spatial eigenmode to the interferometer eigenmode.

7.2.2   Photodiodes

Advanced LIGO is currently using four in-vacuum photodiodes in parallel to measure the required 500 mW of light [166]. This is a sub-optimal arrangements for several reasons including reliability and alignment issues. To get a quantum limited measurement of the power fluctuation of 500 mW of light, new photodetectors need to be developed with sufficient power handling capability, spatial uniformity and quantum efficiency. First experiments showed that back-illuminated InGaAs diodes show promising features. However neither the spatial uniformity nor a sufficiently high quantum efficiency has been demonstrated so far. Furthermore current power stabilization experiments seem to be limited by 1/f electronic noise in photodiodes. The origin of this noise needs to be better understood and either the noise source has to be reduced or easily applicable selection criteria need to be found to get the best devices from the available vendors.

Further R&D in close collaboration between the material and device experts, electrical engineers and groups that can test the photodiodes is needed to develop better photodiodes for LIGO Voyager and later generation gravitational wave detectors, especially with respect to the longer 1.5μm to 2μm wavelength range where quantum efficiency is currently inferior to 1μm systems.

7.2.3   Electro-Optic Modulators

Length and alignment sensing schemes rely heavily on the generation of optical sidebands which co-propagate with the carrier field into the interferometer. These sidebands are currently generated by RTP-based electro-optic modulators which withstand several 100 W of continuous laser power without degrading the beam profile. LIGO Voyager and LIGO Cosmic Explorer detectors are likely to work at different wavelengths and/or at higher power levels for which suitable electro-optic modulators are not yet available or have not been tested. The main problems encountered in high power applications are photo refractive damage and variations in optical path length across the beam profile caused by the residual absorption of the laser beam.

Photo refractive damage has a fairly well defined threshold in specific nonlinear crystals and can be increased by doping the crystal. The most promising family of crystals in the near infrared region are crystals belonging to the $MTiOXO_4$-family such as RTP; M is an alkaline metal such as K, Rb, or Cs, and X is either P or As. These crystals have fairly large electro-optical coefficients, good thermal properties, and, in principle, very low optical absorption coefficients between 1 and $2\mu m$ laser wavelength. Optical absorption in the $MTiOXO_4$-family increases at lower wavelength and potentially limits the laser power to a 10's of Watts for visible lasers.

β-barium borate (BBO) and its derivatives are often used in the visible and near-UV region of the spectrum. BBO is uniaxial and has a very high damage threshold. Values larger than 3 kW/cm^2 for cw-light have been quoted by multiple vendors. It's negative thermo-optical coefficient prevents self-focusing. However, the electro-optical coefficient is low compared to other electro-optical crystals and BBO appears to be of limited value unless the laser wavelengths is reduced to well below 500 nm.

Magnesium-oxide doped lithium niobate (MgO:LiNbO$_3$) might be a potential alternative for IR lasers. The doping increases the photo refractive damage threshold significantly [167] and the crystal has a $\sim 10\%$ larger modulation coefficient than RTP. However, going to laser powers beyond 1kW and laser wavelength below 1 um requires significant testing of electro-optical materials to ensure that electro-optical modulators will be available for LIGO Voyager and future detector generations.

7.2.4   Faraday Isolators

The aLIGO Faraday isolator uses two TGG crystals, a quartz rotator, and a waveplate to compensate the depolarization inside the TGG crystals. It is optimized to suppress thermal effects that would distort the laser mode. Scaling this to kW-class power levels requires further reductions in the optical absorption in TGG while the large number of components already increases the number of ghost beams significantly. Other options are to increase the Verdet constant by cooling the crystal, to use stronger magnetic fields, and to use other magneto-optical materials such as GGG or YAG.

Increased absorption in TGG will likely prevent the use at wavelength longer than 1.3 μm and in addition make the crystals very long. At 2 μm the crystals would need to be twice as long as the 12 mm crystals used in aLIGO, but the telecommunication sector developed

ferromagnetic rare earth iron garnets (RIGs) such as yttrium iron garnet (YIG) and more recently $\{BiRE\}_3(FeGaAl)_5O_{12}$ to rotate the polarization. Unlike paramagnetic Faraday materials, these ferromagnetic materials can be magnetized such that they don't require any external magnetic field. These materials are typically grown in sub-mm thick films on lattice-matched substrates such as GGG for 45 deg rotation. However, the absorption is still in the 1-10 ppm/cm range at interesting wavelengths which prohibits high power laser operation. At shorter wavelength, optical absorption increases in all materials pronouncing thermal effects. Faraday isolators using potassium dihydrogen phosphate (KDP) and its isomorphs have been developed for the UV but the absorption is still fairly high. A targeted research program to study these materials at higher power levels at all interesting wavelength (1.06 μm, 1.5 μm and 2 μm), is required to develop Faraday isolators for the next generation of gravitational wave detectors.

7.2.5 Cryogenics

It has long been known that cryogenically cooled test masses can have much improved material parameters which lead to significant reductions in thermal noise. However, operating at cryogenic temperatures presents multiple new challenges which need to be addressed. The most pressing is to find ways to cool the temperature, to isolate the mirrors from their hot surroundings and to constantly extract the deposited laser heat without short-circuiting the suspension and seismic isolation system. Detailed thermal models have to be developed and tested to maximize radiative and conductive cooling paths.

An additional challenge is the strong possibility of contamination through condensation on the surfaces. Methods will need to be developed to (i) mitigate the level of contamination in cryogenic mirrors, (ii) quantify the magnitude and type of contaminants, and (iii) if necessary, clean contaminated mirrors in situ. One idea which should be pursued is to use fs laser spectroscopy to identify the contaminant and potentially also to remove it.

Cryogenics: Radiative Cooling Operation at cryogenic temperatures poses formidable challenges including heat extraction from the cooled test masses, required both under steady state operation and for cooling from room temperature in a reasonable time. The system needs to work without adding noise or short-circuiting the mechanical isolation. In the steady state, the circulating power may be in the range 0.5 to 1 MW, and with anticipated coating losses of 0.5 to 1 ppm, power loss in the arm coatings is of order 0.3 to 1 W per optic. For cooling a reasonable estimate is between 2 and 100 W of heat conduction from the test masses to the cold environment.

Studies are underway of a novel method of heat removal: near-field radiative coupling between two objects: one hot and one cold. The basic idea is that many thermal fluctuations in the hot object do not couple to radiation; instead, they produce evanescent fields outside the object. If a cold object with appropriate properties is introduced into this evanescent field region, energy is transferred, cooling the hot object. This approach is potentially capable of removing more than 200 W from a test mass. The heat transfer can be greatly enhanced using a small gap but this is accompanied by force coupling and this effect needs to be taken into account. Room-temperature experiments to explore this method of heat transfer have

observed and are characterizing in detail the heat transfer in the near-field regime. Cryogenic experiments are planned, as are measurements to determine the effects of coatings on the heat transfer, and to attempt to optimize the coatings for maximum transfer with spacing around 0.1-1 μm.

7.3   LIGO Cosmic Explorer

The current LIGO facilities, while extraordinary in their capabilities, present significant limitations to potential long term improvement. The Ultimate stage will allow for a complete redesign and major expansion of the detector. The following topics are future developments within this project phase.

7.3.1   PSL for LIGO Cosmic Explorer

Most ideas regarding the LIGO LIGO Cosmic Explorer detectors target the low frequency performance where the sensitivity is limited by radiation pressure noise, thermal noise and Newtonian noise and not by shot noise or the available laser power. The laser needs for silicon test masses for these detectors can probably be met by LIGO Voyager PSLs assuming that **both** types of lasers will be developed in time. To further explore the high frequency region of the GW-spectrum, potential further increases of the laser power might be required.

If new test mass materials other than silicon become available changes towards a shorter wavelength might be advantageous. Shorter wavelengths generally require thinner coating layers which could reduce coating thermal noise; however, it should be kept in mind that shorter wavelength also generate smaller beam sizes for identical cavity g-parameters. The general scaling of coating thermal noise with thickness of coating layers and beamsize is in first order independent of the wavelength (for identical cavity g-parameters). The most obvious way to reduce the wavelength is via frequency doubling a powerful 1064 or 1030nm laser but many other laser concepts are currently being explored by industry and many scientific institutions.

High power concepts - spatial mode filtering and adaptive optics   To convert distorted laser beam profiles into the target eigenmode of the interferometer either static or dynamic wave front correction systems or passive filtering will be required. Advanced LIGO uses optical cavities (the mode cleaner) to filter the fundamental 00-mode and suppress all higher order modes. This technology is slowly reaching its limits as the high power build up inside these optical cavities starts to distort the filter cavities themselves. Other spatial modes such as Laguerre Gauss 33-modes or Mesa beams require modified filter cavities which are resonant only for these specific spatial modes.

For higher power levels intrinsic problems are expected with the filtering method and hence dynamic adaptive beam correction methods should be designed. These could be based on well known Shack-Hartmann detectors and adaptive optic techniques currently employed in astronomical telescopes. These techniques have also significant commercial potential for many other high power laser applications.

7.4 General R&D

The R&D projects listed in the following section require constant improvements and are relevant to all envisioned detector generations, from A+ to LIGO Cosmic Explorer.

7.4.1 Auxiliary Lasers

Auxiliary lasers serve several functions in interferometric gravitational wave detectors.

- CO_2 lasers at 10 μm are used to write a heating pattern into the compensation plate placed next to the ITM.

- Diode lasers at various wavelengths are used together with Hartmann sensors to sense thermal deformations in the test masses and the compensation plate.

- Frequency doubled Nd:YAG lasers are injected at the end stations for lock acquisition of interferometer length degrees of freedom.

The status and planned R&D on these laser types is described as part of the subsystems they are used in: CO_2 lasers as part of the TCS actuation in Section 7.4.2, diode lasers for Hartmann sensors as part of TCS sensing and control in the AIC working group.

7.4.2 Thermal Correction System

The goal of the Thermal Correction System is to optimize the spatial mode inside the interferometer. This spatial mode can be degraded by imperfections in the mirrors caused by radii of curvature or surface figure errors as well as non-homogeneous heating of the optics by the science beam. Untreated, this will reduce the mode matching between the two arm cavities and the recycling cavities and change the beam size inside the interferometer. Advanced LIGO uses ring heaters to optimize the radii of curvatures of the ITMs and ETMs and CO_2 lasers to compensate the thermal lens in the ITM substrate by acting on the compensation plate [41].

Ring Heater   The ring heater has to meet several requirements. It has to generate a homogeneous heating profile with minimal heating of the suspension structure. Its location very close to the test masses requires that it has to meet very stringent cleanliness requirements. Advanced LIGO is currently using a ringheater which uses nichrome wire wound around a bent glass rod, an alternative design developed by the UF group sandwiches the nichrome wire between two alumina coated aluminum surfaces [168]. Both heaters are embedded inside a gold coated thermal shield to maximize the heat transferred to the mirror and minimize the radiative heat transfer into the suspension.

The heat loss at the end points due to thermal conductivity generates an asymmetric heating profile which will also distort the mirror surface and the thermal lens inside the substrate. At higher heating powers, these asymmetries will start to reduce the optical build-up inside the arm cavities and increase the contrast defect at the beam splitter. The development of

ring heaters which produce more symmetric heating profiles could already be crucial for high power operation in Advanced LIGO.

One way to reduce the heating by the ringheater or even eliminate it is to coat the barrel of the optic with a thin layer (a few microns) or an IR reflecting metal such as gold [41]. This would reduce the radial heat flow and homogenize the temperature distribution inside the substrate. Adding a gold barrel coating to the optics would have implication for other aspects of the design, notably thermal noise, charge mitigation, and parametric instabilities. Measurements of the mechanical loss of a thin gold coating indicate that the gold coating can be applied without adversely affecting thermal noise. Gold coating applied to the barrel for thermal compensation purposes might not reduce the optics modal Q's enough to cause significant improvement in parametric instability performance. Tests of a gold coatings interaction with possible charge mitigation schemes, including UV, should be explored. Results of these tests might require follow-ups with other materials and/or coating methods or with additional modeling. This technique may be ready for use in a 3$^{\text{rd}}$ generation detector.

CO_2 laser   Power fluctuations of the CO_2 laser are one of the dominant noise sources associated with the TCS. Commercially available CO_2 lasers do not meet the stringent requirements on power stability for Advanced LIGO during high power operation (125 W input power in the science beam) and R&D has started to develop better CO_2 lasers for Advanced LIGO.

A scanning (or, more generally, a directed-beam) thermal compensation system that can vary the compensation profile in real time without injecting noise into the signal band would be very valuable to correct non-radial symmetric beam distortions. Such a system could already be important for high power operation in 3$^{\text{rd}}$ generation detectors. This will require research on carbon dioxide or other potential heating lasers, to reduce noise and possibly boost power, and potentially on measurement and control issues. In addition, by moving to shorter wavelengths it might be possible to develop MEMS or other technology based spatial light modulators to allow a programmable heating beam profile.

7.4.3   Beam Shaping

Mirror thermal noise is one of the fundamental factors limiting the sensitivity of gravitational wave detectors. A Gaussian beam profile is not the best shape to average over thermal fluctuations and different, carefully chosen shapes allow for sensitivity improvements. Non-spherical mirrors, shaped to support flat intensity mesa profile beams, have been designed and fabricated using specialized coating techniques. These mirrors are being tested on a dedicated interferometer to assess ease of mode-matching and locking. Recent efforts have shown that the tilt sensitivity of the fundamental mesa mode agrees with expectations. It is possible to extend this study, producing useful alignment correction signals via the wavefront sensing technique. The Sidles-Sigg tilt instabilities must also be examined. In addition, continued modeling needs to examine how thermal effects alter the mode profile in a detector arm cavity and help develop thermal compensation strategies. One option involves depositing a static thermal compensation profile to mitigate these effects.

Modeling and experimental work is being carried out on Laguerre-Gauss and other optical

modes that show promise for reducing thermal noise. Laguerre-Gauss modes may avoid some of the instability issues that cause concern with mesa beams. There are, however, questions about the strict requirements on the figure and polish of the optics necessary for these higher order modes. There has been modeling of the effects of different beam shapes on parametric instabilities. Further modeling and experimental testing will be necessary to truly evaluate the potential and limitations of these beam shapes.

7.4.4 Photon Calibrator

The calibration of the interferometer requires to move the mirrors by a known amount and observe the changes in the gravitational wave channel. One way to apply the required forces to the test masses is photon pressure. This photon calibrator uses an amplitude modulated auxiliary laser which is reflected off the test mass. The integration, calibration, and performance of the photon calibrator is still an ongoing research subject and improvements include multiple simultaneous modulation frequencies and beam localization.

References

[1] Einstein Telescope Science Team, "Einstein gravitational wave Telescope conceptual design study," *ET Document: ET-0106C-10*, 2011. http://www.et-gw.eu/.

[2] C. D. Ott, Y. Chen, and R. X. Adhikari, "Astrophysical Motivations for the Third Generation LIGO Detectors," *LIGO Document: LIGO-P1200099*, 2012. https://dcc.ligo.org/cgi-bin/private/DocDB/ShowDocument?docid=87934.

[3] J. Miller, L. Barsotti, P. Fritschel, and M. Evans, "Prospects for doubling the range of Advanced LIGO," *LIGO Document: LIGO-T0900144*, 2014. https://dcc.ligo.org/LIGO-P1400164.

[4] S. Chua, B. Slagmolen, D. Shaddock, and D. McClelland, "Quantum squeezed light in gravitational-wave detectors," *Classical and Quantum Gravity*, **29**, 145015, 2012.

[5] J. Abadie and et al., "Enhanced sensitivity of the LIGO gravitational wave detector by using squeezed states of light," *Nature Photonics*, **7**, pp. 613–619, 2013.

[6] H. Grote, K. Danzmann, K. Dooley, R. Schnabel, J. Slutsky, and H. Vahlbruch, "First Long-Term Application of Squeezed States of Light in a Gravitational-Wave Observatory," *Phys. Rev. Lett.*, **110**, 2013.

[7] M. Stefszky, C. Mow-Lowry, *et al.*, "Quantum squeezed light in gravitational-wave detectors," *Classical and Quantum Gravity*, **31**, 183001, 2014.

[8] P. Kwee, J. Miller, T. Isogai, L. Barsotti, and M. Evans, "Decoherence and degradation of squeezed states in quantum filter cavities," *Physical Review D*, **90**, 062006, 2014.

[9] H. J. Kimble, Y. Levin, A. B. Matsko, K. S. Thorne, and S. P. Vyatchanin, "Conversion of conventional gravitational-wave interferometers into quantum nondemolition interferometers by modifying their input and/or output optics," *Phys. Rev. D*, **65**, 022002, 2001.

[10] J. Harms and et al., "Squeezed-input, optical-spring, signal-recycled gravitational-wave detectors," *Phys. Rev. D*, **68**, 042001, 2003.

[11] M. Evans, L. Barsotti, P. Kwee, and J. Harms, "Loss in long-storage-time optical cavities," *Physical Review D*, **88**, 022002, 2013.

[12] T. Isogai, J. Miller, P. Kwee, and L. arsottiand M. Evans, "Loss in long-storage-time optical cavities," *Optics Express*, **21**, 30114, 2013.

[13] E. Oelker, T. Isogai, J. Miller, M. Tse, L. Barsotti, N. Mavalvala, and M. Evans, "Audio-band frequency-dependent squeezing via storage of entangled photons," *LIGO Document: LIGO-P1500062*, 2015. https://dcc.ligo.org/LIGO-P1500062.

[14] G. M. Harry, A. M. Gretarsson, P. R. Saulson, S. E. Kittelberger, S. D. Penn, W. J. Startin, S. Rowan, M. M. Fejer, D. R. M. Crooks, G. Cagnoli, J. Hough, and N. Nakagawa, "Thermal noise in interferometric gravitational wave detectors due to dielectric optical coatings," *Class. Quantum Grav.*, **19**, no. 5, 897, 2002.

[15] editors G. Harry, T. Body, and R. de Salvo, "Optical Coatings and Thermal Noise in Precision Measurement ," *CUP*, pp. ISBN–13: 978–1107003385, 2012.

[16] G. M. Harry, M. R. Abernathy, A. E. Becerra-Toledo, H. Armandula, E. Black, K. Dooley, M. Eichenfield, C. Nwabugwu, A. Villar, D. R. M. Crooks, G. Cagnoli, J. Hough, C. R. How, I. MacLaren, P. Murray, S. Reid, S. Rowan, P. H. Sneddon, M. M. Fejer, R. Route, S. D. Penn, P. Ganau, J.-M. Mackowski, C. Michel, L. Pinard, and A. Remillieux, "Titania-doped tantala/silica coatings for gravitational-wave detection," *Class. Quantum Grav.*, **24**, no. 2, 405, 2007.

[17] M. Evans, S. Ballmer, M. Fejer, P. Fritschel, G. Harry, and G. Ogin, "Thermo-optic noise in coated mirrors for high-precision optical measurements," *Phys. Rev. D*, **78**, 102003, 2008.

[18] G. D. Cole, W. Zhang, M. J. Martin, J. Ye, and M. Aspelmeyer, "Tenfold reduction of Brownian noise in optical interferometry," *ArXiv e-prints*, Feb. 2013.

[19] A. Cumming and . others, "Measurement of the mechanical loss of prototype GaP/AlGaP crystalline coatings for future gravitational wave detectors," *Classical and Quantum Gravity*, 2014. https://dcc.ligo.org/LIGO-P1400059.

[20] A. Lin, R. B. S. Omar, *et al.*, "Epitaxial growth of GaP/AlGaP mirrors on Si for low thermal noise optical coatings," *LIGO Document: LIGO-P1400236*, 2014. https://dcc.ligo.org/LIGO-P1400236.

[21] P. R. Saulson, "Thermal noise in mechanical experiments," *Phys. Rev. D*, **42**, pp. 2437–2445, 1990.

[22] J. A. Sidles and D. Sigg, "Optical torques in suspended Fabry–Perot interferometers," *Phys. Lett. A*, **354**, pp. 167–172, 2006. http://dx.doi.org/10.1016/j.physleta.2006.01.051.

[23] L. Barsotti and M. Evans, "Modeling of Alignment Sensing and Control for Advanced LIGO," *LIGO Document: LIGO-T0900511*, 2011. https://dcc.ligo.org/LIGO-T0900511.

[24] L. Barsotti, M. Evans, and P. Fritschel, "Alignment sensing and control in advanced LIGO," *Classical and Quantum Gravity*, **27**, no. 8, 084026, 2010. https://dcc.ligo.org/LIGO-P0900258.

[25] G. Hammond, "Suspension Thermal Noise," *LIGO Document: LIGO-G1200579*, 2012. https://dcc.ligo.org/G1200579.

[26] R. Abbott, R. Adhikari, S. Ballmer, L. Barsotti, M. Evans, P. Fritschel, V. Frolov, G. Mueller, B. Slagmolen, and S. Waldman, "AdvLIGO Interferometer Sensing and Control Conceptual Design," *LIGO Document: LIGO-T070247-01*, 2007. https://dcc.ligo.org/cgi-bin/DocDB/ShowDocument?docid=5306.

[27] K. Arai, M. Ando, S. Moriwaki, K. Kawabe, and K. Tsubono, "New signal extraction scheme with harmonic demodulation for power-recycled Fabry-Perot-Michelson interferometers," *Phys. Lett. A*, **273**, pp. 15–24, 2000. http://dx.doi.org/10.1016/S0375-9601(00)00467-9.

[28] T. Fricke, N. Smith-Lefebvre, R. Abbott, R. Adhikari, K. L. Dooley, M. Evans, P. Fritschel, V. Frolov, K. Kawabe, J. S. Kissel, and S. Waldman, "DC readout experiment in Enhanced LIGO," *Class. Quantum Grav.*, 2012. http://dx.doi.org/10.1088/0264-9381/29/6/065005.

[29] The LIGO Scientific Collaboration, J. Abadie, B. P. Abbott, R. Abbott, T. D. Abbott, M. Abernathy, C. Adams, R. Adhikari, C. Affeldt, B. Allen, and et al., "A gravitational wave observatory operating beyond the quantum shot-noise limit," *Nature Physics*, **7**, pp. 962–965, 2011. http://dx.doi.org/10.1038/nphys2083.

[30] S. Hild, H. Grote, J. Degallaix, S. Chelkowski, K. Danzmann, A. Freise, M. Hewitson, J. Hough, H. Lück, M. Prijatelj, K. A. Strain, J. R. Smith, and B. Willke, "DC-readout of a signal-recycled gravitational wave detector," *Class. Quantum Grav.*, **26**, no. 5, 055012, 2009. http://dx.doi.org/10.1088/0264-9381/26/5/055012.

[31] K. Goda, O. Miyakawa, E. E. Mikhailov, S. Saraf, R. Adhikari, K. McKenzie, R. Ward, S. Vass, A. J. Weinstein, and N. Mavalvala, "A quantum-enhanced prototype gravitational-wave detector," *Nature Physics*, **4**, pp. 472–476, 2008. http://dx.doi.org/10.1038/nphys920.

[32] O. Miyakawa, R. Ward, R. Adhikari, M. Evans, B. Abbott, R. Bork, D. Busby, J. Heefner, A. Ivanov, M. Smith, R. Taylor, S. Vass, A. Weinstein, M. Varvella, S. Kawamura, F. Kawazoe, S. Sakata, and C. Mow-Lowry, "Measurement of optical response of a detuned resonant sideband extraction gravitational wave detector," *Phys. Rev. D*, **74**, 022001, 2006. http://link.aps.org/doi/10.1103/PhysRevD.74.022001.

[33] R. L. Ward, R. Adhikari, B. Abbott, R. Abbott, D. Barron, R. Bork, T. Fricke, V. Frolov, J. Heefner, A. Ivanov, O. Miyakawa, K. McKenzie, B. Slagmolen, M. Smith, R. Taylor, S. Vass, S. Waldman, and A. Weinstein, "DC readout experiment at the Caltech 40m prototype interferometer," *Class. Quantum Grav.*, **25**, no. 11, 114030, 2008. http://dx.doi.org/10.1088/0264-9381/25/11/114030.

[34] Y. Aso, M. Ando, K. Kawabe, S. Otsuka, and K. Tsubono, "Stabilization of a Fabry–Perot interferometer using a suspension-point interferometer," *Phys. Lett. A*, **327**, no. 1, pp. 1–8, 2004. http://dx.doi.org/10.1016/j.physleta.2004.04.066.

[35] M. Evans, P. Fritschel, D. McClelland, J. Miller, A. Mullavey, D. Shaddock, B. Slagmolen, S. Waldman, and et al., "Adv. LIGO Arm Length Stabilization Design," *LIGO Document: LIGO-T0900144*, 2012. https://dcc.ligo.org/cgi-bin/private/DocDB/ShowDocument?docid=1625.

[36] A. J. Mullavey, B. J. J. Slagmolen, J. Miller, M. Evans, P. Fritschel, D. Sigg, S. J. Waldman, D. A. Shaddock, and D. E. McClelland, "Arm-length stabilisation for interferometric gravitational-wave detectors using frequency-doubled auxiliary lasers," *Opt. Express*, **20**, pp. 81–89, 2012. http://dx.doi.org/10.1364/OE.20.000081.

[37] K. Izumi, K. Arai, B. Barr, J. Betzwieser, A. Brooks, K. Dahl, S. Doravari, J. C. Driggers, W. Z. Korth, H. Miao, J. G. Rollins, S. Vass, D. Yeaton-Massey, and R. Adhikari, "Multi-color Cavity Metrology," *LIGO Document: LIGO-P1200019*, 2012. https://dcc.ligo.org/cgi-bin/private/DocDB/ShowDocument?docid=87878.

[38] N. Smith-Lefebvre and N. Mavalvala, "Modematching feedback control for interferometers with an output mode cleaner," *LIGO Document: LIGO-P1200034*, 2012. https://dcc.ligo.org/cgi-bin/private/DocDB/ShowDocument?docid=89076.

[39] N. Smith-Lefebvre, S. Ballmer, M. Evans, S. Waldman, K. Kawabe, V. Frolov, and N. Mavalvala, "Optimal alignment sensing of a readout mode cleaner cavity," *Opt. Lett.*, **36**, no. 22, pp. 4365–4367, 2011. http://dx.doi.org/10.1364/OL.36.004365.

[40] M. Smith, K. Mailand, A. Brooks, and P. Willems, "Advanced LIGO Thermal Compensation System Preliminary Design," *LIGO Document: LIGO-T0900304-v2*, 2009. https://dcc.ligo.org/cgi-bin/private/DocDB/ShowDocument?docid=3162.

[41] M. Evans and P. Fritschel, "TCS and the Golden Shield," *LIGO Document: LIGO-T0900359-v2*, 2009. https://dcc.ligo.org/cgi-bin/private/DocDB/ShowDocument?docid=3967.

[42] R. Lawrence, *Active Wavefront Correction in Laser Interferometric Gravitational Wave Detectors*. PhD thesis, Massachusetts Institute of Technology, 2003. http://dspace.mit.edu/handle/1721.1/29308.

[43] P. Willems, "TCS Actuator Noise Couplings," *LIGO Document, LIGO-T060224-v7*, 2006. https://dcc.ligo.org/cgi-bin/private/DocDB/ShowDocument?docid=9248.

[44] H. Yamamoto, "SIS (Stationary Interferometer Simulation) manual," *LIGO Document, LIGO-T070039-v6*, 2007. https://dcc.ligo.org/cgi-bin/DocDB/ShowDocument?docid=160.

[45] P. Willems, "Implications of ETM02 HR Coating Absorption for Thermal Compensation," *LIGO Document, LIGO-T1100250-v2*, 2011. https://dcc.ligo.org/cgi-bin/private/DocDB/ShowDocument?docid=60664.

[46] A. F. Brooks and et al., "Ultra-sensitive wavefront measurement using a Hartmann sensor," *Opt. Express*, **15**, pp. 10370–10375, 2007. http://www.opticsinfobase.org/oe/abstract.cfm?uri=oe-15-16-10370.

[47] A. F. Brooks, *Hartmann Wavefront Sensors for Advanced Gravitational Wave Interferometers*. PhD thesis, The University of Adelaide, 2007. http://digital.library.adelaide.edu.au/dspace/handle/2440/57100.

[48] J. C. Driggers, M. Evans, K. Pepper, and R. Adhikari, "Active noise cancellation in a suspended interferometer," *Rev. Sci. Instrum.*, **83**, 2012. http://dx.doi.org/10.1063/1.3675891.

[49] B. N. Shapiro, *Adaptive Modal Damping for Advance LIGO Suspensions.* PhD thesis, Massachusetts Institute of Technology, 2012. https://dcc.ligo.org/cgi-bin/private/DocDB/ShowDocument?docid=91198.

[50] K. Arai, J. Betzwieser, P. Kalmus, and R. Adhikari, "Simulated Plant Approach," *LIGO Document: LIGO-G1000546*, 2010. https://dcc.ligo.org/cgi-bin/private/DocDB/ShowDocument?docid=11804.

[51] H. Yamamoto, B. Bhawal, M. Evans, E. Maros, M. Rakhmanov, J. R. L. Savage, G. Cella, S. Klimenko, and S. Mohanty, "End to End Simulation Program for Gravitational-Wave Detectors," , in *Gravitational Wave Detection II* (S. Kawamura and N. Mio, eds.), vol. 32 of *Frontiers Science Series*, pp. 331–336, Universal Academy Press, 2000.

[52] LIGO, "GWINC: Gravitational Wave Interferometer Noise Calculator." http://ilog.ligo-wa.caltech.edu:7285/advligo/GWINC.

[53] T. Corbitt and N. Mavalvala, "Review: Quantum noise in gravitational-wave interferometers," *Journal of Optics B: Quantum and Semiclassical Optics*, **6**, no. 8, S675, 2004. http://dx.doi.org/10.1088/1464-4266/6/8/008.

[54] D. McClelland, N. Mavalvala, Y. Chen, and R. Schnabel, "Advanced interferometry, quantum optics and optomechanics in gravitational wave detectors," *Laser & Photonics Reviews*, **5**, 677, 2011.

[55] C. M. Caves, "Quantum-mechanical noise in an interferometer," *Phys. Rev. D*, **23**, 1693, 1981.

[56] R. Schnabel, N. Mavalvala, D. D. E. McClelland, and P. K. P. Lam, "Quantum metrology for gravitational wave astronomy.," *Nature communications*, **1**, 121, jan 2010. http://www.ncbi.nlm.nih.gov/pubmed/21081919.

[57] A. Buonanno and Y. Chen, "Signal recycled laser-interferometer gravitational-wave detectors as optical springs," *Phys. Rev. D*, **65**, 042001, 2002.

[58] H. J. Kimble, Y. Levin, A. B. Matsko, K. S. Thorne, and S. P. Vyatchanin, "Conversion of conventional gravitational-wave interferometers into quantum nondemolition interferometers by modifying their input and/or output optics," *Phys. Rev. D*, **65**, 022002, 2001. http://link.aps.org/doi/10.1103/PhysRevD.65.022002.

[59] F. Y. Khalili and Y. Levin, "Speed meter as a quantum nondemolition measuring device for force," *Phys. Rev. D*, **54**, pp. 4735–4737, 1996. http://link.aps.org/doi/10.1103/PhysRevD.54.4735.

[60] P. Purdue, "Analysis of a quantum nondemolition speed-meter interferometer," *Phys. Rev. D*, **66**, 022001, 2002. http://link.aps.org/doi/10.1103/PhysRevD.66.022001.

[61] P. Purdue and Y. Chen, "Practical speed meter designs for quantum nondemolition gravitational-wave interferometers," *Phys. Rev. D*, **66**, 122004, 2002. http://link.aps.org/doi/10.1103/PhysRevD.66.122004.

[62] Y. Chen, "Sagnac interferometer as a speed-meter-type, quantum-nondemolition gravitational-wave detector," *Phys. Rev. D*, **67**, 122004, 2003. http://link.aps.org/doi/10.1103/PhysRevD.67.122004.

[63] S. P. Vyatchanin and E. A. Zubova, "Quantum variation measurement of a force," *Phys. Lett. A*, **201**, pp. 269–274, 1995. http://dx.doi.org/10.1016/0375-9601(95)00280-G.

[64] H. Rehbein, H. Müller-Ebhardt, K. Somiya, S. L. Danilishin, R. Schnabel, K. Danzmann, and Y. Chen, "Double optical spring enhancement for gravitational-wave detectors," *Phys. Rev. D*, **78**, 062003, 2008. http://link.aps.org/doi/10.1103/PhysRevD.78.062003.

[65] H. Rehbein, H. Müller-Ebhardt, K. Somiya, C. Li, R. Schnabel, K. Danzmann, and Y. Chen, "Local readout enhancement for detuned signal-recycling interferometers," *Phys. Rev. D*, **76**, 062002, 2007. http://link.aps.org/doi/10.1103/PhysRevD.76.062002.

[66] H. Vahlbruch, M. Mehmet, K. Danzmann, and R. Schnabel, "Detection of 15 dB squeezed states of light and their application for the absolute calibration of photoelectric quantum efficiency," 2016. https://dcc.ligo.org/P1600153.

[67] S. Dwyer. personal communication, 2012.

[68] R. Adhikari, "Upgrades to the Advanced LIGO Interferometer," *LIGO Document: LIGO-G1000524*, 2010. https://dcc.ligo.org/cgi-bin/private/DocDB/ShowDocument?docid=11613.

[69] G. Rempe, R. J. Thompson, H. J. Kimble, and R. Lalezari, "Measurement of Ultralow Losses in an Optical Interferometer," *Opt. Lett.*, **17**, pp. 363–365, 1992. http://www.opticsinfobase.org/abstract.cfm?id=11045.

[70] N. Uehara, A. Ueda, K. Ueda, H. Sekiguchi, T. Mitake, and et al., "Ultralow-loss mirror of the parts-in 10^{-6} level at 1064 nm," *Opt. Lett.*, **20**, pp. 530–532, 1995. http://www.opticsinfobase.org/abstract.cfm?uri=ol-20-6-530.

[71] A. Buonanno and Y. Chen, "Scaling law in signal recycled laser-interferometer gravitational-wave detectors," *Phys. Rev. D*, **67**, 062002, 2003. http://link.aps.org/doi/10.1103/PhysRevD.67.062002.

[72] A. Thüring, R. Schnabel, H. Lück, and K. Danzmann, "Detuned Twin-Signal-Recycling for ultra-high precision interferometers," *Opt. Lett.*, **32**, pp. 985–987, 2007.

[73] A. Thuring, C. Graf, H. Vahlbruch, M. Mehmet, K. Danzmann, and R. Schnabel, "Broadband squeezing of quantum noise in a Michelson interferometer with Twin-Signal-Recycling," *Opt. Lett*, 181101, 2009.

[74] V. B. Braginsky and F. Y. Khalili, *Quantum Measurement.* ed. K. S. Thorne, Cambridge University Press, 1992. http://www.amazon.com/Quantum-Measurement-Vladimir-B-Braginsky/dp/052141928X.

[75] A. Wade, K. Mckenzie, Y. Chen, D. Shaddock, J. Chow, and D. McClelland, "A Polarization Speed Meter for Gravitational-Wave Detection," *LIGO Document: P1100205*, 2011. https://dcc.ligo.org/cgi-bin/private/DocDB/ShowDocument?docid=77471.

[76] H. Miao, H. Yang, R. Adhikari, and Y. Chen, "Comparison of Quantum Noise in 3G Interferometer Configurations," *LIGO Document: LIGO-T1200008-v3*, 2012. https://dcc.ligo.org/cgi-bin/private/DocDB/ShowDocument?docid=78229.

[77] N. A. Robertson, G. Cagnoli, D. R. M. Crooks, E. Elliffe, J. E. Faller, P. Fritschel, S. Goßler, A. Grant, A. Heptonstall, J. Hough, H. Lück, R. Mittleman, M. Perreur-Lloyd, M. V. Plissi, S. Rowan, D. H. Shoemaker, P. H. Sneddon, K. A. Strain, C. I. Torrie, H. Ward, and P. Willems, "Quadruple suspension design for Advanced LIGO," *Class. Quantum Grav.*, **19**, pp. 4043–4058, 2002.

[78] A. V. Cumming, A. S. Bell, L. Barsotti, M. A. Barton, G. Cagnoli, D. Cook, L. Cunningham, M. Evans, G. D. Hammond, G. M. Harry, A. Heptonstall, J. Hough, R. Jones, R. Kumar, R. Mittleman, N. A. Robertson, S. Rowan, B. Shapiro, K. A. Strain, K. Tokmakov, C. Torrie, and A. A. van Veggel, "Design and development of the advanced LIGO monolithic fused silica suspension," *Class. Quantum Grav.*, **29**, no. 3, 035003, 2012. http://stacks.iop.org/0264-9381/29/i=3/a=035003.

[79] N. A. Robertson for the LSC, "Seismic isolation and suspension systems for Advanced LIGO," *Proceedings of SPIE*, **5500**, 81, 2004.

[80] P. R. Saulson, "Terrestrial gravitational noise on a gravitational wave antenna," *Phys. Rev. D*, **30**, pp. 732–736, 1984.

[81] J. C. Driggers, J. Harms, and R. Adhikari, "Subtraction of Newtonian Noise Using Optimized Sensor Arrays," *LIGO Document: P1200017*, 2012. https://dcc.ligo.org/P1200017.

[82] T. Hong, H. Yang, E. K. Gustafson, R. Adhikari, and Y. Chen, "Brownian Thermal Noise in Multlayer Coated Mirrors," *in prep.*, 2012. in prep.

[83] G. de Vine, D. A. Shaddock, and D. E. McClelland, "Variable reflectivity signal mirrors and signal response measurements," *Class. Quantum Grav.*, **19**, 1561, 2002. http://dx.doi.org/10.1088/0264-9381/19/7/345.

[84] S. L. Danilishin and F. Y. Khalili, "Practical design of the optical lever intracavity topology of gravitational-wave detectors," *Phys. Rev. D*, **73**, 022002, 2006. http://link.aps.org/doi/10.1103/PhysRevD.73.022002.

[85] T. Corbitt, Y. Chen, F. Khalili, D. Ottaway, S. Vyatchanin, S. Whitcomb, and N. Mavalvala, "Squeezed-state source using radiation-pressure-induced rigidity," *Phys. Rev. A*, **73**, 023801, 2006. http://link.aps.org/doi/10.1103/PhysRevA.73.023801.

[86] T. Corbitt, Y. Chen, and N. Mavalvala, "Mathematical framework for simulation of quantum fields in complex interferometers using the two-photon formalism," *Physical Review A*, **72**, pp. 013818+, July 2005. http://dx.doi.org/10.1103/physreva.72.013818.

[87] M. Zhou, Z. Zhou, and S. M. Shahriar, "Quantum noise limits in white-light-cavity-enhanced gravitational wave detectors," *Phys. Rev. D*, **92**, 082002, Oct 2015. http://link.aps.org/doi/10.1103/PhysRevD.92.082002.

[88] M. Zhou, Z. Zhou, and S. M. Shahriar, "Catastrophic breakdown of the Caves model for quantum noise in some phase-insensitive linear amplifiers or attenuators based on atomic systems," *Phys. Rev. A*, **93**, 033858, Mar 2016. http://link.aps.org/doi/10.1103/PhysRevA.93.033858.

[89] E. E. Mikhailov, K. Goda, T. Corbitt, and N. Mavalvala, "Frequency-dependent squeeze-amplitude attenuation and squeeze-angle rotation by electromagnetically induced transparency for gravitational-wave interferometers," *Phys. Rev. A*, **73**, 053810, 2006. http://link.aps.org/doi/10.1103/PhysRevA.73.053810.

[90] M. Zhou, Z. Zhou, and S. M. Shahriar, "Realizing the GEIT System Using Zeeman Sublevels in Rb for Enhancing the Sensitivity-Bandwidth Product in Next Generation LIGO," 2016. https://dcc.ligo.org/G1600440.

[91] Y. Levin, "Internal thermal noise in the LIGO test masses: A direct approach," *Phys. Rev. D*, **57**, pp. 659–663, 1998. http://link.aps.org/doi/10.1103/PhysRevD.57.659.

[92] W. A. Phillips, "Two-level states in glasses," *Reports on Progress in Physics*, **50**, 1657, 1987. http://dx.doi.org/10.1088/0034-4885/50/12/003.

[93] "Spectral Shape of Relaxations in Silica Glass," *Physical Review Letters*, **84**, 2718, 2000.

[94] S. Chao *et al.*, "Low Loss Dielectric Mirrors with Ion Beam Sputtered $TiO_2 - SiO_2$ Mixed Films," *Opt. Lett*, **40**, 2177, 2001.

[95] S. Ushakov *et al.*, "Crystalization in Hafnia and Zirconia Based Systems," *Phys. Stat. Sol*, **241**, 2268, 2004.

[96] S. Chao *et al.*, "Thickness-dependent crystallization on thermal anneal for the titania/silica nano-layers deposited by ion-beam-sputter method." LIGO Document: LIGO G1300921.

[97] M. Liu *et al.*, "Microstructure and Interfacial Properties of HfO_2/Al_2O_3 Nanolaminate Films," *Appl. Surf. Sci.*, **252**, 6206, 2006.

[98] S. D. Penn, P. H. Sneddon, H. Armandula, J. C. Betzwieser, G. Cagnoli, J. Camp, D. R. M. Crooks, M. M. Fejer, A. M. Gretarsson, G. M. Harry, J. Hough, S. E. Kittelberger, M. J. Mortonson, R. Route, S. Rowan, and C. C. Vassiliou, "Mechanical loss in tantala/silica dielectric mirror coatings," *Class. Quantum Grav.*, **20**, no. 13, 2917, 2003. http://dx.doi.org/10.1088/0264-9381/20/13/334.

[99] I. Pinto *et al.*, "Interdiffused coatings." LIGO Document G-1200976.

[100] M. Principe *et al.*, "Chapter 12, Reflectivity and thickness optimization," , in *Optical Coatings and Thermal Noise in Precision Measurements* (G. Harry *et al.*, eds.), Cambridge University Press, 2012.

[101] A. Villar *et al.*, "Measurement of Thermal Noise in Multilayer Coatings with Optimized Layer Thicknesses," *Phys. Rev. D*, **81**, 122001, 2010.

[102] W. Yam, S. Gras, and M. Evans, "Multi-Material Coatings with Reduced Thermal Noise," *LIGO Document: LIGO-P1400206-v4*, 2014. https://dcc.ligo.org/LIGO-P1400206.

[103] J. Steinlechner *et al.*, "Thermal Noise Reduction and Absorption Optimisation via Multi-Material Coatings," *LIGO Document: LIGO-P1400227-v1*, 2014. https://dcc.ligo.org/LIGO-P1400227.

[104] M. Evans, L. Barsotti, and P. Fritschel, "A general approach to optomechanical parametric instabilities," *Phys. Lett. A*, **374**, no. 4, pp. 665–671, 2010. http://dx.doi.org/10.1016/j.physleta.2009.11.023.

[105] R. X. Adhikari, "Gravitational Radiation Detection with Laser Interferometry," *Reviews of Modern Physics*, 2013.

[106] C. Zhao *et al. Phys. Rev. Lett.*, **4**, 121102, 2005.

[107] S. Gras *et al. Class. Quantum Grav.*, **27**, 205019, 2010.

[108] S. Strigin *et al. Phys. Lett. A*, **372**, 5727, 2008.

[109] A. C. Lin, J. S. Harris, and M. M. Fejer, "Two-dimensional III-V nucleation on Si for nonlinear optics," *Journal of Vacuum Science Technology B: Microelectronics and Nanometer Structures*, **29**, no. 3, 030000, 2011.

[110] I.Martin *et al.*, "Mechanical loss of crystalline and amorphous coatings." GWADW 2014. http://www.gravity.ircs.titech.ac.jp/GWADW2014/slide/Iain_Martin.pdf.

[111] B. Lantz, R. Schofield, B. O'Reilly, D. E. Clark, and D. DeBra, "Review: Requirements for a Ground Rotation Sensor to Improve Advanced LIGO," *Bulletin of the Seismological Society of America*, **99**, pp. 980–989, 2009. http://bssa.geoscienceworld.org/cgi/content/abstract/99/2B/980.

[112] V. Dergachev and R. DeSalvo, "A high precision mechanical ground rotation sensor ," *LIGO Document: LIGO-G1200187*, 2012. https://dcc.ligo.org/G1200187.

[113] K. Venkateswara, "TiltWash: Update on tiltmeter work at UW," *LIGO Document: LIGO-G1200225*, 2012. https://dcc.ligo.org/G1200225.

[114] W. Korth, A. Heptonstall, R. Adhikari, E. Gustafson, and B. Lantz, "Status of the Caltech Laser Gyro," *LIGO Document: LIGO-G1200261*, 2012. https://dcc.ligo.org/G1200261.

[115] M. Evans and F. Matichard, "Tilt Free Inertial Sensing," *LIGO Document: LIGO-T0900628*, 2009. https://dcc.ligo.org/cgi-bin/private/DocDB/ShowDocument?docid=7974.

[116] K. Venkateswara, "Improving active seismic isolation in aLIGO using a ground rotation sensor," *LIGO Document: LIGO-G1600083*, 2016. https://dcc.ligo.org/LIGO-G1600083.

[117] G. Rajalakshmi, P. K. Madhu, and C. Unnikrishnan, "Atomic Spin Gyroscopes for Rotation Sensing," *LIGO Document: LIGO-G1601427*, 2016. https://dcc.ligo.org/LIGO-G1601427.

[118] T. W. Kornack, R. K. Ghosh, and M. V. Romalis, "Nuclear Spin Gyroscope Based on an Atomic Comagnetometer," *Phys. Rev. Lett.*, **95**, 230801, Nov 2005. http://link.aps.org/doi/10.1103/PhysRevLett.95.230801.

[119] B. Lantz, "Thoughts on Hanford Wind," *LIGO Document: LIGO-G1501371*, 2015. https://dcc.ligo.org/LIGO-G1501371.

[120] D. Tshilumba, L. Nuttall, T. Mac Donald, R. Mittleman, B. Lantz, F. Matichard, and C. Collette, "Vibration analysis and control of the LIGO observatories large chambers and support piers," , in *PROCEEDINGS OF ISMA2014 INCLUDING USD2014*, pp. 187–200, 2014. https://dcc.ligo.org/LIGO-p1400109.

[121] T. MacDonald, "BSC HEPI Motion Measurements and Modeling," *LIGO Document: LIGO-G1401167*, 2014. https://dcc.ligo.org/G1401167.

[122] J. Driggers, V. Frolov, D. Atkinson, H. Miao, M. Landry, R. Adhikari, and R. DeRosa, "Global feed-forward vibration isolation in a km scale interferometer," *LIGO-Document: LIGO-P1000088*, 2010. https://dcc.ligo.org/P1000088.

[123] R. Kurdyumov, C. Kucharczyk, and B. Lantz, "Blend Switching User Guide," *LIGO-Document: LIGO-T1200126*, 2012. https://dcc.ligo.org/T1200126.

[124] M. Coughlin *et al.*, "Earthquake monitoring for aLIGO," *LIGO Document: LIGO-G1400811*, 2014. https://dcc.ligo.org/G1400811.

[125] C. Collette and F. Matichard, "Sensor Fusion Methods for High Performance Active Vibration Isolation Systems," *Journal of Sound and Vibration*, no. P1400022, 2014. https://dcc.ligo.org/LIGO-P1400022.

[126] C. Collette and F. Matichard, "Vibration control of flexible structures using fusion of inertial sensors and hyper-stable actuator/sensor pairs," *LIGO Document: LIGO-P1400099*, 2014. https://dcc.ligo.org/LIGO-P1400099.

[127] K.-F. J. Tseng, "System Failure Diagnosis for the Advanced LIGO HAM Chamber Seismic Isolation System," *LIGO Document: LIGO-P1000086*, 2010. https://dcc.ligo.org/P1000086.

[128] B. N. Shapiro, R. Adhikari, J. Driggers, J. Kissel, B. Lantz, J. Rollins, and K. Youcef-Toumi, "Noise and control decoupling of Advanced LIGO suspensions," *Classical and Quantum Gravity*, **32**, no. 1, 015004, 2015. http://stacks.iop.org/0264-9381/32/i=1/a=015004.

[129] P. Fritschel, "Potential Advanced LIGO post-Project upgrades," Tech. Rep. T1300176, LIGO Laboratory, Mar 2013. https://dcc.ligo.org/LIGO-T1300176.

[130] N. A. Robertson, H. Miller, and C. Torrie, "Risk Reduction Work on Advanced LIGO Suspensions," *LIGO Document: LIGO-G1400804*, 2014. https://dcc.ligo.org/LIGO-G1400804.

[131] N. Robertson and M. Barton, "Design of a Larger Beamsplitter Suspension," *LIGO Document: LIGO-T1400296*, 2014. https://dcc.ligo.org/LIGO-P1400296.

[132] N. Robertson and H. Miller, "Revised Design of HSTS with Improved Vertical Isolation," *LIGO Document: LIGO-T1400290*, 2014. https://dcc.ligo.org/LIGO-P1400290.

[133] N. A. Robertson and J. Hough, "Gas Damping in Advanced LIGO Suspensions," *LIGO Document: LIGO-T0900416-v2*, 2009. https://dcc.ligo.org/cgi-bin/DocDB/ShowDocument?docid=5085.

[134] A. Cavalleri, G. Ciani, R. Dolesi, A. Heptonstall, M. Hueller, D. Nicolodi, S. Rowan, D. Tombolato, S. Vitale, P. J. Wass, and W. J. Weber, "Increased Brownian Force Noise from Molecular Impacts in a Constrained Volume," *Phys. Rev. Lett.*, **103**, 140601, 2009. http://link.aps.org/doi/10.1103/PhysRevLett.103.140601.

[135] R. Dolesi, M. Hueller, D. Nicolodi, D. Tombolato, S. Vitale, P. J. Wass, W. J. Weber, M. Evans, P. Fritschel, R. Weiss, J. H. Gundlach, C. A. Hagedorn, S. Schlamminger, G. Ciani, and A. Cavalleri, "Brownian force noise from molecular collisions and the sensitivity of advanced gravitational wave observatories," *Phys. Rev. D*, **84**, 063007, 2011. http://link.aps.org/doi/10.1103/PhysRevD.84.063007.

[136] G. Billingsley, N. Robertson, and B. Shapiro, "Annular End Reaction Mass Conceptual/Final Design Document," *LIGO Document: LIGO-E1500264*, 2015. https://dcc.ligo.org/LIGO-E1500264.

[137] N. Robertson and C. Torrie, "Recent Results and Conclusions from Tests of the UIM Blade Non-Magnetic Damper," *LIGO Document: LIGO-T1600046*, 2016. https://dcc.ligo.org/LIGO-T1600046.

[138] N. Robertson and C. Torrie, "A Tale of Two Dampers: Bounce and Roll Mode Damping for the Quads," *LIGO Document: LIGO-G1600371*, 2016. https://dcc.ligo.org/LIGO-G1600371.

[139] G. Hammond *et al.*, "Progress on silica and silicon suspensions," *LIGO Document: LIGO-G1400849*, 2014. https://dcc.ligo.org/G1400849.

[140] D. Madden-Fong, "LIGO III Quad Pendulum Conceptual Design Optimization," *LIGO Document: LIGO-T1300786*, 2013. https://dcc.ligo.org/T1300786.

[141] B. Shapiro, "Alternative design approach for caging, sensing and control next generation suspensions," *LIGO Document: LIGO-G1601426*, 2016. https://dcc.ligo.org/LIGO-G1601426.

[142] N. Lockerbie, K. Tokmakov, and S. Jawahar, "New OSEM results using a displacement-doubling prism-based flag," *LIGO Document: LIGO-G1601136*, 2016. https://dcc.ligo.org/LIGO-G1601136.

[143] C. C. Speake and S. M. Aston, "An interferometric sensor for satellite drag-free control," *Class. Quantum Grav.*, **22**, S269, 2005. http://dx.doi.org/10.1088/0264-9381/22/10/019.

[144] A. Cumming, R. Jones, M. Barton, G. Cagnoli, C. A. Cantley, D. R. M. Crooks, G. D. Hammond, A. Heptonstall, J. Hough, S. Rowan, and K. A. Strain, "Apparatus for dimensional characterization of fused silica fibers for the suspensions of advanced gravitational wave detectors," *Rev. Sci. Instrum.*, **82**, 044502, 2011. http://link.aip.org/link/doi/10.1063/1.3581228.

[145] A. Heptonstall, M. Barton, C. Cantley, A. Cumming, G. Cagnoli, J. Hough, R. Jones, R. Kumar, I. Martin, S. Rowan, C. Torrie, and S. Zech, "Investigation of mechanical dissipation in CO2 laser-drawn fused silica fibres and welds," *Class. Quantum Grav.*, **27**, 035013, 2010. http://dx.doi.org/10.1088/0264-9381/27/3/035013.

[146] A. Heptonstall, M. A. Barton, A. Bell, G. Cagnoli, C. A. Cantley, and et al., "Invited Article: CO2 laser production of fused silica fibers for use in interferometric gravitational wave detector mirror suspensions," *Rev. Sci. Insrum.*, **82**, 011301, 2011. http://link.aip.org/link/doi/10.1063/1.3532770.

[147] L. Cunningham, P. Murray, A. Cumming, E. Elliffe, G. Hammond, K. Haughian, J. Hough, M. Hendry, R. Jones, I. Martin, S. Reid, S. Rowan, J. Scott, K. Strain, K. Tokmakov, C. Torrie, and A. van Veggel, "Re-evaluation of the mechanical loss factor of hydroxide-catalysis bonds and its significance for the next generation of gravitational wave detectors," *Phys. Lett. A*, **374**, no. 39, pp. 3993 – 3998, 2010. http://dx.doi.org/10.1016/j.physleta.2010.07.049.

[148] D. Clark, B. Lantz, and D. DeBra, "Seismic Platform Interferometer - Progress at Stanford," *LIGO Document: LIGO-G1200178*, 2012. https://dcc.ligo.org/G1200178.

[149] D. Clark, "Control of Differential Motion Between Adjacent Advanced LIGO Seismic Isolation Platforms," Tech. Rep. P1300043, LIGO Laboratory, Mar 2013. https://dcc.ligo.org/LIGO-P1300043.

[150] K. Dahl, A. Bertolini, M. Born, Y. Chen, D. Gering, S. Goßler, C. Gräf, G. Heinzel, S. Hild, F. Kawazoe, O. Kranz, G. Kühn, H. Lück, K. Mossavi, R. Schnabel, K. Somiya, K. A. Strain, J. R. Taylor, A. Wanner, T. Westphal, B. Willke, and K. Danzmann, "Towards a Suspension Platform Interferometer for the AEI 10 m Prototype Interferometer," *J. Phys.: Conf. Ser.*, **228**, 012027, 2010. http://dx.doi.org/10.1088/1742-6596/228/1/012027.

[151] C. Collette, F. Nassif, J. Amar, C. Depouhon, and S.-P. Gorza, "Prototype of inter-ferometric absolute motion sensor," *Sensors and Actuators A: Physical*, 2015.

[152] J. vanHeijningen and J. van den Brand, "An interferometric readout for a monolithic accelerometer, towards a fm/rtHz resolution," *LIGO Document: LIGO-G1300971*, 2013. https://dcc.ligo.org/LIGO-G1300971.

[153] B. Sorazu, K. A. Strain, I. S. Heng, , and R. Kumar, "Violin mode amplitude glitch monitor for the presence of excess noise on the monolithic silica suspensions of GEO 600," *Class. Quantum Grav.*, **27**, 155017, 2010. http://dx.doi.org/10.1088/0264-9381/27/15/155017.

[154] X. Ni, E. Quintero, and G. Vajente, "Proposal for an Upgrade of the Crackle Experiment," *LIGO Document: LIGO-T1400407*, 2014. https://dcc.ligo.org/LIGO-T1400407.

[155] G. Vajente, E. A. Quintero, X. Ni, K. Arai, E. K. Gustafson, N. A. Robertson, E. J. Sanchez, J. R. Greer, and R. X. Adhikari, "An in-strument to measure mechanical up-conversion phenomena in metals in the elastic regime," *Review of Scientific Instruments*, **87**, no. 6, 2016. http://scitation.aip.org/content/aip/journal/rsi/87/6/10.1063/1.4953114.

[156] Y. Ikushima, R. Li, T. Tomaru, N. Sato, T. Suzuki, T. Haruyama, T. Shintomi, and A. Yamamoto, "Ultra-low-vibration pulse-tube cryocooler system - cooling ca-pacity and vibration," *Cryogenics*, **48**, no. 9-10, pp. 406 – 412, 2008. http://www.sciencedirect.com/science/article/pii/S0011227508000490.

[157] B. Shapiro, "Cryogenic Test Mass Work at Stanford," *LIGO Document: LIGO-G1400926*, 2014. https://dcc.ligo.org/G1400926.

[158] O. Aguiar, "Multi-Nested Pendula System: measured, calculated and simulated cooling performances," *LIGO Document: LIGO-G1400845*, 2014. https://dcc.ligo.org/G1400845.

[159] O. Aguiar, M. Constancio, E. Ferreira, A. Silva, and M. Okada, "Multi-Nested Pen-dula System: Mechanics and Cryogenics Update," *LIGO Document: LIGO-G1500172*, 2015. https://dcc.ligo.org/G1500172.

[160] B. Shapiro, "A Cryogenic LIGO Mirror for 3rd Generation Observatories," *LIGO Doc-ument: LIGO-G1600766*, 2016. https://dcc.ligo.org/G1600766.

[161] D. I. G. Jones, *Handbook of Viscoelastic Vibration Damping.* Chichester: J. Wiley, 2001. pp. 171-174.

[162] L. Winkelmann, O. Puncken, R. Kluzik, C. Veltkamp, P. Kwee, J. Poeld, C. Bo-gan, B. Willke, M. Frede, J. Neumann, P. Wessels, and D. Kracht, "Injection-locked single-frequency laser with an output power of 220 W," *Applied Physics B: Lasers and Optics*, **102**, pp. 529–538, 2011. http://www.springerlink.com/content/t2r71860p963l681/.

[163] M. Frede, B. Schulz, R. Wilhelm, P. Kwee, F. Seifert, B. Willke, and D. Kracht, "Fundamental mode, single-frequency laser amplifier for gravitational wave detectors," *Opt. Express*, **15**, pp. 459–465, 2007. http://www.opticsinfobase.org/oe/abstract.cfm?URI=oe-15-2-459.

[164] M. Frede, R. Wilhelm, D. Kracht, and C. Fallnich, "Nd:YAG ring laser with 213 W linearly polarized fundamental mode output power," *Opt. Express*, **13**, pp. 7516–7519, 2005. http://www.opticsinfobase.org/oe/abstract.cfm?URI=oe-13-19-7516.

[165] M. Ganija, D. Ottaway, P. Veitch, and J. Munch, "Cryogenic, high power, near diffraction limited, Yb:YAG slab laser," *Opt. Express*, **21**, pp. 6973–6978, Mar 2013. http://www.opticsexpress.org/abstract.cfm?URI=oe-21-6-6973.

[166] P. Kwee, B. Willke, and K. Danzmann, "Shot-noise-limited laser power stabilization with a high-power photodiode array," *Opt. Lett.*, **34**, pp. 2912–2914, 2009. http://www.opticsinfobase.org/abstract.cfm?URI=ol-34-19-2912.

[167] D. A. Bryan, R. Gerson, and H. E. Tomaschke, "Increase optical damage resistance in lithium niobate," *Appl. Phys. Lett.*, **44**, 847, 1984. http://dx.doi.org/10.1063/1.94946.

[168] G. Mueller, M. Arain, P. Sainathan, and G. Ciani, "aLIGO TCS Ring Heater development at UF - Krakow 2010 talk," *LIGO Document: LIGO-G1000945-v1*, 2010. https://dcc.ligo.org/cgi-bin/private/DocDB/ShowDocument?docid=21294.